EUROPEAN SCHOOL OF MOLECULAR MEDICINE

SEDE DI NAPOLI

UNIVERSITA' DEGLI STUDI DI NAPOLI "FEDERICO II"

Ph.D. in Molecular Medicine – Ciclo IV/XXI

Curriculum scelto (Human Genetics)

"Molecular development and laminar distribution of GABAergic interneurons of the cerebral cortex"

Tutor:
Prof. Brunella Franco

Co-tutor:
Prof. Michèle Studer

Internal Supervisor:
Prof. Antonio Simeone

External Supervisor:
Prof. Paola Arlotta

Coordinator:
Prof. Francesco Salvatore

Ph.D. student: Simona Lodato

Academic Year: 2009-2010

Acknowledgments

First and foremost, I would like to thank you my two advisors and mentors, Michèle Studer and Paola Arlotta for welcoming me in their laboratories and encouraging me over the past years. I have been an extremely lucky student to have the opportunity to train in their two laboratories, incredible places fulfilled with great science and amazing people. I have greatly benefited from the guidance and the insightful advices received by the members of my PhD thesis advisory Committee, Prof. Antonio Baldini, Prof. Brunella Franco, Prof. Tommaso Russo, and Prof. Antonio Simeone. I would like to thank Valeria Rotoli for her endless help on every kind and sort of administrative problems I encountered during my training.

I would like to thank all the members of the Studer lab for sharing their knowledge and skills with me; in particular, Eva Coppola, Maria Armentano and Gennaro Andolfi have been terrific colleagues to work with and fantastic friends. Thank you all guys for making the lab such an enjoyable and pleasant place to work. I also would like to thank all the members of the Arlotta lab; they all made me feeling home. I thank William Hendriks and Melissa Lin for their endless tips and tricks in tissue culture techniques; Zachary Trayes-Gibson, Amanda Merlino and Alyssa Melesky for their outstanding technical assistance; our dear "Book" Chanati Jantrachotechatchawan, for his untiring willingness in learning and working at the bench. I also would like to thank Eiman Azim for his generous advices and genuine interest for my work. Caroline Rouaux has been a great teacher and, most importantly, an amazing friend: it has been a pleasure and a trill sharing all the moments of my lab life with such a brilliant person like you, Caro. And Giulio Srubek Tomassy, an almost-constant presence in my whole scientific carrier: it has been a joy sharing with you the fascinating discoveries of science and life, my friend.

I also would like to thank all my friends, from “here and there” in the world, that, independently for the physical distances, have always been on my side, supporting an encouraging. Cheers guys!

And of course, I would like to thank my family. They offered me the opportunity of becoming a scientist. I wish I could make them proud of a good person, together with a good scientist. Thank you, Mamma, Papa’ and my “big bro” Mario.

A special thank goes to my always-here husband, Roberto, for his endless support of my work. He is the “north” of my life. Now more than ever.

Abstract

GABAergic interneurons of the cerebral cortex represent one of the most diversified populations of cells of the Central Nervous System. It is well established that different subtypes of interneurons populate and integrate into the cortical layers, where they critically modulate the firing activity of their excitatory projection neuron partners. The developmental origin of interneurons has been extensively studied, and elegant prior work has demonstrated that in rodents, the vast majority of interneurons are born in the ventral telencephalon within the medial and caudal ganglionic eminences (MGE and CGE).

Although great progress has been made over the last decade in understanding the molecular diversity and fate-specification of MGE-derived interneuron subtypes, the mechanisms controlling the birth and diversification of CGE-derived interneurons, as well as their functional roles within cortical circuitry, remain poorly understood. Here, I addressed this question directly, by investigating a potential role over CGE-derived interneurons of COUP-TFI, a transcription factor highly expressed in the embryonic CGE. I generated and studied conditional, null-mutant mice where the COUP-TFI gene was selectively deleted from the ventral telencephalon (COUP-TFI$^{fl;fl}$ x Dlx5/6CRE-IRES-GFP). In this mouse model, all GABAergic interneurons that arise from the subventricular zone of the ventral telencephalon lack COUP-TFI, without loss of this gene from neurons within the cerebral cortex. These conditional mutants are viable and survive to adulthood, thus enabling investigation of the birth and differentiation of interneuronal subtypes through postnatal stages of development, when local cortical microcircuitry is built. I found that conditional loss-of-function of COUP-TFI in subventricular precursors and post-mitotic cells of the basal ganglia led to a decrease within the cortex of late-born, CGE-derived, VIP- and CR-expressing bipolar interneurons, which was compensated by a concurrent increase of early-born, MGE-derived, PV-expressing interneurons. Strikingly,

COUP-TFI mutants were more resistant to pharmacologically induced seizures, a phenotype that we found is dependent on GABAergic signaling.

Together, the data support a model by which COUP-TFI regulates the delicate balance between MGE- and CGE-derived interneurons that reach the cortex, likely by influencing intermediate progenitor cell division in the CGE.

Upon fate-specification in the ventral telencephalon, interneurons travel long distances to reach and enter the cerebral cortex. Here, they precisely distribute into cortical layer and contact projection neuron partners. The developmental events governing the integration of excitatory projection neurons and inhibitory interneurons into balanced local circuitries are still poorly understood. In order to investigate the role of projection neurons in cortical interneuron lamination, I analyzed the cortex of *Fezf2*$^{-/-}$ mice, a unique mutant model in which a single population of projection neurons, subcerebral projection neurons, is absent and replaced by callosal projection neurons, without any effect on interneuron cell-autonomous fate specification and differentiation. Using this model, I found that replacement of one projection neuron type with another was sufficient to cause distinct abnormalities of interneuron lamination and altered GABAergic inhibition. The data indicate that different subtypes of projection neurons uniquely and differentially determine the laminar distribution of interneurons in the cerebral cortex. In agreement, in parallel gain-of-function experiments, I found that distinct populations of projection neurons (i.e. corticofugal projection neurons or upper layer II/III callosal projection neurons) that were experimentally generated below the cortex could recruit cortical interneurons to these ectopic locations. Strikingly, the identity of the projection neurons generated, rather than strictly their birthdate, determined the specific types of interneurons recruited. These data demonstrate that in the neocortex individual populations of projection neurons cell-extrinsically control the laminar fate of interneurons and the assembly of local inhibitory circuitry.

Together, the work identifies a new transcriptional control over cell-autonomous development of CGE-derived interneurons, and provides a first demonstration that neuronal subtype-specific interactions among excitatory and inhibitory neurons is critically necessary for the building of balanced local microcircuitry in the cerebral cortex.

Table of Contents

Figures Index

Chapter 1

Introduction

Cortical development

The central nervous system (CNS) is one of the most complex tissues of the body, with unparalleled cellular diversity and very complex connectivity. The region of the CNS responsible for cognitive function, sensory perception, motor function and consciousness, and as such, that has undergone pronounced expansion and development during evolution, is the cerebral cortex (Tomassy et al., 2010b). Here, a highly organized six-layered structure, the neocortex, contains an extraordinary variety of glial and neuronal subtypes that are generated during embryogenesis from distinct pools of tissue-specific neural stem and progenitor cells, which are progressively specified to different cellular fates. Then, hundreds of different cell types coordinately assembly to generate the cortical circuitries. Defects in cortical neural circuitry are likely to underlie important neurological and psychiatric illnesses. Circuitry development occurs during brain formation and requires the precise timing of cell migration and differentiation, as well as synaptogenesis. Inherited disruption of these developmental events in the cerebral cortex commonly leads to human neurological and psychiatric disorders such as epilepsy, anxiety and depression with a developmental onset during childhood or adolescence. In particular, proper cortical activity depends on a delicate balance of synaptic excitation and inhibition, which relies on the coordinated assembly of local microcircuitry between two broad neuronal populations of the neocortex: excitatory glutamatergic projection neurons and inhibitory GABAergic interneurons (Hensch, 2005). In spite of representing only the 20% of the total neuronal population in the mouse cerebral cortex, intreneurons play a key role in the regulation of cortical intrinsic activity through their direct effect on excitatory neurons. GABA neurotransmitter acts predominantly via postsynaptic chloride-permeable ionotropic $GABA_A$ receptors to shunt or hyperpolarize target cells. As such, GABAergic interneurons are crucial for regulating the firing activity and entraining the principal neuronal component of the cerebral cortex: the glutamatergic projection neurons.

Glutamatergic projection neurons of layer II-VI are characterized by a typical pyramidal morphology and transmit information between different regions of the neocortex and to other regions of the brain. During development, they are generated from progenitors in the dorsal telencephalon (pallium) and migrate into the cortex primarily via radial glia-guided migration (Anderson, 2001; Anderson et al., 2002; Rakic, 1972; Tan et al., 1998; Ware et al., 1999). In contrast, in rodents a wealth of evidence has accumulated indicating that the majority of cortical GABAergic interneurons are generated in the ventral telencephalon deriving from subpallial germinal zones, including the medial and caudal ganglionic eminences, the septum and the preoptic area, each of which contributes distinct sets of interneurons that undergo tangential migration to reach their final destinations in the cortex (Anderson et al., 2001; Anderson et al., 1997; Marin and Rubenstein, 2001; Nery et al., 2002; Tamamaki et al., 1997; Tan et al., 1998; Wichterle et al., 2001). Additionally, different subtypes of layer I Cajal-Retzius cells are derived from at least three regions – the caudomedial cortical hem (Meyer et al., 2002; Takiguchi-Hayashi et al., 2004), the pallial-subpallial boundary (Bielle et al., 2005), and the septum (Bielle et al., 2005).

Here, I will present an overview of the development of excitatory projection neurons and of cortical GABAergic interneurons, focusing in particular on the molecular and cellular mechanisms governing development of cortical interneurons.

Development of cortical excitatory projection neurons

Neocortical excitatory projection neurons are born from progenitors residing in the ventricular and subventricular zone of the developing dorsal telencephalon in a tightly controlled temporal order (Angevine and Sidman, 1961; Rakic, 1974) and position themselves in the developing cortex *via* defined modes of radial migration (Rakic, 1972, 2003). Similarly to other regions of the developing CNS, different types of neural

progenitor cells are present at different stages of development; these have distinct characteristics, different plasticity and fate potentials. At the earliest stages of corticogenesis, before cortical neurons are generated, neural progenitors are defined as neuroepithelial (NE) cells due to their appearance as a sheet of polarized, cycling cells with epithelial features, including tight and adherent junctions in the apico-lateral plasma membrane. NE cells are multipotent neural progenitors that expand *via* symmetrical divisions (Aaku-Saraste et al., 1996; Gotz and Huttner, 2005; Zhadanov et al., 1999). As corticogenesis progresses NE cells become more fate-restricted and give rise to a second type of cortical progenitor cells known as radial glia (RG). RG have a unique bipolar shape and while their cell bodies are located in the ventricular zone (VZ), they maintain connections with both the ventricular and pial (i.e. external) surface of the developing cortical wall (Kriegstein and Gotz, 2003; Malatesta et al., 2008). RG retain some hallmarks of NE cells like the presence of adherent (but not tight) junctions and the expression of the intermediate filament protein *Nestin* (Chenn et al., 1998; Gotz and Huttner, 2005; Malatesta et al., 2000) but they are a more fate-restricted population of neural progenitors (Chenn et al., 1998; Williams and Price, 1995). When cortical neurogenesis begins, RG begin to divide asymmetrically to generate both progenitors and postmitotic neurons (Gotz and Huttner, 2005; Noctor et al., 2004). The discovery that radial glial cells are progenitor cells represents a significant advance toward characterizing the different populations of stem cells and multipotent progenitors. Earlier, radial glial cells have long been known to play critical roles in guiding migrating neurons to their final locations in the cortical plate by serving as migratory scaffolding with long processes extending from the ventricular wall to the pial surface (Rakic, 1972, 2003). However, there is now direct evidence that radial glia are also progenitors that make significant contributions to cortical neurogenesis (Anthony et al., 2004; Hartfuss et al., 2001; Heins et al., 2002; Malatesta et al., 2003; Malatesta et al., 2000; Noctor et al., 2001). By directly

observing radial glial division and the migration of individual progenitors and their progeny, more recent work has started to define the cellular dynamics of neurogenesis and migration of clonally related families of cortical neurons on the radial glia cell that produced them (Noctor et al., 2001; Noctor et al., 2002; Noctor et al., 2004).

Neuronal progeny, in turn, migrate radially away from the VZ such as the earliest born neurons form the preplate. As more neuroblasts migrate away from the germinal zone and into the preplate, they form a new layer, called the cortical plate (CP), which effectively splits the preplate in two. The portion of the preplate above the newly formed cortical plate becomes the marginal zone (MZ) and the portion below the cortical plate forms the subplate (SP) (Bayer and Altman, 1991). When later-born neuroblasts arrive at the cortical plate, they migrate past earlier-born neurons, resulting in an "inside-out" pattern of cortical development such that early generated neurons populate the deeper layers of the neocortex, while later-born neurons position within more superficial layers (Angevine and Sidman, 1961; Rakic, 1974). Elegant birth-dating studies using H^3–thymidine have also confirmed that projection neurons of the different layers are generated in a specific temporal order, such that SP and deep layer VI and V neurons are born first (between E10.5 and E13.5 in the mouse) while neurons of the superficial layers IV and II/III are born later (between E14.5 and E16.5 in the mouse) (Bayer and Altman, 1991; Molyneaux et al., 2007).

Major insights into the molecular mechanisms underlying cortical lamination have come from studies of reeler mice (Rice and Curran, 2001; Tissir and Goffinet, 2003). In the reeler cortex, the normal inside-out pattern is replaced by a roughly inverted pattern of cortical lamination where newborn neurons fail to migrate past older ones and end up occupying deeper layers of the cortex (Caviness and Sidman, 1973). Reeler mutation affects the *reln* gene (D'Arcangelo et al., 1995; Ogawa et al., 1995), which encodes a large extracellular matrix glycoprotein highly expressed in Cajal-Retzius (Alcantara et al.,

1998). The Reelin signal is received in migrating neurons by two redundant cell surface receptors, Very Low Density Lipoprotein Receptor (Vldlr) and Apolipoprotein E Receptor 2 (ApoER2). Double mutation of Vldlr and ApoER2 results in cortical lamination defects similar to reeler mutants (D'Arcangelo et al., 1999; Dulabon et al., 2000; Hiesberger et al., 1999; Howell et al., 1999; Senzaki et al., 1999; Trommsdorff et al., 1999). Downstream of Vldlr and ApoER2, the adaptor protein Disabled-1 (Dab-1) is required for mediating Reln signaling and Dab-1 mutant mice also display reeler-like cortical lamination phenotypes (Howell et al., 1997; Sheldon et al., 1997). Thus, Reelin signaling to cortical neurons is essential for proper radial neuron migration and cortical layer formation.

The laminar cytoarchitecture of the cortex is relatively similar in all mammals; however, a big expansion of the cortex occurred during recent evolution, which led to the transformation of a lissencephalic cortex (i.e. smooth and without folds) characteristic of rodents, into a gyrencephalic one (i.e. folded with gyri and sulci) characteristic of primates. The need to accommodate the disproportionate growth of the cortex appears to have been at least in part met by the appearance and enlargement of a second germinal zone, the subventricular zone (SVZ), located away from the luminal surface (Kriegstein et al., 2006) and with it, the generation of another class of cortical neural progenitors: the basal progenitor (BP) cells. BP progenitors are different from both NE and RG progenitors in that they divide in the SVZ, and they are further restricted in their fate potential (Haubensak et al., 2004; Noctor et al., 2004; Pontious et al., 2008). It is intriguing to consider that BP progenitors may have different fate potential than RG progenitors, at least in part because they divide away from the ventricular surface, and thus do not receive VZ derived signals (Schematic 1.1). Upon differentiation, progenitor cells and their postmitotic progeny behave very differently, the former remaining in the germinal zones (VZ or SVZ) to divide and generate new progeny, the latter migrating away to populate the cortical plate. A dividing progenitor cell thus bears the “responsibility” to choose

between very different fates: undergoing a neurogenic division (i.e. giving rise to at least one postmitotic neuron) or continuing with proliferative divisions (i.e. giving rise to two progenitor cells). The precise identity of the different progenitor cell types, in relationship with the different fates of their progeny and together with the degree of restriction of each type, is not known but has been the subject of intense study (Desai and McConnell, 2000; McConnell, 1988; McConnell and Kaznowski, 1991; Mizutani and Saito, 2005). Changes in progenitor fate potential are dependent on intrinsic as well as environmental signals and were initially described in a series of transplantation experiments where the potential of cortical progenitors at different stages was tested by transplanting them into cortex at earlier or later stages. Progenitors transplanted from the germinal zone at early stages of development (when deep layer neurons are normally generated) have the potential to form either deep layer neurons or upper layer neurons depending on the environment they are transplanted into and the stage of the cell cycle they are in at the time of transplantation. In contrast, later in development, progenitors become more restricted and if transplanted into a younger cortex, they only generate upper layer neurons, appropriate for the host but not the recipient (Desai and McConnell, 2000; McConnell, 1988). More recently, these results have been extended by demonstrating that even progenitors that are prevented from asynchronous division by constitutively active Notch expression still undergo changes in fate potential – later stage neurons are appropriately generated when the constitutively active Notch activity is removed (Mizutani and Saito, 2005).

By several sophisticated mechanisms, over time, cortical neural progenitors give rise to an impressive diversity of projection neuron subtypes that are located in different layers and areas of the cortex, and have unique morphological features, molecular "fingerprints", distinctive connectivity targets and, ultimately, serve different functions. Projection neurons are indeed classified into numerous subtypes based on their location within different cortical layers and areas; their axonal projections to distinct intracortical,

subcortical and subcerebral targets; and the combinatorial expression of different neuron type-specific genes (Bayer and Altman, 1991). Among them, corticofugal projection neurons include corticothalamic projection neurons, which are found in layer VI and project to the thalamus, as well as corticospinal motor neurons (CSMN), corticotectal projection neurons and several other types of subcerebral projection neurons, which are located in different areas of layer V and project to the spinal cord, the superior culliculus and other targets in the brainstem and below the brain, respectively (Molyneaux et al., 2007). In addition, the cortex includes several types of callosal projection neurons (CPN), which are located in layers II/III and V (and in small numbers in layer VI) and connect to targets in the contralateral hemisphere (i.e. *via* the corpus callosum), the striatum and the frontal cortex (Lindwall et al., 2007; Mitchell and Macklis, 2005; Molyneaux et al., 2009; Richards et al., 2004) (Schematic 1.2).

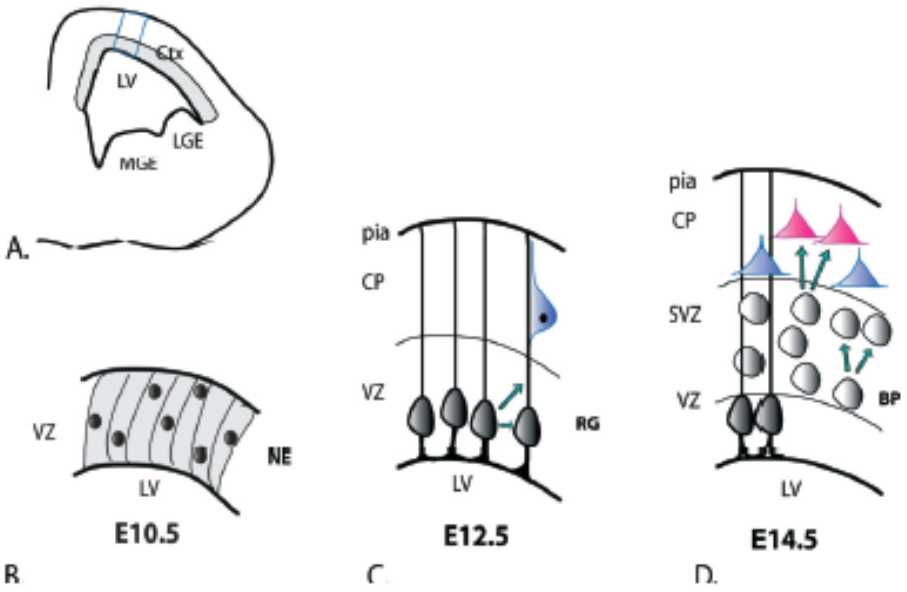

Schematic 1.1 Different classes of neural progenitors generate projection neurons of the cerebral cortex. (A) Schematic representation of the developing forebrain. Cortical progenitors are located in the VZ, highlighted in grey. (B) At the earliest stages of corticogenesis, neural progenitors are defined as neuroepithelial (NE) cells. (C) Later, NE cells give rise to Radial Glia (RG) cells, which give rise to immature projection neurons (highlighted in light blue) and provide a scaffold for neuronal migration to the cortical plate (CP). (D) Basal progenitor (BP) cells appear in the subventricular zone during later stages of corticogenesis and mostly give rise to upper layer projection neurons (highlighted in pink). (Adapted from Tomassy et al., 2010).

Specification of cortical projection neurons

Although great progress has been recently made in identifying markers of different subtypes of projection neurons once they have reached the cortical plate, it is not clearly defined for most populations which signals are responsible for driving the early steps of specification and overall development of individual types of neurons. However, among the projection neurons, corticospinal motor neurons (CSMN), and, to a smaller extent, callosal projection neurons (CPN) are notable first exceptions (Arlotta et al., 2005; Molnar et al., 2006; Molyneaux et al., 2009; Molyneaux et al., 2005; Molyneaux et al., 2007). CSMN are located in layer Vb of motor cortex and they extend axonal projections through the internal capsule and the pons to the spinal cord, where they synapse with lower motor neurons (*via* interneurons in rodents) (Canty and Murphy, 2008; Liang et al., 1991). Together with highly related neuronal types that make axonal projections from layer Vb to targets below the brain, CSMN are also classified as subcerebral projection neurons (Molyneaux et al., 2007). Recently, the development of experimental approaches to label and isolate CSMN and other projection neuron subtypes from the cortex has led to the identification of a first series of genes that, with different degrees of restricted expression, distinguish CSMN at the molecular level (Arlotta et al., 2005). Genes that define the CSMN population include transcription factors (e.g., *Ctip2*, *Bcl6*, *Sox5, Fezf2*); cell surface proteins (e.g., *Encephalopsin*, *Itm2a*, *Daf1*); calcium signaling proteins (e.g., *Pcp4*, *S100a10*); cell adhesion proteins (e.g., *Cdh22, Cdh13*, *Cntn6*), and axon guidance molecules (e.g., *Neto1, Netrin-G1*) (Arlotta et al., 2005). Most importantly, beyond their roles as CSMN molecular markers, some of these genes have been shown to control central steps of development of CSMN, including the timing of birth, fate specification and axonal connectivity (Arlotta et al., 2005). Among key transcription factors, the zinc finger protein *Fezf2* has been shown to be essential for CSMN early specification, *in vivo* (Hirata et al., 2004; Molyneaux et al., 2005). In the absence of *Fezf2* in null-mutant mice,

CSMN and all subcerebral projection neurons are not specified and are absent from the cortex. In line with this finding, the corticospinal tract (and all cortical connections to the brainstem) does not form (Molyneaux et al., 2005). This effect is neuron type-restricted since upper layer IV and II/III neurons appear to develop normally, and layer VI neurons, despite some morphologic and molecular abnormalities, are specified and locate correctly in layer VI of the *Fezf2*$^{-/-}$ cortex (Molyneaux et al., 2005). Further adding to the "master" role of *Fezf2* in CSMN development, elevated levels of *Fezf2* expression in progenitor cells of upper layer neurons of the cortex (mostly CPN), is in part sufficient to instruct a switch of fate and the generation of deep layer neurons that make connections to subcortical and subcerebral targets (Chen et al., 2005a; Molyneaux et al., 2005). Likely acting after *Fezf2*, another CSMN specific transcription factor, *Ctip2*, is important for the establishment of appropriate axonal connectivity by CSMN to the spinal cord (Arlotta et al., 2005; Chen et al., 2008). Similarly, *Sox5* and *Bhlhb5* have been demonstrated to control the timing of generation and the arealization of the CSMN population, respectively (Chen et al., 2005b; Lai et al., 2008).

Although our understanding of the mechanisms that produce distinct subtypes of subcortical projection neurons in the deep layers is growing, much less is known about how the brain produces the classes of neurons that populate the upper layers, mainly represented by callosal projection neurons. Recent work has revealed that callosal projection neurons require the chromatin remodeling protein Satb2 for the formation of their normal projections, and that in the absence of *Satb2*, these cells extend axons toward subcortical targets (Alcamo et al., 2008; Leone et al., 2008). In addition to adopting the axon trajectory of deep layer neurons, *Satb2* mutants display alterations in the expression of several axon guidance molecules and a dramatic expansion of Ctip2 expression into the upper layers and within the deep layers. These data suggest that Satb2 functions to repress *Ctip2* expression in callosal projection neurons. Indeed, the ectopic expression of *Satb2* in

neurons markedly reduces the fraction of cells that express *Ctip2* (Chen et al., 2008; Fukumitsu et al., 2006), and alters the projections of deep layer neurons, such that the axons of electroporated cells fail to extend past the cerebral peduncle (Fukumitsu et al., 2006). This axonal phenotype is reminiscent of that observed in *Ctip2*−/− brains (Arlotta et al., 2005), suggesting that ectopic expression of *Satb2* might alter the fate of deep layer neurons by regulating *Ctip2* expression. Collectively these data suggest that *Satb2* promotes a callosal projection neuron identity in the cortex by repressing *Ctip2* expression. Indeed, the repression of *Ctip2* by Satb2 appears to be direct: Satb2 binds directly to matrix attachment regions (MARs) in the *Ctip2* locus, where it recruits histone deacetylases (Fukumitsu et al., 2006; Olsson et al., 1997) and modifies chromatin configuration to assume a less activated state (Chen et al., 2008; Olsson et al., 1997).

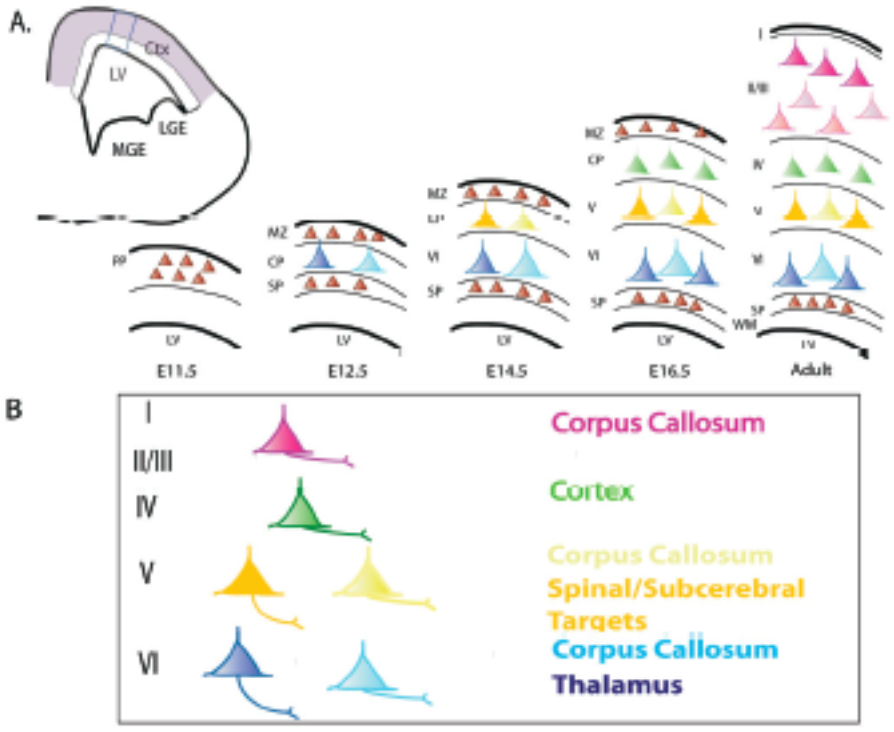

Schematic 1.2 The cortex contains many subtypes of cortical projection neurons. (A) Projection neuron types are born at different stages of development. Layers contain more than one type of projection neuron (indicated by the different colours). (B) Different projection neurons connect to different targets within the cortex (via the corpus callosum and to local ipsilateral targets), and to subcortical (exemplified by the thalamus) and subcerebral (exemplified by the spinal cord) targets. (Adapted from Tomassy et al., 2010)

Development of cortical inhibitory interneurons

Firstly identified and classified based on their morphology in 1899 by Ramon y Cajal, who described them as ‘‘short axon cells’’, GABAergic intereurons are now known to be locally projecting cells that control and synchronize the output of pyramidal neurons, accounting for about 20–30% of the cortical neuronal population. Despite years of research, however, it is still unclear how many different types of cortical interneurons actually exist. This is due, among other reasons, to the difficulties in defining what a cortical interneuron is (Ascoli et al., 2008), which complicates the concerted effort of many neuroscientists, recently attempted, to formalize a unique and comprehensive nomenclature (Petilla Nomenclature). Despite some reservations, it is now largely accepted that distinct types of interneurons exist and that they are defined by a constellation of neurochemical, anatomical and electrophysiological characteristics. Based on this definition, four major classes of interneurons have been identified: (1) fast-spiking, PV-containing basket and chandelier cells; (2) somatostatin (SST)-containing interneurons which typically display intrinsic burst spiking or adapting non-fast-spiking electrophysiological profiles and many of which have long axons that extend into layer I; (3) rapidly adapting interneurons with bipolar or double-bouquet morphologies, which frequently express calretinin (CR) and⁄or vasointestinal peptide (VIP); and (4) rapidly adapting interneurons with multipolar morphologies and that express neuropeptide Y (NPY) and⁄or reelin, but not SST (Ascoli et al., 2008; Gupta et al., 2000; Markram et al., 2004). Although this general classification is now largely accepted, many other types of interneurons are left out of this major classification. This is due, at least in part, to activity-dependent changes in the levels of some neurochemical markers, cross-species differences and lack of comprehensive analyses of the heterogeneous characteristics of cortical interneurons (Gelman and Marin, 2010).

Various transplantation experiments and elegant fate mapping studies have

demonstrated that such a wide diversity is intimately dependent on their origin (where interneuron progenitors are located) and birth-dates (Butt et al., 2005; Fogarty et al., 2007; Miyoshi et al., 2007; Miyoshi and Fishell, 2010).

Research over the past decades has provided strong evidence that the majority of cortical interneurons, in rodents and ferrets, is generated from multiple proliferative regions in the ventral telencephalon, that are the lateral, medial and caudal ganglionic eminences (LGE, MGE and CGE, respectively), the recently recognized preoptic area (POA), and perhaps the anterior entopedunculate region (AEP) (Corbin et al., 2001; Gelman et al., 2009; Marin and Rubenstein, 2001). After being generated in these ventral structures, interneurons begin their journey migrating tangentially over long distances to populate the cortex, including the piriform cortex, the neocortex and the hippocampus (Marin and Rubenstein, 2003).

Several molecules, including transcription factors, have been demonstrated to be involved in controlling fate specification and/or migration of interneurons (Marin and Rubenstein, 2003). Alteration of these proteins leads to abnormal specification and migration of the interneurons to the cortex.

In a temporal pattern, the generation of cortical INs extends through a lengthy period of embryonic neurogenesis in the telencephalon from embryonic day (E) 10.5 to birth. Intereurons migrate from the ventral telencephalon through two different streams that go around the corticostriatal boundary and follow tangentially orientated paths to eventually enter the cortex. Around E12.5, an early cohort that originates in the MGE innervates the cortical preplate (a layer of tangentially oriented cells that often show features typical of Cajal-Retzius cells). A second and more prominent cohort, composed also of MGE-derived cells, has been observed to migrate mainly through the intermediate zone (IZ) and the subventricular zone (SVZ) of the cortex slightly later (E13.5-15.5) (Kriegstein and Noctor, 2004; Lavdas et al., 1999). After reaching the pallium, migrating

interneurons invade the cortical plate by changing their mode of migration from tangential to radial (Ang et al., 2003; Polleux et al., 2002; Tanaka et al., 2003b) and disperse within the six layers of the cortex to acquire their laminar position. It has long been recognized that, cortical interneurons show the same inside-out pattern of generation that is observed in pyramidal cells (Anderson et al., 2002; Cavanagh and Parnavelas, 1989; Fairen et al., 1986; Peduzzi, 1988). Different subtypes of MGE-derived interneurons are produced at particular developmental times and end up in different layers of the cortex. Early-born MGE-derived interneurons end up in deep layers, while late-born interneurons occupy superficial layers of the mature cortex, and each cohort possesses unique electrophysiological properties characteristic of their birthdate (Miyoshi et al., 2007).

Although cortical interneurons have to cover long distances to reach their final laminar position, they tend to occupy the same cortical layer of projection neurons born at the same time (Lopez-Bendito et al., 2004; Tanaka et al., 2003b). Little is known about the mechanism controlling the acquisition of laminar position by cortical interneurons. In Chapter 3, I will analyze the role of projection neurons on interneuronal cortical positioning and their integration in the cortical network.

Interneuron specification: the where and when

The question of how interneuron diversity is established has been a central point of debate in the field over the last decade. Despite a multitude of attempts to reveal the mechanisms by which an interneuron acquires its mature properties, we still do not have a definitive answer to this question. Multiple lines of evidence show that interneuron subtypes identity is related to both its spatial and temporal embryonic origin (Batista-Brito and Fishell, 2009; Butt et al., 2005).

Recent studies in humans and in non-human primates provide intriguing and definitive evidence for a cortical origin of interneurons in primates (Letinic et al., 2002;

Petanjek et al., 2009). In contrast, in rodents, the field is currently lacking any in vivo evidence for an embryonic cortical source of interneurons. Nevertheless, there are multiple indications that post-natal generation of cortical interneurons can occur within the cortex itself, especially under specific circumstances (Dayer et al., 2005; Inta et al., 2008; Ohira et al., 2010).

Anatomical origin

To date, the vast majority of cortical interneurons have been shown to arise from the ganglionic eminences, with a recently found small contribution by the preoptic area, and a controversial contribution by the septal region (Gelman et al., 2009; Rubin et al., 2010) (Schematic 1.3).

The MGE and LGE were the first ganglionic eminences described in the murine telencephalon, by analogy with structures originally described in human embryos (Sturrock and Smart, 1980); in contrast, the CGE was proposed much later as a distinct entity by Anderson et al. (2001) as the eminence that is posterior to the fusion of the MGE and LGE. These three structures also appear in a different timeframe during the mouse development, with the MGE emerging first, followed by the LGE and only few days later by the CGE (Smart, 1976). However, while a clear anatomical separation exists between the LGE and the MGE, the *sulcus*, no physical borders define the CGE extension, making its definition very controversial. According to some neuro-developmental biologists, the CGE could results by the caudalization of the LGE (Flames et al., 2007) and the MGE protruding at later developmental stages.

The MGE gives rise to the vast majority of cortical interneurons (around 60%) expressing the calcium-binding protein Parvalbumin (PV) and the peptide hormone Somatostatin (SST) as demonstrated by numerous transplanting experiments *in utero* or into postnatal cortex, as well as plating of dissociated MGE progenitors onto cortical

layers in vitro (Valcanis and Tan, 2003; Wichterle et al., 1999; Wichterle et al., 2001; Xu et al., 2004). After the MGE, the CGE is the most prominent source of cortical interneurons (Anderson, 2001; Nery et al., 2002). Isolated late CGE progenitors on feeder layer of cortical neurons produce mainly bipolar Calretinin (CR)- and Vasointestinal Peptide (VIP) expressing interneurons (Xu et al., 2004). These experiments, together with *in vivo* transplantation studies, suggest that the CGE generates a remarkable diversity of interneurons in addition to CR- VIP- that includes Neuropeptide (NPY)- and Reelin-expressing cells (Butt et al., 2005; Miyoshi et al., 2007).

While very well recognized is the origin of interneurons from the MGE and the CGE, still much debated is their origin from the LGE: originally identified together with the MGE as source of cortical interneurons, and then revised in lights of several evidences (Anderson, 2001; Wichterle et al., 2001), now only one study performed on rat embryos is still supporting the original hypothesis (Jimenez et al., 2002). Should the LGE give rise to a small fraction of cortical interneurons, however those do not include the SST-and PV-expressing subgroups (Xu et al., 2004).

The preoptic area, a hypothalamic region located immediately in front of the optic recess, just ventral to the MGE, has been recently identified as source of small number of cortical interneurons (Gelman et al., 2009). These were found mainly in the superficial layers of the cortex, and about a third expresses NPY but not SST, and tended to have a distinctive, rapidly adapting electrophysiological property.

Still controversial is instead the contribution of the septal region, originally considered as a possible source of tangentially migrating interneurons destined to the cerebral cortex (Taglialatela et al., 2004). A more recent study of genetic lineage tracing excludes that the septum generates cortical interneurons (Rubin et al., 2010).

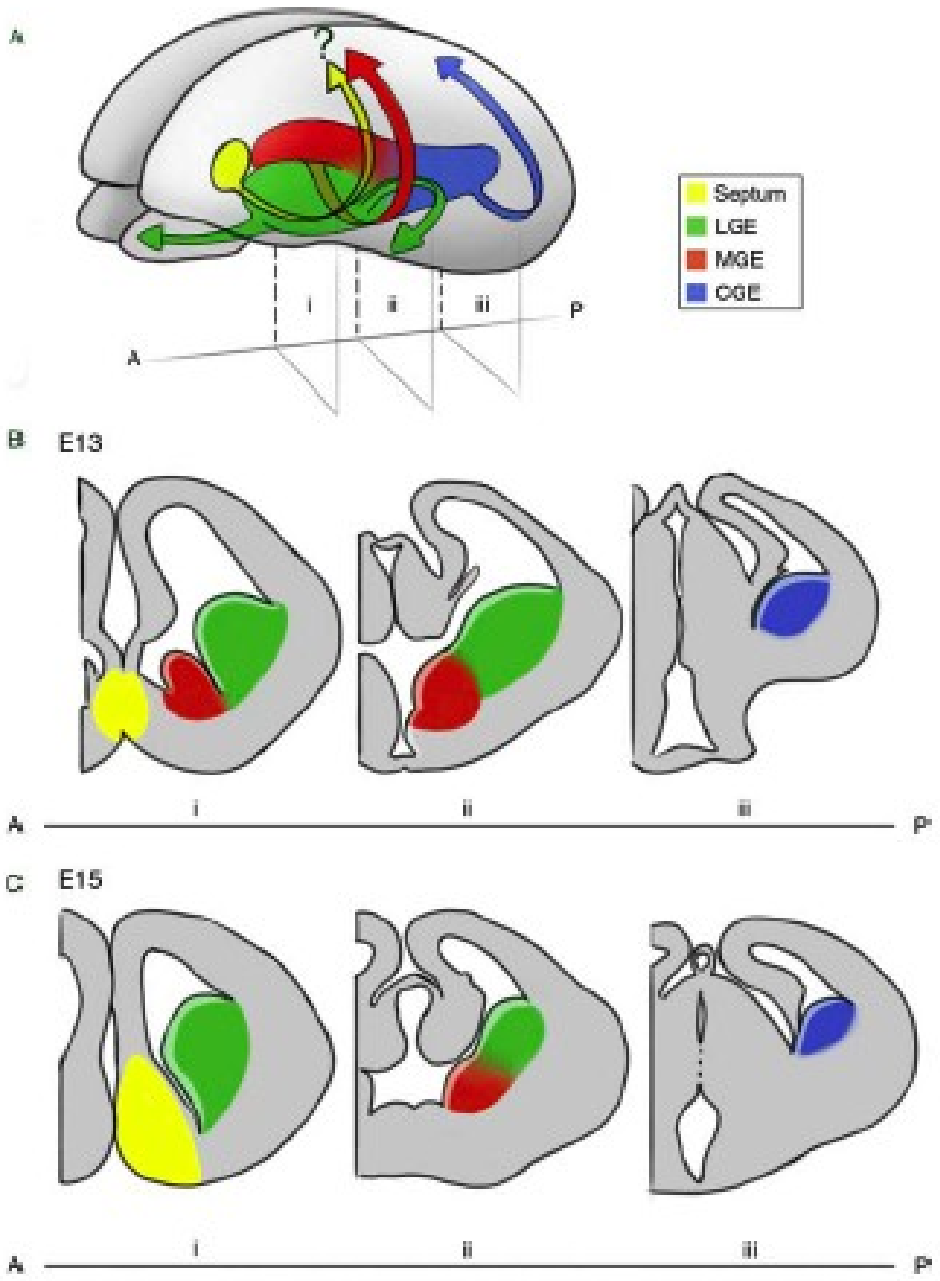

Schematic 1.3 Representation of the developing mouse brain. (A) Threedimensional view of a developing brain indicating the ventral anatomical regions that give rise to interneurons and their correspondent migratory pathways. The LGE (green) generates interneurons that migrate to the olfactory bulb and striatum. Both the MGE (red) and CGE (blue) produce cortical interneurons. Whether the septum produces cortical interneurons (yellow) is still a matter of debate. (B–C) Coronal views of the brain in (A) at three locations (i–iii) along the anterior (A)–posterior (P) axis at the embryonic ages E13 (B) and E15 (C) (adapted from Batista-Brito and Fishell, 2010).

Molecular origin

The ventral telencephalon undergoes gradual morphological changes during development. This quick rearrangement of the anatomical structures definitely complicates the

identification of the eminences solely on the basis of morphological features. To overcome this limitation, in the last decade, a concerted effort from many different laboratories has been made to identify molecular landmarks that could correspond to these anatomical structures (Batista-Brito and Fishell, 2009; Flames et al., 2007). Many genes are broadly expressed within the ventral telencephalon and are known to be essential for the generation for cortical interneuron development. In particular, members of the *Dlx* gene family, which are expressed throughout the subpallial subventricular zone (SVZ), have been shown to be critical for interneuron specification (Petryniak et al., 2007; Pleasure et al., 2000). Mice containing compound Dlx1/Dlx2 mutations die at birth and have a severe reduction in the tangential migration of interneurons from the ventral eminences to the neocortex, resulting in a massive loss of neocortical GABAergic cells at birth (Anderson et al., 1997). Furthermore, Dlx1/Dlx2 nulls have abnormal striatal differentiation (Anderson et al., 1997), and virtually no olfactory bulb interneurons (Bulfone et al., 1998). Similarly, null mutations in *Mash1*, a proneural gene expressed throughout the subpallial SVZ (Porteus et al., 1994) display a marked loss of GABAergic cortical and olfactory bulb interneurons (Casarosa et al., 1999). While *Dlx* family and *Mash1* genes are broadly expressed within the subpallium, other genes show more restricted expression patterns.

A few years ago, the concerted effort of several scientists evidenced a novel mechanism of specification of interneuron subtypes taking into account the molecular identity of their origin (Flames et al., 2007). It was hypothesized that, akin to what happens in the spinal cord, the ganglionic eminences contain multiple distinct pools of progenitors, each of which gives rise to specific interneuron subtypes. Using a combinatorial approach, based on the examination of the patterns and levels of expression of different transcription factors, both the MGE and LGE were divided into nine subdomains. Although this effort to map the eminences into microdomains greatly contributed to the discovery of novel gene expression patterns, it cannot yet account for

the diversity of interneuron subtypes that arise from the only MGE (Miyoshi et al., 2007). Therefore, although the hypothesis of distinct MGE progenitor subdomains specified through the actions of unique transcriptional combinations is very attractive, a finer subdivision within the eminences will need to be established (Batista-Brito and Fishell, 2009).

The majority of the MGE domain is delimited by the expression of the transcription factor Nkx2.1, excluding the dorsal MGE that expresses Nkx6.2, Gli1 and is partially Nkx2.1 negative (Fogarty et al., 2007; Rallu et al., 2002; Wonders et al., 2008). Nkx2.1 null mice show a dramatically reduced MGE and present a drastic reduction of cortical interneurons at birth (Sussel et al., 1999). Years later the first null model was published, it has been demonstrated indeed that Nkx2.1 is required for the correct specification of MGE-derived interneuron subtypes and for the establishment and maintenance of MGE identity (Butt et al., 2008). Conditional removal of Nkx2.1 leads to an interneuron subtype fate-witch in a time-dependent manner. Similar to what was observed in Nkx2.1 nulls (Sussel et al., 1999), early conditional removal (E10.5) of Nkx2.1 leads to a decrease of cortical interneurons and a corresponding increase in striatal spiny neurons (Butt et al., 2008). It also results in the remaining cortical interneurons acquiring characteristics normally found in the CGE-derived population. Later removal of Nkx2.1 at E12.5 resulted in a decrease of MGE-derived PV/SST cortical interneuron subtypes, and an increase in the normally CGE-derived CR/VIP population. Also, it has recently been shown that Nkx2.1 is an upstream regulator of another important transcription factor, the LIM-homeobox Lhx6, and specifies interneuron fate by directly activating this gene (Du et al., 2008). Lhx6 pattern of expression resembles very much Nkx2.1, if excluded its absence from the MGE VZ progenitors; MGE-derived progenitors indeed start to express Lhx6 as soon as they leave the ventricular zone (Grigoriou et al., 1998). Lhx6 expression persists throughout adulthood in most parvalbumin (PV)- and

somatostatin (SST)-expressing cortical interneurons, while is virtually absent from VIP- and CR-expressing intereneurons (Cobos et al., 2006; Du et al., 2008; Fogarty et al., 2007; Gong et al., 2003; Lavdas et al., 1999; Liodis et al., 2007). Lhx6 loss of function analysis has shown that this gene is required for the normal specification and migration of MGE-derived GABAergic cells, and null animals exhibit a loss of PV and SST interneurons in the neocortex and hippocampus, without any alteration is the total number of cortical GABAergic interneurons generated (Liodis et al., 2007).

In concordance with the transplantation studies from the MGE, genetic fate mapping of this structure by using the allele *Nkx2.1Cre* shows that this region produces primarily PV, SST, and CB, and to a lesser extent NPY and CR neurons (Fogarty et al., 2007; Xu et al., 2004). Genetic fate mapping of Nkx6.2 progenitors (expressed in the sulcus) using an *Nkx6.2Cre* allele shows that this region, similar to the Nkx2.1 domain, produces CB, SST, PV, NPY, and CR neurons with the difference of a proportionally greater contribution to the NPY and CR subtypes than the Nkx2.1 domain fate map, suggesting that the latter two subtypes preferentially originate in the most dorsal part of the MGE (Fogarty et al., 2007; Xu et al., 2008). Fate mapping of Lhx6-expressing cells reveals a total overlap of the Lhx6 lineage with the cortical PV, SST, and CB interneurons (Fogarty et al., 2007; Xu et al., 2008), and the contribution of Lhx6 for NPY and CR subtypes is similar to that observed for Nkx6.2 (Fogarty et al., 2007; Xu et al., 2008). Altogether these results confirm that the MGE constitutes the region that accounts for the majority of cortical interneurons generated (Anderson et al., 2001; Lavdas et al., 1999; Wichterle et al., 1999; Wichterle et al., 2001).

The CGE, originally thought to contribute to the generation of solely 15% of cortical interneurons (Nery et al., 2002), has been recently reconsidered to account for almost 40% of them (Miyoshi et al., 2010), conferring to this structure an importance so far almost neglected. Although it has been recently shown that CGE-derived interneurons

specifically express the serotonin receptor 5HT3a, and that Nkx6.2 and the transcription factors COUP-TF1/2 are widely expressed within the CGE (Sousa et al., 2009), to date, no CGE-master gene has been identified. Therefore genetic fate mapping of any gene that specifically labels the CGE has been hampered.

Recently, the fortuitous expression of a BAC *Mash1CreER* transgenic line selectively in the CGE and not MGE, has allowed a preliminary study of genetic fate-maping of this region. This analysis has confirmed the results from previous CGE transplant experiments, and has expanded upon them by indicating that the contribution of CGE lineages to the cortical interneuron population is higher than previously estimated (about 40% of the total). Of the cells fate mapped from the CGE, a large percentage are late-spiking interneurons expressing Reelin or bipolar VIP/calretinin populations (Miyoshi et al., 2010). In line with these findings, very recently it has been shown that the population of 5-HT3AR-expressing interneurons is particularly large in supragranular layers, in which it represents the major interneuron population (Lee et al., 2010; Vucurovic et al., 2010). More interestingly, nearly all interneurons that do not express parvalbumin (PV) or somatostatin (SST) are 5-HT3AR expressing, suggesting that the CGE is the origin of most interneurons that do not express these markers (Butt et al., 2005; Cobos et al., 2006; Miyoshi et al., 2010; Nery et al., 2002; Xu et al., 2004). This includes the reelin-expressing late-spiking neurogliaform cells as well as bipolar/bitufted VIP-expressing cells. Using genetic fate mapping, the authors directly show the CGE origin of a majority of 5-HT3AR-expressing neurons and exclude the MGE as a source (Lee et al., 2010) (Schematic 1.4).

The mechanisms underlying the specification of CGE-derived interneurons are still poorly understood and the lack of any specific CGE master transcription factor still leaves a big “black box” in our understanding of the generation of such a molecular diversity of cortical GABAergic interneurons.

The preoptic area has been recently identified as a novel source of cortical intereurons and it shares with the MGE Nk2.1 expression; in contrast, many of the cells that emerge from this structure do not seem to express Lhx6, a feature that may distinguish POA- and MGE derived cells (Flames et al., 2007). Because Nkx2-1 is expressed by POA progenitors, it is conceivable that the analysis of the derivatives of *Nkx2-1-Cre* mice includes cells not only derived from the MGE but also from other structures that express this gene, such as the POA. To overcome this difficulty, a fate mapping study of a small population of cells from the POA, which exclusively express the transcription factor Nkx5-1 (not expressed in the MGE), has been performed. This study revealed that the POA is the origin of a small population of multipolar GABAergic cells with an electrophysiological profile of rapidly adapting interneurons (Gelman et al., 2009) (Schematic 1.5).

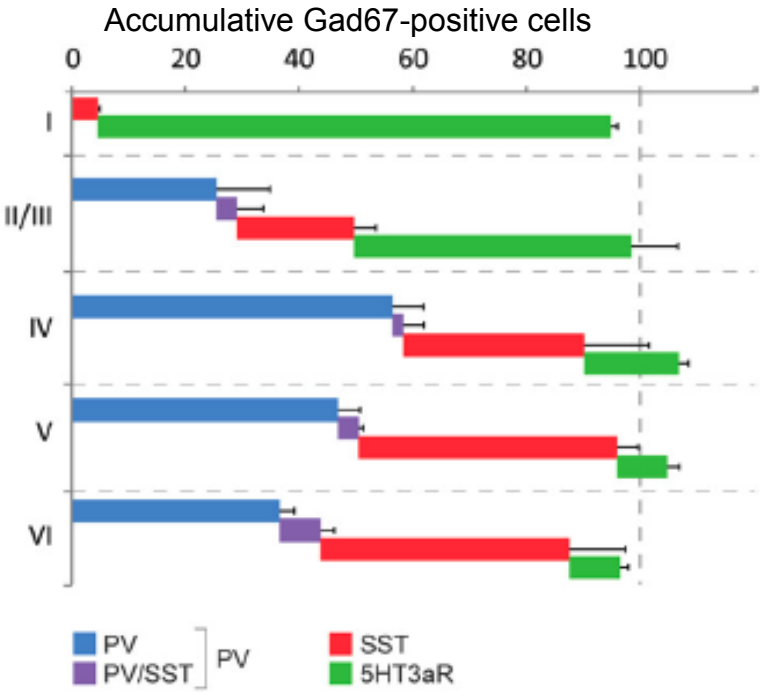

Schematic 1.4 Cumulative graphical representation of the percentage of *Gad67* cells expressing each interneuronal marker. Notably, 100 +/- 5% of interneurons of all layers can be accounted for using these three markers and that 5-HT3AR-expressing neurons predominantly occupy superficial layers. Notably we observed some overlap in the *in situ* signal between *SST* and *PV* even though this cannot be seen at the protein level. (Adapted from Lee et al., 2010)

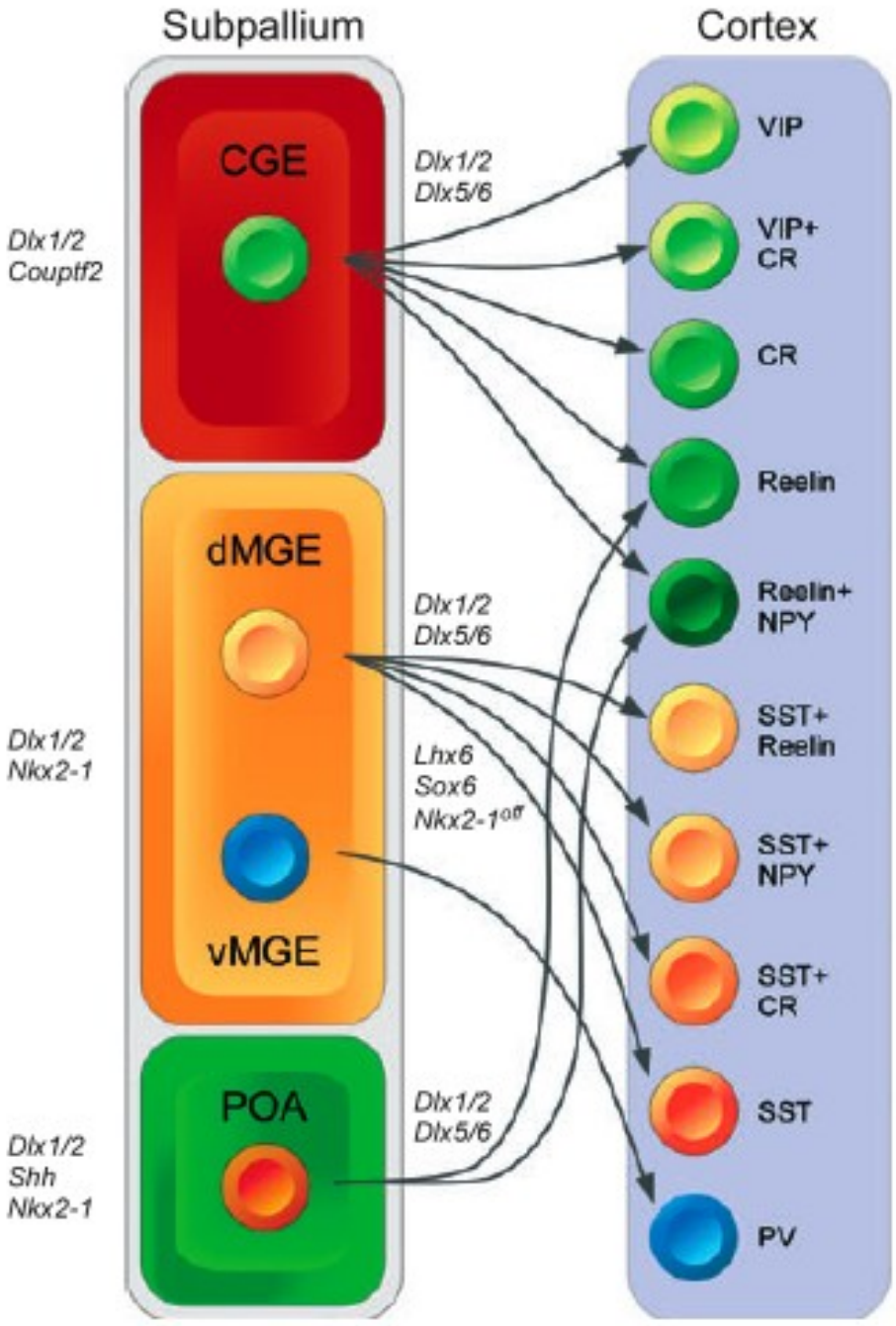

Schematic 1.5 Schamtic representation of the main sources of cortical interneurons, CGE, MGE and POA, which contain progenitor cells that can be distinguished by their expression of transcription factors and other proteins. CGE cells express both Dlx1 / 2 and Couptf2, MGE cells express Dlx1 / 2 and Nkx2-1, and POA cells express Dlx1 / 2, Nkx2-1 and Shh. Each progenitor region produces a particular group of interneurons, although some interneuron classes may emerge from different progenitor domains. This is the case for multipolar reelin / NPY-containing interneurons, which derive from both CGE and POA. It is possible, however, that these cells derive from a progenitor domain that bridges the two structures and that is characterized by the expression of Couptf2. (Adapted from Gelman and Marin, 2010).

Time of generation

MGE- and CGE- derived cortical interneurons are generated with different temporal profiles. While most of MGE-derived interneurons are born around E13.5, the generation of CGE-derived interneurons peaks at later ages (around E15.5) (Butt et al., 2005; Nery et al., 2002). It has long been recognized that, in general, cortical interneurons show the same inside-out pattern of generation that is observed in pyramidal cells (Anderson et al., 2002; Cavanagh and Parnavelas, 1989). Early-born MGE-derived interneurons end up in deep layers, while late-born interneurons occupy superficial layers of the mature cortex, and each cohort possesses unique electrophysiological properties characteristic of their birthdate (Miyoshi et al., 2007). These finding are confirmed by heterochronic transplants of progenitors demonstrating that the fate of transplanted cells is determined by the age of the donor and not the age of the recipient (Butt et al., 2005). Altogether, these evidences suggest that MGE progenitors have different potentials at different times during development, that influence the subtype of interneurons generated and the final location in the cortex.

However, recent genetic fate-mapping analysis, have recently shown that, contrary to the MGE, the subtypes of interneurons generated within the CGE does not significantly change over time. Furthermore, the birthdate of CGE neurons does not predict their cortical layer destination, unlike their MGE counterparts (Miyoshi et al., 2010). In fact, at least one subpopulations of CGE-derived cells, the CR interneurons, have an outside–in gradient of generation (Rymar and Sadikot, 2007), while VIP interneuron layer specificity does not appear to be correlated with their time of birth (Cavanagh and Parnavelas, 1989) (Schematic 1.6).

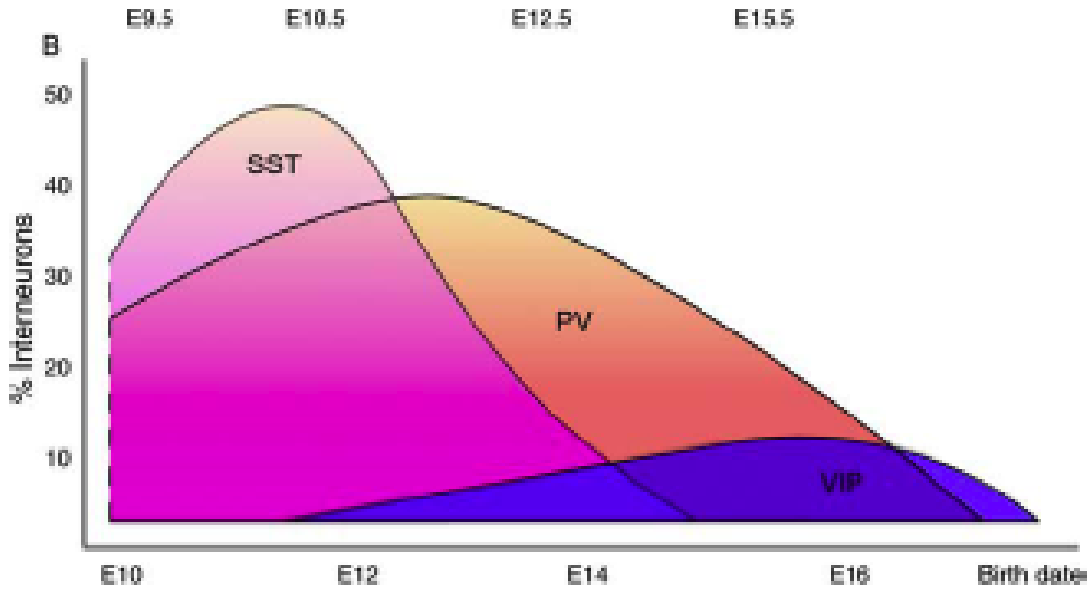

Schematic 1.6 Diagram of temporal origin of three subtypes of MGE interneurons, the somatostatin (SST—pink), the parvalbumin (PV—orange), and a subtype of CGE-derived interneuron (VIP—blue). (Adapted from Batista-Brito and Fishell, 2010)

Migration of interneurons: a long journey on the road

Cortical interneurons have a distinct and characteristic tangential mode of migration to enter the six-layered cortex (Corbin et al., 2001; Marin and Rubenstein, 2001). Tangentially migrating interneurons enter the cortical plate through two different migratory routes: a superficial path within the marginal zone (MZ); and a deep route positioned at the subplate/SVZ interface (Lavdas et al., 1999). The molecular cues guiding interneurons to each of these routes are currently unknown, as is whether there exist preferred routes for different interneuron subtypes. Tangential migration is mediated by a combination of molecular cues that function to both selectively repel and attract cortical interneuron populations (Marin and Rubenstein, 2003). This process is directly influenced by the guidance molecules themselves (e.g., Semaphorins, Slits, Neuregulin), playing key role in facilitating the journey of these interneurons. In fact, Neuregulin-1 (Nrg1), a molecule with widespread function in neural development, plays a major role in guiding the dorsal migration of interneuron precursors via the regulation of two different isoforms able to play distinct roles along the migratory path followed by interneurons. A membrane

bound isoform of Nrg1, which is permissive for interneuron migration, was found highly expressed throughout the LGE including the SVZ but not the VZ. Since the chemorepulsants Sema3A and 3F are expressed in the emerging striatum (Marin and Rubenstein, 2001), this may thus explain the corridor along the SVZ that is normally adopted by interneurons migrating across the LGE. A secreted isoform of Nrg1, on the other hand, was found not only highly expressed in the cortex but also chemo-attractive toward interneurons. This suggests that this isoform may play a role in long-range attraction of interneurons to the cortex. Indeed, mutations in Nrg1 or its receptor ErbB4 result in not only failure by interneurons to enter the LGE corridor but also reduced numbers of interneurons in the cortex (Flames et al., 2004).

The glial-derived neurotrophic factor (GDNF) is highly expressed along interneuron migratory pathways in the cortex and has been reported to be an important signal involved in guiding interneuron migration (Pozas and Ibanez, 2005). *In vitro* GDNF not only enhances the maturation and motility of interneurons but also acts as a strong chemo-attractant. Most importantly, in mutants of GDNF co-receptor GFRα1, interneurons were found misrouted in the MGE and significantly reduced in the cortex. Interestingly, the effects of GDNF appear to be independent of its two known transmembrane receptors, the RET tyrosine kinase and the neural cell adhesion molecule NCAM, suggesting involvement of novel GDNF transmembrane receptors. Nonetheless, these results strongly implicate GDNF as a key cortical player in attracting the dorsal migration of interneuron precursors. Together with the role of Nrg1 (Flames et al., 2004), these results thus indicate that Nrg1 and GDNF act in parallel as cortical chemo-attractants for interneurons, suggesting that multiple cortical signals are involved in guiding the dorsal migration of interneurons.

The responsiveness of migrating interneurons to these extrinsic cues is also regulated by subtype specific transcription factors. A clear example of this has been

elegantly reported for Nkx2.1, which has been demonstrated to be a negative regulator of semaphorin receptor Nrp2 (Nobrega-Pereira et al., 2008). As a result, the Sema3a (the repellent ligand for the Nrp2 receptor) expression in the striatum prevents cortical interneurons from invading this structure. By contrast, the persistent Nkx2.1 expression in interneurons destined for the striatum prevents Nrp2 expression in this population and as a result permits them to invade this region.

At the cellular level, migrating interneurons have been observed to develop branched leading processes that undergo complex morphological changes. Their centrosomes also go through large amplitude forward movements that are associated with centriole splitting (Bellion et al., 2005). These observations suggest potential new mechanisms of microtubules dynamics during interneuron migration. Indeed, recent findings showed that interneurons appear to rely on biased selection of leading process branches for changes in migration direction (Martini et al., 2009). Transcription factors have also been shown to control the intracellular machinery required for migration. Dlx1/2 compound double mutants have impaired cortical interneuron migration (Anderson et al., 1997) at least in part through their control of the p21-activated serine/threonine kinase PAK3, a downstream effector of the Rho family of GTPases (Cobos et al., 2006).

In addition, tangential migration of interneurons appears to be largely independent of cell autonomous requirement for Cdk5 or p35 (Gilmore and Herrup, 2001; Hammond et al., 2006; Hammond et al., 2004), although recent evidence indicates that p35 deficient interneurons show retarded migration in vitro, delayed cortical entry in vivo, and increased process branching that can be rescued by cell-autonomous p35 expression (Rakic et al., 2009). Nonetheless, there appear to be significant similarities between tangential and radial migration in that both include cyclical steps of leading process extension followed by nuclear translocation, suggesting substantial levels of regulatory conservation. Indeed, both Lis1 and Dcx have been found required for interneuron migration (Friocourt et al.,

2007; Kappeler et al., 2006).

Radial migration

After entering the cortex, interneurons shift to a radial mode of migration to invade cortical layers for integrating into the cortical circuitries (Ang et al., 2003; Polleux et al., 2002). Little is known about the mechanisms behind this switch in their mode of migration; however, the timing of this shift seems to be regulated by chemokines. Recent studies, in fact, found that the chemokine Cxcl12 (also known as stromal cell derived factor- SDF-1) plays a key role in this process (Li et al., 2008; Lopez-Bendito et al., 2008; Stumm et al., 2003; Tiveron et al., 2006). Cxcl12 is highly expressed along the streams of migrating interneurons in the MZ and SVZ by both the meninges and pyramidal cells, whereas its receptor Cxcr4 is expressed in interneurons (Stumm et al., 2003; Tiveron et al., 2006). It has been also reported that Cxcl12 soaked beads potently attract migrating interneurons and, interestingly, this attraction depends strongly on the age of interneurons. The beads are highly effective on embryonic interneurons but not on those from neonatal stages (Li et al., 2008). This change in Cxcl12 responsiveness coincides with the timing of radial invasion into the CP by interneurons, suggesting that these two processes may be linked. Indeed, the impairment of this signaling pathway due to either the absence of the chemokine (Cxcl12) or its receptor (Cxcr4) leads to abnormal entrance into the cortical plate by migrating interneurons, and subsequent abnormal interneuron lamination. Removal of Cxcr4 from interneurons after they have reached the MZ precipitated their premature entry into the CP. Constitutive deletion of Cxcr4 from interneurons, on the other hand, resulted in interneuron accumulation in the ventral pallium as well as disorganization of their migratory streams in the cortex, which led to interneuron laminar positioning defects in postnatal brains (Lopez-Bendito et al., 2008; Tiveron et al., 2006). These results thus argue that changes in Cxcl12 responsiveness are responsible for

controlling the timing of interneuron invasion of CP and a delayed entry is essential for their proper integration into the cortical circuitry. In line with these findings, it has recently been reported that interneurons only tend to invade the CP when confronted with relatively older CP tissues (2 days older), suggesting a role for cortical signals in determining the timing of interneuron invasion (Lopez-Bendito et al., 2008).

Remarkably, in the last issue of *Neuron*, while this thesis was in preparation, two independent studies revealed the critical role of the chemokine receptor Cxcr7 in interneuron migration (Sanchez-Alcaniz et al., 2011; Wang et al., 2011). Cxcr7 is required in migrating interneurons to regulate the levels of Cxcr4 receptors expressed by these cells, through a process that requires the interaction of migrating cells with the chemokine Cxcl12. Previous studies have suggested that the main function of Cxcr7 is to sequester Cxcl12 from undesirable locations, thereby contributing to dynamically shape the chemokine gradients for cell migration (Boldajipour et al., 2008). The expression of Cxcr7 in the early CP suggests that this receptor may play such a role in the developing cortex. Thus, Cxcr7 expression in the early CP may contribute to the organization of the routes of interneuron migration in the cortex, and the analysis of null mutants for Cxcr7 is consistent with this possibility. However, the similarity of the defects found in Cxcr7$^{-/-}$ and IN-Cxcr7 mutants suggest that the expression of Cxcr7 in migrating neurons is indispensable for normal migration. Thus, although the CP may play a role in buffering chemokines through the function of Cxcr7, these recent results demonstrate that this receptor is uniquely required for normal migration in cells that also express Cxcr4 receptors. Although, these newest finding greatly enhance our understanding of the molecular mechanism regulating the entrance by interneurons into the cortical plate, it is note worth that the chemokine signaling may have a strong regional bias, since the lamination defect observed in the Cxcr7 mutants is confined to the somatosensory area. This could either suggests that chemokine signaling might be particularly important to

prevent the concentration of interneurons in the first region they encounter when they enter the cortex, the developing parietal cortex; alternatively, other chemokines/molecules expressed in the developing brain may play additional roles in controlling the distribution of interneurons in other cortical regions.

Interneuron integration in the cortical circuitry

Several studies over the last twenty years (Miller, 1985; Miyoshi et al., 2007; Valcanis and Tan, 2003) have shown that cortical interneurons derived from the ganglionic eminences follow an inside-out pattern of layer integration within the cortex by approximately matching the birthdates of pyramidal cells within the same cortical lamina. Despite the fact that these two neuronal population are generated in different proliferative zones of the developing telencephalon and they follow different routes of migration, projection neurons and interneurons in fact ultimately coexist in the cortex, where they assemble into local microcircuitry. This clearly requires coordinated migration and development of these two broad neuronal populations.

The cellular and molecular events that direct interneurons to position precisely within specific cortical layers are much debated and poorly understood. It is although known that both cell intrinsic and cell extrinsic factors can influence the laminar positioning of cortical interneurons.

Indeed, correct cell-autonomous development of cortical interneurons is a critical factor for the radial positioning of GABAergic interneurons. Defective laminar distribution is observed in mutant mice that have abnormal interneuronal differentiation such as Nkx2.1, Lhx6 and Sox6 mutants, where the lack of specification of SST- and PV-expressing interneurons is observed (Alifragis et al., 2004; Azim et al., 2009; Batista-Brito and Fishell, 2009; Butt et al., 2008). More examples are provided by the analysis of Dlx1 and Dlx 5/6 null mice where, in concomitance of subtype-specific abnormal differentiation

defect, an impaired lamination of Gad67-expressing interneurons was observed (Cobos et al., 2006; Liodis et al., 2007; Wang et al., 2011).

In addition, recent findings reported that interneurons are cell-intrinsically programmed to sense extracellular GABA levels and arrest radial migration (Bortone and Polleux, 2009) by modulating the expression of the KCC2 co-transporter. During their journey towards the cortex, migrating interneurons change their responsiveness to ambient GABA from a motogenic to a stop signal. On the way to the cortex, ambient GABA and glutamate initially stimulate the motility of interneurons through both GABA(A) and AMPA/NMDA receptor activation. Once within the cortex, upregulation of the potassium-chloride cotransporter KCC2 is both necessary and sufficient to reduce interneuron motility through its ability to reduce membrane potential upon GABA(A) receptor activation. In the brain, intracellular chloride concentration is actively regulated by two transporters (NKCC1 and KCC2). NKCC1 imports Cl^- into the cell and is highly expressed in immature neurons. Conversely, KCC2, a Cl^- exporter, expression increases with neuronal maturation and in case of interneurons, at the moment when they stop migrating (Ben-Ari, 2002; Dzhala et al., 2005).

However, several lines of evidence indicate that the environment of the cortex also plays important roles in directing interneuron cortical distribution, pointing to a possible involvement of projection neurons in this process. For example, the preferential distribution of projection neurons and GABAergic interneurons synchronically generated suggests linked mechanisms of layer distribution (Fairen et al., 1986; Miller, 1985; Peduzzi, 1988; Pla et al., 2006; Valcanis and Tan, 2003).

Moreover, several independent studies have reported that interneurons distribute abnormally in the cortex of *reeler* and Dab1 mutant mice, in which projection neuron lamination is nearly inverted (Hammond et al., 2004; Hevner et al., 2004; Pla et al., 2006; Yabut et al., 2007). While it is unequivocally accepted that radial migration and laminar

arrangement of projection neurons depends on Reelin signaling, the dependence on Reelin signal by cortical interneurons is very debated (Hammond et al., 2004; Pla et al., 2006). Interestingly, it has been recently shown that interneurons invade the cortical plate and their target layers well after synchronically generated projection neurons reach their final destination (Lopez-Bendito et al., 2008). These results suggest a model in which cues provided by projection neurons guide cortical interneurons to their appropriate layer, and reveal that, at least for some neuronal types, long-range radial migration does not directly require Reelin.

Testing the validity of this hypothesis and understanding the contribution of cortical projection neurons to interneuron lamination represent the main question of the second part of my thesis project and it will be discussed in larger details in Chapter 3.

Same birthdate, different destination?

Once in the cortex, MGE- and CGE-derived interneurons born at the same time are able to invade the cortical plate simultaneously to show a similar layer distribution by postnatal day 1 (P1) (Miyoshi and Fishell, 2010). Only after this stage, each population sorts itself out into appropriate cortical layers. Furthermore, the critical time window for this postnatal sorting was found to occur several days earlier in the MGEderived population than the age-matched CGE cohort. This radial sorting period coincides well with the increase in potassium/chloride cotransporter KCC2 expression within each interneuron cohort.

This "birth date-matching" has been demonstrated for the majority of cortical interneurons, the MGE-derived population, that are normally generated around E12.5 and mainly populate the deep layers of the cortex. In contrast, cortical interneurons derived from the CGE consistently contribute ~75% of their population to the superficial layers and ~25% to deep layers, regardless of their birthdates (Miyoshi and Fishell, 2010). Thus,

for CGE-derived interneurons, the laminar positioning within the cortex is not strictly dictated by birth date. This feature raises a possibility that the inside-out layering of MGE-derived interneuron populations may just be correlative. Although the mechanisms remain still unknown, it appears very clear now that MGE- and CGE-derived interneurons clearly use different strategies to select their appropriate cortical laminae. Moreover, radial sorting of later born (E16.5) CGE-derived cohorts is found to take a similar time course as the E12.5 CGE-derived cohorts, suggesting that the final laminar location of interneurons is determined during the postnatal period in which they are sorted. We conclude that the selective sorting of interneurons within the early postnatal cortex is a crucial step for the assembly of mature neuronal networks. Moreover, the timing of their segregation into the appropriate cortical laminae is predicted by their region of origin and hence interneuron subtype rather than by their birthdate (Miyoshi and Fishell, 2010).

Thesis overview

The cellular and molecular events that determine unequivocally the "identity" of a certain interneuron type, its connectivity pattern, its cortical location, its firing activity, and ultimately its function in the cerebral circuitry, although intensively investigated, are still poorly understood. Thanks to many works that have been reported in the last few decades, the neurodevelopmental field has made terrific progresses in beginning to understand the intrinsic and extrinsic determinants responsible for the generation of such a variety of cortical interneurons. First, the discovery that cortical interneurons originate from different ventral progenitors residing in a distant germinal zone, and that they undergo a long and characteristic journey to reach, only perinatally, their final position in the cortical laminae, has opened a new chapter in the study of the cortical development (Anderson et al., 2001; Nery et al., 2002). Then, the findings that molecular and anatomical origins of cortical interneurons, together with their time of birth, contribute to the specification of different subtype of cortical interneurons, providing important information about their positions and/or their branching pattern, has also greatly improved our understanding at molecular level of the cellular diversity on the GABAergic system. Importantly, it has been proven that the cortical environment, through which the interneurons migrate, influences their journey and their final destination.

In my thesis project, I investigated different aspects of the development of cortical interneurons. Briefly, in the first part of my project, described in Chapter 2, I focused on the molecular specification of the CGE-derived cortical interneurons, so far poorly investigated, and I found that the transcription factor COUP-TFI is required for their proper differentiation during embryogenesis. In addition, I characterized the role of COUP-TFI in ensuring the balance between the MGE-derived and the CGE-derived interneurons in the cortex. This balance appears to be crucial for proper cortical activity, since electrophysiological analysis of conditional mutants lacking COUP-TFI selectively

in cortical interneurons, results in an epileptic-resistant phenotype. All together, the data provide a better understanding of the moleculat specification of CGE-derived interneurons and their function in the cortical circuitry.

In the second part of my project, described in Chapter 3, I investigated the role of the cortical projection neurons in influencing the final laminar positioning of the interneurons in the cortex. The investigation of the mechanisms that mediate the influence of projection neurons on interneuronal location has been notoriously complicated by the difficulties of uncoupling intrinsic defects of interneuronal fate specification, within the ventral telencephalon, from the environmental cortical components, making it a challenge to establish cause and effect in most of these animal models. Moreover, most *in vivo* models available have broad-spread defects in more then one type of projection neuron types, making the analysis of any interneuronal phenotype very confusing. To overcome these difficulties, I took advantage of the Fezf2 null mutant model that lacks specifically and uniquely the population of subcerebral projection neurons, substituted by another population of excitatory neurons, the callosal projection neurons (Chen et al., 2005a; Chen et al., 2008; Chen et al., 2005b; Molyneaux et al., 2005). The replacement occurs without an overall loss of projection neurons or changes in the total thickness of the cortex. Such a unique model allowed us to analyze the cortical distribution of inhibitory interneurons, that results abnormal in the *Fezf2*$^{-/-}$cortex, with a concomitant aberrant cortical activity due to defective GABAergic inhibition across layers. The defect is projection neuron type-specific, since the generation of other projection neurons (callosal projection neurons) in place of the missing subcerebral projection neurons cannot compensate for the observed interneuron abnormalities in the *Fezf2*$^{-/-}$ cortex. In addition, I found that specific subtypes of projection neurons are sufficient to recruit their own interneuronal partners to ectopic location below the cortex.

These data pointed, for the first time, at a crucial role for the projection neurons in

providing positional infomation to cortical interneurons, influencing the establishment of the ‘circuitry-pairing’ by an identity-mediated mechanism.

In Chapter 4, I discuss the results of my thesis and the impact that these findings have on our understanding of the molecular mechanisms of interneuron diversity and lamination during cortical development. Future work is necessary to identify the molecules controlling cell-cell interactions between projection neurons and interneurons, and determining the selected pairing within the cortical circuitry.

Chapter 2

The transcription factor COUP-TFI and the balance between CGE- and MGE-derived interneurons: implications in epilepsy

Author Contribuitions:

I performed this work as an equal collaboration with Giulio Srubek Tomassy and Elvira De Leonibus. With Giulio, we worked closely together and planned many of our experiments jointly. In general, I did the majority of the molecular analysis on the embryonic and adult COUP-TFI mutants. Giulio perfomed the statistical analysis of the cell counting and collaborated in the analysis of the cell cycle study. Elvira perfomed the whole pharmacological seizure induction study.

Publication:

This work is in press (accepted on January 19th 2011 in *Journal of Neuroscience*)
Lodato S.*, Srubek Tomassy' G.*, De Leonibus E.*, Uzcategui Y.G., Andolfi G., Armentano M., Touzot A., Gaztelu J.M., Arlotta P., Menendez de la Prida L.#, and Studer M#.
Loss of COUP-TFI alters the balance between CGE- and MGE-derived cortical interneurons and results in resistance to epilepsy

Preface

In this part of my project, I focus on the role of the transcription factor COUP-TFI in the specification of CGE-derived interneurons and their function in cortical development. In summary, I found that, during corticogenesis, COUP-TFI expression becomes gradually restricted to the caudal ventral telencephalon and that the conditional inactivation of COUP-TFI, selectively in cortical interneurons, leads to increased PV-expressing interneurons and decreased VIP- and CR-expressing bipolar neurons, without affecting the total number of GABAergic cells generated. Interestingly, COUP-TFI conditional embryos show increased cellular proliferation in the MGE as well as enhanced expression of the cell cycle gene cyclinD2, known to establish the proper density of PV-expressing interneurons within the cortex (Glickstein et al., 2007b). Strikingly, in collaboration with expert neurophysiologists, we found no distinct electroencephalographic (EEG) abnormalities, but, instead, *COUP-TFI* conditional mice are more resistant to pharmacologically induced seizures, a GABA-dependent property.

Taken together, the data indicate an intrinsic property of COUP-TFI in regulating the balance between MGE- and CGE-derived cortical interneurons, thus contributing to the proper formation of the cortical local inhibitory circuitry.

COUP-TF members and their roles in embryogenesis

Chicken ovalbumin upstream promoter-transcription-factors (COUP-TFs) belong to the steroid-thyroid hormone receptor superfamily of nuclear receptor proteins and they are one of the best-characterized orphan nuclear receptors (NR2F subgroup according to the nuclear receptor nomenclature, 1999) (Tsai and Tsai, 1997). This superfamily consists of many ligand-activated transcriptional regulators required in development, differentiation and homeostasis (Beato et al., 1995; Kastner et al., 1995; Mangelsdorf and Evans, 1995; Thummel, 1995; Tsai and O'Malley, 1994). A large number of these proteins are orphan

receptors whose ligands have yet to be identified (Giguere, 1999). The first member, human COUP-TFI, was discovered as a transcription factor that bound the COUP element, which regulates transcription of the ovalbumin gene (Pastorcic et al., 1986; Sagami et al., 1986; Tsai et al., 1987; Wang et al., 1989; Wang et al., 1987). Independently, hCOUP-TFI was cloned as v-ErbA related protein 3, EAR-3 (Miyajima et al., 1988), and subsequently a second human family member, hCOUP-TFII (Wang et al., 1991) was identified, which was also cloned as apolipoprotein regulating protein 1, ARP-1 (Ladias and Karathanasis, 1991). Through homology screening human COUP-TF homologs and orthologs have been obtained from numerous species, making the COUP-TF (NR2F) subgroup of orphan nuclear receptors the largest within the nuclear receptor superfamily (Laudet, 1997). Based on alignment of their putative ligand-binding domains (LBDs) vertebrate COUP-TFs can be subdivided into four groups (Tsai and Tsai, 1997). While most of the higher vertebrates, from human to chicken, contain genes encoding two COUP-TF subfamily members, zebrafish and *Xenopus* have three members, and insects and invertebrates such as *Drosophila*, C*aenorhabditis elegans* and the sea urchin contain only one member. Within a given subgroup, the homology in both the DNA binding domains (DBDs) and the putative LBDs is striking. The DNA Binding Domains of COUP-TFI or -II in different species are virtually identical, implying that they bind to a similar if not identical response element (Tsai and Tsai, 1997). Most surprisingly, the putative LBDs of COUP-TFI and -II are 99.6% identical among vertebrates and 90% between human and fly (Tsai and Tsai, 1997). Such a high degree of sequence conservation strongly suggests that these domains are critical for the biological function of COUP-TFs, although a ligand for COUP-TFs has not been identified. In contrast, the N-terminal domains of COUP-TFI and -II are significantly divergent, having only 45% identity; this may provide distinct functions for the two different members (Ladias and Karathanasis, 1991; Wang et al., 1991; Wang et al., 1989; Zhou et al., 1999). Based on this striking sequence conservation over the millions of

years of evolution, it is reasonable to speculate that COUP-TFs may play a vital role for cellular function. This hypothesis is supported by the finding that null mutants of *Drosophila svp* are lethal (Hoshizaki et al., 1994; Mlodzik et al., 1990) and by the fact that COUP-TFI and -II loss-of-function mouse mutants also lead to perinatal and embryonic lethality, respectively (Pereira et al., 1999; Qiu et al., 1997).

The patterns of COUP-TF expression have been described in the mouse, chick, zebrafish, frog, *C. elegans and Drosophila* (Pereira et al., 1995; Tsai and Tsai, 1997; Zhou and Walthall, 1998). It has been shown that COUP-TFI and -II exhibit overlapping, but distinct, expression patterns in all three germ layers during mouse development, with high expression of COUP-TFI in the nervous system and of COUP-TFII in the mesenchyme of internal organs (Pereira et al., 1995; Qiu et al., 1994a; Qiu et al., 1994b). Expression of COUP-TFI and -II is first detected postgastrulation at embryonic day 7.5 (E7.5) in the neural ectoderm, peaks between E10–12 (Qiu et al., 1997). The expression of COUP-TFs in the developing central nervous system (CNS) suggests a role in patterning and segmentation of the brain (Lutz et al., 1994; Qiu et al., 1994a; Qiu et al., 1997; Qiu et al., 1994b. In the peripheral nervous system (PNS), differential expression of the COUP-TFs is apparent in many developing regions in the brain. COUP-TFI is detected in premigratory and migratory neural crest cells (NCCs) at E8.5, whereas COUP-TFII is not {Qiu, 1997 #2153). In E13.5 mouse embryos, COUP-TFI and –II are detected throughout the developing telencephalon with specific gradient pattern and within the diencephalic neuromeres (CNS). Differential expressions of COUP-TFI and -II are also detected in other neuronal regions, including the midbrain and the spinal cord at midgestation. COUP-TFI is expressed throughout the neural tube, whereas COUP-TFII expression is restricted to the motor neurons (Qiu et al., 1994a). The differential COUP-TF expression patterns during mouse CNS development suggest that they may be required for neuronal development and differentiation.

In addition to neural ectoderm expression, COUP-TFs are also expressed in mesoderm and endoderm during organogenesis (Jonk et al., 1994; Pereira et al., 1995). COUP-TFII is expressed in the mesenchyme of the nasal septum, tongue, follicles of vibrissae and cochlea (Pereira et al., 1995) COUP-TFI is expressed in the same regions, but at a considerably higher level (Pereira et al., 1995). In contrast, COUP-TFII is expressed highly in the mesenchyme of the developing salivary gland, atrium, heart, lung, stomach, pancreas primordium, mesonephros, kidney and prostate, whereas COUP-TFI is expressed at a much lower level in these tissues (Pereira et al., 1995).

COUP-TFI function in the developing nervous system

Given the significant expression of COUP-TFs in the developing central and peripheral nervous system (CNS and PNS), both genes have been objects of intense studies, over several years, to identify their function in the development of specific structures of the brain. Analysis of the loss of function mutant mice has revealed central roles of COUP-TFI and -TFII in specific aspect of brain formation.

In COUP-TFI mutants, defects in the glossopharyngeal nerve impair both sensory and motor functions of the pharynx and the tongue and compromise feeding behavior, resulting in malnutrition, dehydration and usually perinatal death (Qiu et al., 1997). These phenotypes were consistent with the whole-mount *in situ* results for COUP-TFI transcripts, pointing that it is a marker of premigratory and migratory neural crest cells in the hindbrain. Some neural crest precursors of the IX cranial neurons underwent apoptosis prior to formation of the ganglion, resulting in an aberrant formation of the superior component of the IX ganglion. Aside from cranial nerve fusions, arborization of axons is severely reduced in the cervical plexus region as well as in the ophthalmic branch of the trigeminal nerve. This significantly limited axonal arborization in COUP-TFI mutants in comparison to control littermates contributed to the inability to feed, resulting in perinatal

death of mutants (Qiu et al., 1997). The limited arborization was not due to a delay in development, since the same phenotypes were seen at different somite stages. Both phenotypic changes in the mutants suggest that COUP-TFI may modulate axon guidance. Whether the observable defects arise from the lack of guidance cues, the inability to sense the cues or both is still to be defined.

Interestingly, the cortical cytoarchitecture of COUP-TFI mutants is defective. In fact, in the cerebral cortex of COUP-TFI null mice, cortical layer IV is absent, due to excessive cell death, a consequence of the failure of thalamocortical axons to project to their cortical targets. Moreover, subplate neurons undergo improper differentiation and premature cell death during corticogenesis, indicating that the subplate neuron defects lead to the failure of guidance and innervation of thalamocortical projections. Thus, the lack of proper thalamocortical afferent inputs resulted in layer IV neuron cell death, culminating in the apparent absence of layer IV in the COUP-TFI mutant cortex (Zhou et al., 1999). More recently, a conditional deletion of COUP-TFI in cortical progenitors showed a massive expansion of frontal areas, including motor area, to occupy most of the cerebral cortex, paralleled by marked compression of sensory areas to caudal occipital cortex. Strikingly, these area patterning changes are preceded and paralleled by corresponding changes in molecular markers of area identity and altered axonal projections to maintain patterned area-specific input and output connections. These results pointed at a novel role of COUP-TFI in balancing patterning of cerebral cortex into frontal/motor and sensory areas by repressing frontal/motor area identities and promoting sensory area identities (Armentano et al., 2007). These findings are supported by the low-rostral high-caudal gradient of COUP-TFI expression in the developing telencephalon. This particularly interesting expression profile, with different levels in presumptive sensory and motor cortices leaded the authors to assume that COUP-TFI might control sensory area formation by repressing a “motorizing” genetic program of differentiation in neurons of

the somatosensory cortex. Indeed, in the absence of COUP-TFI function, CSMN are born prematurely in somatosensory cortex, at a time when layer VI corticothalamic neurons are normally born. In contrast, layer V is expanded at the expense of layer VI, with a corresponding redistribution of neurons expressing CSMN specific genes and projecting to the spinal cord. In the context of an aberrantly expanded motor cortex and a corticospinal tract consisting largely of abnormally specified corticothalamic axons, adult COUP-TFI conditional mutant mice exhibit impaired fine motor skills, reinforcing the necessity for precision in both areal and temporal control of CSMN differentiation. These results enhanced our understanding of the role of COUP-TFI in controlling the emergence of the area-specific cytoarchitectural and functional features of sensory and motor cortical areas during corticogenesis, via specific areal and temporal repression of a CSMN differentiation program in corticofugal neurons of the somatosensory cortex (Tomassy et al., 2010a).

Based on the genetic manipulations of COUP-TFI expression pattern, a recent study has been conducted to investigate the mechanism through which COUP-TFI regulates areal patterning in respect of laminar fate and neurogenesis. By using loss- and gain-of-function manipulations, COUP-TFI has been found to promote cell cycle exit and neural differentiation, to regulate the balance of early- and late-born neurons, and regulate the balanced production of different types of layer V cortical projection neurons, by repressing Mapk/Erk, Akt, and b-catenin signaling (Faedo et al., 2008). Intimately related with these latter two studies, a recent work put in evidence the role of COUP-TFI and -II in controlling the timing of the switch of progenitor cells from neurogenesis to gliogenesis in the developing cortex (Naka et al., 2008a).

COUP-TFI has also been identified as a critical player in axonal growth in vivo during development. Fibers of the corpus callosum, the hippocampal commissure and the anterior commissure project aberrantly and fail to cross the midline in COUP-TFI null

mutants, indicating that COUP-TFI is intrinsically required for proper axonal growth and guidance of all major forebrain commissures; hippocampal neurons lacking COUP-TFI have also a defect in neurite outgrowth and show an abnormal axonal morphology (Armentano et al., 2006). Finally, in addition to its intrinsic role in axonal development, COUP-TFI has been shown to be required in axonal myelination, as demonstrated by its function in oligodendrocytes differentiation (Yamaguchi et al., 2004).

As far as the function of COUP-TFs in interneuronal development is concerned, very little is known. Only two reports so far have put in evidence the role of both receptors COUP-TFI and –II, with restricted expression in the CGE, in the caudal migration of cortical interneurons (Kanatani et al., 2008; Tripodi et al., 2004). In the first study, COUP-TFI and COUP-TFII expression was identified in migrating cells in specific pathways within the ventral telencephalon, including in cortical GABAergic interneurons. Moreover, ectopic expression of COUP-TFI and COUP-TFII in the ganglioni eminences resulted in an increased rate of migrating cells towards the cerebral cortex, suggesting novel functions of COUP-TFs in regulating cell migration in the developing forebrain (Tripodi et al., 2004). As far as concerned COUP-TFII, it has been shown that it is sufficient and required for the caudal migration of interneurons destined to the causal cortex and the hyppocampus, suggesting that COUP-TFII plays an important role in specifying the unique migratory behavior of CGE-derived cells (Kanatani et al., 2008).

Introduction

In rodents, interneurons are born in basal telencephalic structures, such as the medial (MGE) and the caudal (CGE) ganglionic eminences (GE) from which they migrate to populate the neocortex (Corbin et al., 2001; Marin and Rubenstein, 2001, 2003). Various transplantation and fate mapping experiments have shown that such a wide diversity is intimately dependent on their birth-date and location (Butt et al., 2005; Fogarty et al., 2007; Miyoshi et al., 2007; Miyoshi and Fishell, 2010; Miyoshi et al., 2010). Early-born interneurons originate from the MGE and produce mainly the PV- and somatostatin (SST)-expressing subtypes, which contribute primarily to deep cortical layers; late-born interneurons derive predominantly from the CGE, generate CR- and VIP-expressing interneurons and preferentially occupy superficial cortical layers.

Transcription factors expressed either broadly within the two eminences or predominantly in restricted domains of the ganglion eminences have been shown to play fundamental roles in the specification and maturation of these cells (Batista-Brito and Fishell, 2009). While loss of Dlx1/Dlx2 function results in a massive decrease of neocortical GABAergic interneurons at birth (Anderson et al., 1997), mice lacking only the *Dlx1* gene show reduction of CR- and SST-expressing interneurons without affecting the PV-expressing population (Cobos et al., 2005). These mice have cortical dysrhythmia and generalized seizures. Early removal of the transcription factor Nkx2.1, restricted to the MGE domain, results in a molecular and cellular switch of MGE-derived cortical interneurons (PV- and SST-positive subpopulations) to CGE-derived neurons (VIP- and CR-expressing cells), leading ultimately to seizure activities (Butt et al., 2008). Downstream of Nkx2.1, the transcription factors Lhx6 is involved in the specification and migration of PV- and SST-expressing interneurons (Liodis et al., 2007), whereas Sox6, acting downstream to Lhx6 (Batista-Brito and Fishell, 2009) as well, is required for the correct balance of PV-, SST- and NPY-expressing subpopulations (Azim et al., 2009;

Batista-Brito and Fishell, 2009). Loss-of-function of Sox6 results in a dramatic reduction of PV- and SST-expressing interneurons, whereas NPY+ interneurons outnumber the normal level without affecting the CGE-derived CR- and VIP- subpopulations. Interestingly, similarly to Dlx1 and Nkx2.1 mutant mice, Sox6 mutants suffer from generalized epileptic seizures (Batista-Brito and Fishell, 2009).

While many reports have characterized genetic determinants of MGE-derived cortical interneurons, little is known about the regional and cell-type specification of CGE-derived interneurons, which comprises around 30% of all cortical interneurons with an unexpected higher diversity than previously anticipated (Miyoshi and Fishell, 2010). The orphan nuclear receptors Chicken Ovalbumin Upstream Protein-Transcription Factors I and II are expressed in the basal ganglia (Kanatani et al., 2008; Willi-Monnerat et al., 2008) and required for the caudal migration of cortical interneurons (Kanatani et al., 2008; Tripodi et al., 2004). Moreover, in Nkx2.1 conditional mutant mice, where a high number of CR- and VIP-expressing cortical interneurons are generated, COUP-TFII is ectopically expressed in the MGE (Butt et al., 2008). Altogether, these reports strongly suggest that COUP-TF members might be directly involved in the migration and specification of CGE-derived cortical interneurons.

Material and Methods

Mice

COUP-TFI$^{flox/+}$ mice were generated as previously reported (Armentano et al., 2007), and propagated by backcrossing to C57BL/6 in bred mice. Homozygous *COUP-TFI*$^{flox/flox}$ mice were obtained by intercrossing heterozygous mice and mated to the *Dlx5/6-Cre-IRES-GFP* transgenic line (Stenman et al., 2003), a kind gift from K. Campbell (Children's Hospital Research Foundation, Cincinnati, Ohio), to generate conditional *COUP-TFI CKO-Dlx5/6* mice and embryos (*COUP-TFI*$^{flox/flox}$ homozygous-*Dlx5/6 Cre* heterozygous). We found no differences between males and females mutant mice. Homozygous *COUP-TFI*$^{flox/flox}$ mice and the *Dlx5/6-Cre-IRES-GFP* line have no phenotypic abnormalities, as previously described (Armentano et al., 2007; Stenman et al., 2003) and are used as control together with WT mice. Genotyping was performed as previously described (Armentano et al., 2007; Stenman et al., 2003). Midday of the day of the vaginal plug was embryonic day 0.5 (E0.5). All experiments were conducted following guidelines of the Institutional Animal Care and Use Committee, Cardarelli Hospital, Naples, Italy.

Immunocytochemistry and *in situ* hybridization

Mice were perfused with 4% buffered paraformaldehyde (PFA), and decapitated heads (E12.5-E14.5) or brains (P21) were post-fixed in 4% PFA for 12 to 24 hours at 4° C. Brains were either sectioned on a vibratome at 50 µm, or cryosectioned in OCT medium (Tissue-Tek) at 20 µm. Vibratome sections were processed free floating and standard non radioactive *in situ* hybridization and immunofluorescence protocols were used. *In situ* hybridization and combined immunohistochemistry were performed as previously described (Tripodi et al., 2004). The following primary antibodies were used: COUP-TFI (rabbit, 1:500) (Tripodi et al., 2004); BrdU (mouse, 1:300, Sigma); Ki67 (rat, 1:250,

Dako); GABA (rabbit, 1:1000, Sigma); NPY (rabbit, 1:3000, Diasorin); Calretinin (rabbit, 1:5000, SWANT); Parvalbumin (mouse, 1:1000, Millipore); Lhx6 (rabbit, 1:500, kind gift from V. Pachnis) and GFP (rabbit, 1:1000, Millipore). The following secondary antibodies were used: 1:400, Alexafluor 488 α-rabbit; Alexafluor 594 α-rabbit; Alexafluor 594 α-mouse (Molecular probes). Non-radioactive *in situ* hybridization on 16-20 μm thick cryostat sections were performed as previously described (Armentano et al., 2007). Antisense RNA probes were labeled using a DIG-RNA labeling kit (Roche). The following probes were used: *COUP-TFI*, *Gad67*, *SST*, *VIP*, *CyclinD2 and Nkx2.1*.

BrdU birthdating

Timed pregnant females received a single intraperitoneal injection of bromodeoxyuridine (BrdU) (50 mg/kg) one *hour* before sacrifice and embryos were collected at E13.5. A set of three WT and *COUP-TFI CKO-Dlx5/6* embryos were examined for BrdU-positive cell distribution in the MGE and CGE, as previously described (Tomassy et al., 2010a). Sections from the rostral, middle and caudal levels of the basal telencephalon were photographed at 10X magnification on a Leica DM5000B equipped with Leica IM image management software (Leica Microsystems, Wetzlar, Germany) and then imported into Adobe Photoshop for counting. The percentage of BrdU-positive was calculated as the ratio of double BrdU/DAPI-positive cells divided by the total of DAPI-positive cells.

Cell counting

For the quantification of interneuron subpopulations in *COUP-TFI CKO-Dlx5/6* and wild type cortices, three coronal anatomically matched sections within the sensorimotor area in the rostro-caudal axis (Bregma:0.50, -0.34 and) were selected from littermate mice and processed by immunocytochemistry to detect GABA, PV, NPY and CR, and *in situ* hybridization to detect *SST* and *VIP* transcript (n = 3 *COUP-TFI CKO-Dlx5/6*; n = 3 wild

type, 6 hemispheres per area, for each mouse at P21). Digital boxes of fixed width were superimposed on each coronal section and they were divided into ten sampling areas (bins) with a dorso-ventral extent from the *pial* surface to the white matter (corpus callosum). Deep layer were assigned to bin 1 to 5 and upper layers were assigned to bin 6 to 10, based on anatomical features. Cell detection and counting was performed using a customized imaging processing software. The automated algorithm has been developed in Matlab (version 7.6, The MathWorks, Inc., Natick, MA, USA) by an investigator blinded to the study design and consisted in a series of processing steps. In the first one, original fluorescent or bright-field images, taken at 4X magnification, are corrected for uneven illumination and background noise. Image segmentation is then obtained through edge detection, in which minimum and maximum levels of the intensity gradient are established *a priori* for each staining analyzed and kept constant throughout the counting analysis. Then, morphological characteristics were added to the filtering process. The eccentricity parameter –where 1 indicates a linear shape and 0 a circular shape- was used to identify cell bodies, by using a threshold values established *a priori*. In combination with the eccentricity parameter, thresholds for the cell size were established *a priori* based on the normal distribution of cell area for each staining analyzed. In addition, the area parameter was used to discriminate single cells within clusters. For the quantification of the percentage of interneuron subtypes that express COUP-TFI in P8 and P21 wild type cortices, three coronal sections spanning within the somatosensory area in the rostro-caudal axis (Bregma: -0.34) were selected from littermate mice (n=3, 6 hemispheres per area, for each wild type mouse at P8 and P21). Digital boxes of fixed width were superimposed on each coronal section and cell counting was performed on images taken at 10X magnification by an investigator blinded to the study design. Counting criteria were established *a priori*.

Data analysis

All cell counting data and the graphs were constructed using Microsoft Excel software. For each animal a mean value was calculated from all the sections counted, and for each genotype a mean value was obtained by pooling the means of the three sampled animals. EEG data was analyzed using the Mann-Whitney U test for comparison of the power spectra between groups and an ANOVA or a Kruskal-Wallis test for comparison of the four different frequency bands between group and gender (see the EEG section in Methods). All behavioral pharmacological data were analyzed using either one-way ANOVA (genotype, 2 levels: WT and CKO) or two-way ANOVA [genotype (2 levels: WT and CKO) and pre-treatment (2 levels: vehicle and CGP 35348)]. Post-hoc analysis was performed using Duncan post-hoc test. All error bars represent the standard error of the mean (s.e.m.). Statistical significance was determined using two-tailed Student's *t*-tests. *$p<0.05$, **$p<0.01$.

Electroencephalographic recordings

Freely moving mice aged between 7 and 13 weeks were tested for spontaneous EEG activity. Animals were anesthetized with ketamine (100 mg/kg) and xylaxine (10 mg/kg i.p.) and placed in a stereotaxic apparatus. Cortical EEG recordings were obtained from 100 μm-wide tungsten wires implanted over the parietal cortex at 0.2-0.4 mm depth from the cortical surface using bone cement. Two screws were used to serve as a reference and ground at the occipital region. In a group of animals, two wires were bilaterally implanted in the dorsal hippocampus in order to obtain simultaneous cortical and hippocampal EEG activity. After recovering from surgery, EEG was recorded from individual mice over several days, for a maximum of 2 h per day, by using a Grass EEG Neurodata system. Total recording time per mouse ranged from 18 to 36 hours over the course of 12 to 20 days. Animals were simultaneously video-taped for identifying different behavioural

states. EEG recordings during awaken states were band-pass FIR filtered between 1 and 200 Hz and sampled at 500 Hz. After completing EEG recordings brains were fixed in 4% paraformaldehyde for electrode placement verification.

EEG data was analyzed with Spike 2 and routines developed in Matlab. The spectral power was calculated using the fast Fourier transform with Hamming window and 1024 points for artefact-free recording windows of 10 minutes duration. In order to study the frequency content independently of amplitude changes, each EEG spectrum was normalized by the total power in the 1-100 Hz band. The mean power spectrum for each group is represented together with the 95% confidence intervals. To look at spectral differences between types of oscillations four different frequency bands were defined: 1-4 Hz (delta), 4-10 Hz (theta), 10-40 Hz (beta) and 40-100 Hz (gamma). The power spectrum value for each band was calculated by integrating the normalized power spectrum in the corresponding frequency interval. For statistical comparisons, we first tested data for normal distribution using the Kolmogorov-Smirnov test. Power spectral values in a logarithmic scale were normally distributed except for the 40-100 Hz gamma band. Thus, to quantify statistical differences, spectra from the two experimental groups were compared using a non-parametric test for multiple comparisons (Mann-Whitney U test). To compare the spectral distribution at the delta, theta and beta bands, a two-way ANOVA was used with the factors group and gender. Differences in the gamma band were compared using the Kruskal-Wallis non-parametric test for the group and for the gender independently.

Pharmacological seizure induction

For pilocarpine-induced seizures, mice were i.p. injected with lithium chloride (423 mg/kg) between 18-20 hours before 100 mg/kg of pilocarpine hydrochloride.

Pentylenetetrazol (PTZ, Sigma) was administered s.c. at a dose of 90 mg/kg. We chose a supra-threshold dose of PTZ to induce clonic seizures independently on the gender and with uniform latency within groups (Loscher et al., 1991). In a group of PTZ experiments we pre-treated mice with the GABAb-receptor antagonist (3-aminopropyl)(diethoxymethyl)-phosphinic acid hydrate- GCP 35348 (Sigma). Mice injected with PTZ and not pre-treated with GCP 35348, were divided in two groups half not injected and half injected with vehicle. Animals were observed for 45 min after the PTZ injection. Three different stages of seizure activity were scored: stage 1: body and tail rigidity; stage 2: characterized by whole-body clonus; and stage 3: characterized by generalized tonic-clonic hindlimb extensions.

Results

COUP-TFI is preferentially expressed in the dorsal MGE, in the CGE and in a subpopulation of mature cortical interneurons

To investigate the function of COUP-TFI in the development of GABAergic interneurons, we first characterized its expression profile in the developing ganglionic eminences on coronal sections. From E10.5 to E12.5 COUP-TFI is expressed in the subpallium, and within the lateral ganglionic eminence (LGE) and MGE, respectively, in progenitor and precursor cells (Armentano et al., 2007; Faedo et al., 2008) (Fig. 2.1*A*). However, at E13.5 COUP-TFI expression becomes highly regionalized with a low rostral to high caudal expression gradient (Fig. 2.1*B-D*). In more rostral coronal sections, COUP-TFI expression is restricted to the corticostriatal boundary and the dorsal MGE (dMGE) (Fig. 2.1*B*). In intermediate regions COUP-TFI is expressed at high levels in the caudal/dorsal part of the MGE and at low levels in the caudal LGE (Fig. 2.1*C*). Interestingly, expression levels of COUP-TFI are highest in the caudalmost basal telencephalon, particularly in the ventricular (VZ) and subventricular zone (SVZ) of the ventral (v)CGE, while in the LGE and dorsal (d)CGE expression of COUP-TFI is lower (Fig. 2.1*D*). Thus, we found that at E13.5 COUP-TFI becomes restricted in a rostral to caudal and dorsal to ventral expression gradient in the basal telencephalon, being strongest in the VZ and SVZ of the ventrocaudal ganglionic eminence, the vCGE.

As previously reported by a study conducted in our laboratory, COUP-TFI is also expressed in immature interneurons migrating tangentially from the basal telencephalon to the developing neocortex (Tripodi et al., 2004); then, we decided to investigate its expression in mature cortical interneuron subtypes at post-natal stages (Fig. 2.1*E-J'''*). Double labeling for COUP-TFI protein and the glutamate decarboxylase *GAD67* transcript shows a high proportion of postnatal GABAergic interneurons positive for COUP-TFI in the somatosensory cortex (83.1±2.2%, n=3, average ± SEM, P8) (Fig. 2.1*E, E'*). To

further address whether specific subtypes of cortical interneurons express COUP-TFI, we performed double labeling for COUP-TFI and different molecular markers of mature cortical interneurons including the peptide hormone somatostatin (*SST*), the neurotransmitter peptide Y (NPY), the vasoactive intestinal peptide (*VIP*) at P8, (n=3) (Fig. 2.1*F-H'*), as well as the calcium-binding proteins calretinin (CR) and parvalbumin (PV) at P21 (n=3) (Fig. 2.1*I-J'''*) within the somatosensory cortex. At P8, COUP-TFI was found in 55.8±1.1% of *SST*-expressing, in about 70.0±2.1% of NPY-expressing and in 78.1±5.4% of *VIP*-expressing interneurons (Fig. 2.1F-H'). At P21, we found only a 4.0±0.3% overlapping between COUP-TFI and PV, and 51.6±5.3% co-labeling between COUP-TFI and CR (Fig. 2.1*I-J'''*). However, detailed morphological analysis indicates that COUP-TFI is highly expressed (89.2±5.9%) in a subpopulation of CR+ cells that shows a characteristic vertically oriented bipolar morphology (Fig. 2.1*I'-I'''*). Taken together, these data indicate that at post-natal stages COUP-TFI is expressed in most mature cortical interneuron subtypes, with a preference to CGE-derived interneurons, such as bipolar VIP+ and CR+ cells, and to a subpopulation of NPY+ cells (Karagiannis et al., 2009), while it is generally excluded from the early-born MGE-derived PV-expressing cells.

Specific inactivation of COUP-TFI in SVZ intermediate progenitors of the basal telencephalon

To investigate the role of COUP-TFI in interneuron diversity and in the maturation and specification of different cortical interneuron subtypes, we took advantage of a conditional genetic approach in which the *COUP-TFI lox/lox* (*COUP-TFI*^{flox}) mouse (Armentano et al., 2007) was mated to the *Dlx5/6-Cre-IRES-GFP* transgenic line (Stenman et al., 2003), making the CRE activity exclusively within the basal telencephalic SVZ and MZ (Fig.

2.2*A*). Mice homozygous for *COUP-TFI*^{flox} and heterozygous for *Dlx5/6-Cre-IRES-GFP* are viable and fertile, and will be named *COUP-TFI CKO-Dlx5/6* throughout this study.

Before starting the phenotypical analysis of the generated mutants, we first validated the quality of the designed approach by assessing whether and at what age COUP-TFI was specifically inactivated in Dlx5/6-positive cells. By taking advantage of the endogenous GFP fluorescence of the *Dlx5/6-Cre-IRES-GFP* transgenic line (Stenman et al., 2003), we could follow the destiny of the cells in which the recombination occurred. In the basal telencephalon of *COUP-TFI CKO-Dlx5/6* heterozygotes, in fact, only SVZ progenitors are double positive for GFP and COUP-TFI (Fig. 2.2*E, H*), whereas VZ progenitors express COUP-TFI (labeled in red) but not GFP (labeled in green) (Fig. 2.2*C*, *F, D, G*). No, or very few COUP-TFI/GFP double-positive cells were detected in the SVZ or mantle zone of *COUP-TFI CKO-Dlx5/6* homozygous embryos at E12.5 and E13.5 (Fig. 2.2*E',H'*). This indicates that, already at E12.5, before COUP-TFI becomes regionalized to dMGE and CGE, COUP-TFI function is specifically abolished in SVZ (Dlx5/6-positive domains), but not in progenitors located in the VZ (Dlx5/6-negative domain). Accordingly, at E15.5 COUP-TFI fails to be expressed in post-mitotic neurons of the basal telencephalon (Fig. 2.2*I-J'*), with the exception of the ventrally migrating stream originating from the Dlx5/6 negative IGS region, which co-express COUP-TFI and COUP-TFII (Tripodi et al., 2004). Thus, we generated an efficient conditional COUP-TFI mutant line, in which COUP-TFI is specifically inactivated within the ventral telencephalon, exclusively in SVZ progenitors and post-mitotic interneurons, but not in VZ progenitors.

Conditional loss of COUP-TFI function alters the balance of interneuron subtypes without affecting the total number of GABAergic cortical interneurons

To unravel the role of COUP-TFI in the specification of interneuron subtypes, we investigated whether loss-of-function of COUP-TFI in SVZ progenitors of the basal telencephalon would affect the total number and laminar distribution of interneurons in P21 *COUP-TFI CKO-Dlx5/6* brains compared to WT littermates. Interestingly, when we performed immunofluorescence for GABA (gamma-amminobutirric acid), the specific neurotransmitter of the inhibitory interneurons, we found no difference in the overall number of cortical interneurons in *COUP-TFI* mutant sensorimotor cortices (Fig. 2.3*A, A', G*; p=0.79; n=3), and no difference in the distribution of GABA-positive cells along the cortical wall (Fig. 2.3*H*). Next, we evaluated the total and radial distribution of distinct cortical interneuron subtypes by performing immunostaining and *in situ* hybridization using subtype-defining molecular markers for distinct GABAergic interneuron subpopulations (Ascoli et al., 2008) in P21 WT and *COUP-TFI CKO-Dlx5/6* cortices (Fig. 2.3*B-F'*). As previously reported, PV+ and SST+ interneurons are two MGE early-born subclasses predominantly located in deep layers, whereas VIP+ cells are primarily CGE late-born interneurons located in superficial layers (Butt et al., 2005; Miyoshi et al., 2007; Miyoshi and Fishell; Miyoshi et al., 2010; Wonders and Anderson, 2006). By contrast, CR+ and NPY+ interneurons derive from both the MGE and the CGE and are distributed along the radial extent of the cortex, although bipolar CR+ cells are predominantly located in superficial layers (Caputi et al., 2009; Fogarty et al., 2007; Xu et al., 2004).

Interestingly, we found that loss of COUP-TFI function affects the specification of PV+ interneurons and the VIP+ and CR+ bipolar subpopulations in opposite ways (Fig. 2-3*I*). While the number of PV+ interneurons was increased significantly by 33% (Fig. 2.3*B, B', I*; p=0.0004; n=3), the total number of bipolar CR+ and VIP+ interneurons was decreased significantly by 21% (Fig. 2.3*E, E', I*; p=0.007; n=3) and by 26% (Fig. 2.3*F, F',*

I; p=0.03; n=3), respectively. Conversely, there was no significant change in the total number of SST+ (Fig. 2.3*C, C', I*; p=0.09; n=3) and NPY+ (Fig. 2.3*D, D', I*; p=0.19; n=3) subpopulations, although the number of NPY+ interneurons increased by 25% in deep layers of *COUP-TFI CKO-Dlx5/6* cortices (Fig. 2.3*J*; p=0.0028; n=3). Differences in layer distribution were also detected in the MGE-derived PV+ population, which was strikingly increased by more than 50% in deep layers (Fig. 2.3*J*; p<0.0001; n=3), but not affected in superficial layers (Fig. 2-3*K*; p=0.98) of *COUP-TFI CKO-Dlx5/6* mice. Regarding the CGE-derived subpopulations, the number of VIP-expressing cells was reduced significantly in all layers (36% reduction in deep layers, p=0.02; and 22% in superficial layers, p=0.04; n=3; Fig. 2.3*F, F', I*), whereas the number of CR-expressing cells was decreased by 27% in superficial layers (Fig. 2.3*K*; p=0.0034; n=3), but not altered in deep layers (Fig. 2.3*J*; p=0.57; n=3). Detailed morphological characterization of the CR+ subpopulation demonstrated a 25% decrease (Fig. 2.3*L*; p=0.007; n=3) of bipolar-shaped cells, strongly indicating that the CR+ cohort altered in *COUP-TFI CKO-Dlx5/6* mice was mainly composed by bipolar CR+ cells (Caputi et al., 2009).

Taken together these results indicate that loss of COUP-TFI function alters the balance between PV+ (MGE-derived) and bipolar VIP+, CR+ (CGE-derived) interneuron subpopulations, without affecting the overall cortical interneuron number.

COUP-TFI does not act on cell identity but regulates cell cycle divisions of SVZ precursors in the basal telencephalon

Different mechanisms can motivate an increase of MGE-derived PV+ interneurons at the expense of CGE-derived CR+ and VIP+ interneurons. One possibility could be a molecular switch between MGE and CGE identity. To test the validity of this first hypothesis, we first investigated whether developmental regulators of MGE interneuron cell fate were abnormally expressed in *COUP-TFI CKO-Dlx5/6* embryos. We looked at

the expression of *Nkx2.1*, known to determine the identity of progenitor cells in the MGE (Butt et al., 2008; Nobrega-Pereira et al., 2008; Sussel et al., 1999), and its downstream target Lhx6 (Du et al., 2008), which starts to be expressed as soon as MGE-derived progenitors leave the VZ (Liodis et al., 2007). No obvious changes in the expression pattern of Nkx2.1 and Lhx6 at rostral and caudal levels were observed in E13.5 *COUP-TFI CKO-Dlx5/6* embryos (Fig. 2.4*A-D'*), indicating that loss of COUP-TFI in the SVZ does not induce a molecular fate change between CGE- and MGE-derived interneurons.

An alternative mechanism, among others, that could possibly lead to an increase number of MGE-derived PV+ interneurons at the expense of CGE-derived CR+ and VIP+ interneurons is an imbalance rate of proliferation/differentiation between MGE- and CGE-derived cortical interneurons.

To assess whether inactivation of COUP-TFI would have an effect on cell cycle divisions, similarly to what observed in the neocortex (Faedo et al., 2008; Tomassy et al., 2010a), we performed acute injection of BrdU in pregnant females and compared the percentage of BrdU-positive cells in the MGE and CGE of WT and E13.5 *COUP-TFI CKO-Dlx5/6* embryos (Fig. 2.4E-*F'*). Strikingly, the ratio of proliferating (BrdU+) cells was significantly higher in the MGE, but not in the CGE (Fig. 2.4*G; WT:* MGE, 25.7±2.2%; CGE, 30.2±2.0%; *CKO:* MGE, 47.8±3.9%; CGE, 45.0±4.2%; p value(MGE)=0.04; p value(CGE)=0.097). Similar results were obtained after immunofluorescence of the proliferation marker Ki67, in which the thickness of the Ki67-positive region, with respect to the total ventricular to pial thickness of the basal telencephalon, results larger in the MGE than CGE of mutant embryos (Fig. 2.4*I*; *WT:* MGE, 0.34±0.04; CGE, 0.27±0.02; *CKO:* MGE, 0.47±0; CGE, 0.34±0.02; p(MGE)=0.03; p(CGE)= 0.07). Thus, increased proliferation, particularly in the MGE region, was detected in *COUP-TFI CKO-Dlx5/6* embryos. To further investigate whether cell cycle progression was affected in the absence of COUP-TFI in cortical interneurons, we

assessed the expression of the G1-active cell cycle protein cyclinD2, known to promote SVZ divisions in the telencephalon (Glickstein et al., 2007b). Strikingly, expression of *cyclinD2* is clearly increased in SVZ progenitors of E13.5 and E15.5 *COUP-TFI CKO-Dlx5/6* embryos predominantly at rostral levels (Fig. 2.4*J-K'*). Since COUP-TFI is maintained in VZ progenitors of mutant embryos, we found accordingly no differences in the expression of cyclinD1 (not shown) (Glickstein et al., 2007b).

Altogether, these data strongly suggest that COUP-TFI regulates cell cycle progression by modulating divisions of SVZ interneuron precursors without affecting the identity of MGE determinant genes.

Basal EEG recordings show no apparent abnormalities in mutant mice

Since previous reports have shown that altered balance of interneuronal subtypes correlate with epileptic phenotypes and disruption of cortical EEG rhythms (Batista-Brito and Fishell, 2009; Butt et al., 2008; Cobos et al., 2005; Glickstein et al., 2007; Powell et al., 2003), we decided to investigate the basal activity of the *COUP-TFI CKO-Dlx5/6* mice in collaboration with the help of expert neurophysiologist Dr. Mendez de La Prida at Cajal Institute in Madrid. Therefore, we chose to obtain long lasting recordings of basal EEG activity from adult WT (n=6) and *COUP-TFI CKO-Dlx5/6* mice (n=8). Cortical EEGs from awaken WT mice were characterized by rhythmic activity at 3-7Hz interspersed by episodes of beta activity at 15-20Hz (Fig. 2.5*A*). Strikingly, *COUP-TFI CKO-Dlx5/6* mice showed roughly similar EEG patterns compared with WT (Fig. 2.5*B*). Seizures, and other types of epileptic-like activity, were never observed in mutants and no statistical difference was evident from the normalized mean power spectra from both groups at $p=0.05$ (Fig. 2.5*C*). In a group of mice (n=6 WT, n=10 *CKO*), we obtained simultaneous cortical and hippocampal EEG recordings to check for signs of ictal activity confined to the hippocampus with little cortical manifestation. Again, we did not observe signs of

hyperexcitability in the hippocampus of *CKO* mice, discarding the possibility of non-convulsive subclinical seizures in these animals.

We also looked for differences in the typical frequency bands of the EEG spectrum, i.e. 1-4 Hz (delta), 4-10 Hz (theta), 10-40 Hz (beta) and 40-100 Hz (gamma) (*Fig.2.5D*). We found no difference between groups using a two-way ANOVA comparison for the delta ($F=1.45$, $p=0.25$), theta ($F=0.78$, $p=0.39$) and beta bands ($F=0.26$, $p=0.62$) and the Kruskal-Wallis test for the gamma band ($U=25$, $p=0.49$). Finally, we checked for a possible functional compensation, that is taking place in COUP-TFI mutants as reflected in an age dependence of the cortical EEG activity. We found no correlation with age of the cortical EEG power in the different frequency bands over the course of 40 to 90 days postnatal, neither difference with one-year-old mice in both groups (*Fig. 2.5E*). Furthermore, no gender differences were present. Thus, alterations in the distribution of PV+, VIP+ and CR+ interneuron subpopulations result in no obvious abnormalities in the gross cortical EEG of *COUP-TFI* mutant mice.

COUP-TFI mutants are more resistant to seizures induced by lithium-pilocarpine

The absence of abnormalities in the gross cortical EEG in our mutants suggests that reduced number of VIP+ and CR+ cortical interneurons has no discernible effect on the basal cortical activity of COUP-TFI mutants. This was surprising because a similar reduction, observed in the Dlx1 mutant mice, in the presence of normal numbers of PV+ interneurons results in dysrhythmia and epilepsy (Cobos et al., 2005). We thus reasoned that the increase of PV+, and possibly NPY+ interneurons, observed in our mutants might be functionally compensating the reduction of CGE-derived interneuronal subtypes.

To test this hypothesis, in collaboration with Dr. Mendez de La Prida and Dr. De Leonibus, expert neuropharmachologist and behavioralist, we used the muscarinic receptor agonist pilocarpine to unspecifically increase the excitatory level at doses of 100mg/kg

that induce tonic-clonic seizures and *status epilepticus* in wild-type mice (Groticke et al., 2007). We found that *COUP-TFI CKO-Dlx5/6* mice (n=7) were more resistant to seizures and to develop *status epilepticus* than WT (n=7), as reflected in both the cortical EEG recordings and clinical manifestations (Fig. 2.6*A, B*). Progression to the *status* was characterized by the early appearance of body and tail rigidity, and multiple spikes in the cortical EEG between 2-3 minutes after pilocarpine injection (Fig. 2.6*A, B*). There was no significant difference between groups in the latency to the first EEG spikes (Fig. 2.6*C*). This was followed by whole-body clonic spasms and secondary generalized tonic-clonic seizures with forelimb automatisms, which were associated with ictal EEG patterns. The mean latency to the first electroclinical manifestation of a tonic-clonic seizure was 39.9±6.9 min in mutants versus 14.9±1.6 min in WT animals (Fig. 2-7*C*; F1/12=12.48; p=0.004). Similarly, the onset of the *status epilepticus*, defined from EEG recordings (Fig. 2.6*A, B*), was significantly delayed in *COUP-TFI CKO-Dlx5/6* versus WT mice (Fig. 2-7*C*; CKO, 50.4±6.9 min versus WT, 22.8±3.3 min; F1/12=13.17; p=0.003). Together, these data indicate that *COUP-TFI CKO-Dlx5/6* mice are more resistant to seizures induced by pilocarpine, probably reflecting a functional effect of the increased number of PV-, and eventually, NPY-expressing interneurons in counteracting a decreased number of VIP- and CR-positive neurons.

Seizure resistance in mutant mice is mediated by GABAa- and GABAb- signaling

To further confirm that the seizure-resistance character of these mice was GABA-dependent, we used pentylenetetrazole (PTZ) at 90 mg/kg, a GABAa-receptor antagonist that is widely used for testing seizure susceptibility in mice (Powell et al., 2003). Similarly to pilocarpine, we found an early appearance of body and tail rigidity in both WT (n=22) and *COUP-TFI CKO-Dlx5/6* (n=12) mice and a larger latency of *COUP-TFI*

mutants to the first tonic-clonic seizure (Fig. 2.6*D*; WT: 24 ± 2.7 min versus CKO: 38 ± 3.3 min; F1/32=9.59; p=0.004).

Altogether, this indicates that *COUP-TFI CKO-Dlx5/6* brains are less excitable than WT brains to produce seizures induced by the cholinomimetic convulsant pilocarpine and the GABAa-antagonist pentyneletetrazol. However, latency difference to tonic-clonic seizures can be accounted by other mechanisms, like a different excitability level at the glutamatergic circuits or residual pre- and post-synaptic GABAb-receptor mediated inhibition after PTZ injection. To ascertain that the seizure-resistant character of these mice are indeed GABA-dependent, we pre-injected WT (n=7) and mutant animals (n=8) with the GABAb-receptor antagonist CGP 35348 at the non-convulsive dose of 136 mg/kg i.p. (Karlsson et al., 1992) 30min before PTZ (Fig. 2.6*D*). CGP pre-treatment significantly [genotype (F1/45=1.96; p=0.168); pre-treatment (F1/45=20.773; p<0.0001); genotype x pre-treatment (F1/45=6.93; p=0.01)] reduced the latency to the first tonic-clonic seizure in *COUP-TFI CKO-Dlx5/6* mice (CGP 35348 versus vehicle pre-treated p<0.0001) and eliminated latency difference with the WT group (p=0.38; Fig. 2.6*D*).

Thus, these data indicate that blockage of GABAb-receptor abolishes resistance to seizures induced by the GABAa-receptor antagonist PTZ, and confirm that the seizure-resistant phenotype observed in *COUP-TFI CKO-Dlx5/6* mice is dependent on an altered balance of MGE- versus CGE-derived interneurons acting through both GABAa and GABAb receptors.

Discussion

Until recently, the CGE was not considered a distinct anatomical and molecular entity, mainly due to the absence of a morphologically definite sulcus demarcating the CGE from the MGE and LGE, and to the lack of CGE-restricted molecular markers (Flames et al., 2007). However, a series of experimental evidence including *in vivo* transplantation studies, *in vitro* migratory assays and fate mapping analyses have established the CGE as a separate molecular territory and confirmed that CGE-derived cortical interneurons contribute to a subset of interneuron subtypes with distinct morphological and electrophysiological interneurons (Kanatani et al., 2008; Miyoshi et al., 2010; Nery et al., 2002; Willi-Monnerat et al., 2008; Yozu et al., 2005). Still, no functional studies on genes required for the specification of CGE-derived cortical interneurons have been described to date.

Here, we reported for the first time a molecular determinant required for the proper specification the CGE-derived interneurons, the transcription factor COUP-TFI. We showed that COUP-TFI is a key player in the specification of CGE –derived cortical interneurons and regulates the fine balance between distinct cortical interneuron subtypes in a spatiotemporal controlled manner during corticogenesis. The establishment and the maintenance of this balance enable proper cortical microcircuitry and functional activity.

Conditional inactivation of COUP-TFI solely in interneuron SVZ progenitors leads to a decreased number of CR- and VIP-bipolar GABAergic cells in superficial cortical layers and a concomitant increase of PV- and NPY-expressing interneurons in deep cortical layers of the mature cortex, without affecting the total number of GABAergic cortical interneurons. Physiologically, this alters the balance of both GABAa- and GABAb-receptor mediated inhibition so that mutants become more resistant to pharmacologically induced seizures. Moreover, this work describes for the first time an epilepsy-resistant phenotype

after genetic manipulation of interneuronal subtypes, and suggests a potential role for increased PV+ and NPY+ interneurons in controlling seizures.

COUP-TFI controls the balance between MGE- and CGE-derived interneurons

Differently from COUP-TFII, COUP-TFI is expressed in precursors of the basal telencephalon along the whole rostrocaudal extent at early stages (Armentano et al., 2007; Faedo et al., 2008), before getting restricted to the dorsal MGE and CGE at E13.5, and to CGE-derived cortical interneurons, such as VIP- and CR-expressing bipolar interneurons (appr. 80% and 90%, respectively). Furthermore, 56% of COUP-TFI+ express SST and 70% express NPY+, most presumably originating from the dMGE (for the SST+ cohort) and from both, the dMGE and the CGE, for the NPY+ subpopulation (Fogarty et al., 2007; Karagiannis et al., 2009; Sousa et al., 2009).

Interestingly, although COUP-TFI is expressed in the MGE at early stages during the production of PV+ interneurons, its expression is not maintained in this cell type at P21. In this part of my thesis, I demonstrate that loss of COUP-TFI function affects generation, but not maturation of PV+ interneurons. Differently from Nkx2.1, which normally acts as a cell fate switch between PV+ (MGE-derived) and CR+/ VIP+ (CGE-derived) interneurons (Butt et al., 2008), COUP-TFI acts in the opposite way by limiting generation of PV+ interneurons and promoting specification of CR+ and VIP+ interneurons. The imbalance between MGE- and CGE-derived interneurons induced by loss of COUP-TFI function is not due to a change of cell fate, as observed for Nkx2.1 mutants (Butt et al., 2008), but rather to a control on precursor cell divisions within the MGE, as seen by increased proliferation and expression levels of the cell cycle protein cyclinD2 in SVZ precursors (Glickstein et al., 2007a; Glickstein et al., 2007b). Null mutant mice for cyclinD2 have a selective deficit in cortical PV-expressing interneurons and increased excitability, without affecting other MGE-derived subtypes, such as SST+

interneurons (Glickstein et al., 2007b). Accordingly, overexpression of cyclinD2 in COUP-TFI conditional mutants results in an increase of PV+ neurons (Glickstein et al., 2007b) implying that negative control of SVZ divisions by COUP-TFI normally limits the number of PV+ interneurons. Thus, in the absence of COUP-TFI function, this repression is released and an excess of PV+ interneurons is produced. Since COUP-TFI is expressed in the MGE from E10.5 to E12.5 (Armentano et al., 2007; Armentano et al., 2006) (and this study), and production of PV+ interneurons occurs from E9.5 to E15.5 (Miyoshi et al., 2007), it is reasonable to assume that presumptive PV+ cells express COUP-TFI while proliferating in the SVZ and that COUP-TFI normally controls early SVZ progenitor divisions during generation of PV+ interneurons.

However, beside the increase of PV+ interneurons, loss of COUP-TFI function also affects correct specification of late-born CR+ and VIP+ interneurons. We hypothesize that overproduction of PV+ (and in part NPY+ cells) at a time when normally VIP+ and CR+ cells are generated (from E14.5 to E18.5) (Miyoshi et al., 2010), depletes the progenitor pool in the MGE, resulting in a decrease of VIP+ and CR+ bipolar interneuron precursors in the CGE. Thus, we propose that COUP-TFI normally regulates the number of PV+ cells during generation of CR+ and VIP+ neurons by controlling sequential cell divisions in SVZ progenitors. Excessive cell divisions during the time of PV+ interneuron generation would affect the sequential production of VIP/CR bipolar interneurons. In support of this mechanism, increased PV+ interneurons are found in deep cortical layers (appropriately for their MGE origin), and decreased CR+ and VIP+ interneurons are still located in superficial layers (appropriate for their CGE origin) in COUP-TFI conditional mutants.

Altogether, these data support a model by which COUP-TFI regulates the fine balance between MGE- and CGE-derived interneurons by ensuring proper generation and specification of different subsets of cortical interneurons. This is in accordance with the

control of pyramidal projection neurons by COUP-TFI, which is required to balance motor and sensory cortical areas by repressing corticospinal motor neuron generation during production of corticofugal pyramidal neurons in an area- and temporal-specific manner (Armentano et al., 2007; Tomassy et al., 2010a). Moreover, both COUP-TFs regulate the switch between neurogenesis (early corticogenesis) and gliogenesis (late corticogenesis) and in their absence, neurogenesis is sustained and the generation of early-born neurons is prolonged (Naka et al., 2008a). Finally, the *Drosophila* COUP-TF ortholog, *svp*, controls neuroblast diversity in a temporally controlled mode by regulating the balance between early- and late-born neuroblasts during neurogenesis (Kanai et al., 2005). Overall, we propose that in the basal telencephalon COUP-TFI plays a critical temporal and spatial control over the differentiation of different subtypes of cortical interneurons, thereby enabling the temporal and spatial specification of PV-, and bipolar CR- and VIP-expressing interneurons.

Increased inhibition mediated by altered balance of cortical interneuronal types might account for epilepsy resistance

The role of GABAergic interneurons in the proper operation of cortical circuitry is widely recognized. By means of a precise somatodendritic arrangement of their synaptic contacts, diverse types of interneurons specifically control excitability of principal cells and other neuronal types (Ascoli et al., 2008; Markram et al., 2004), being responsible of setting brain rhythms and local field potential oscillations (Buzsaki et al., 2004). We know that GABAergic cell dysfunction is associated primarily with epilepsy, one of the most frequent neurological disorders occurring in the young population (Baraban, 2007; Cossart et al., 2005). However, we still lack a comprehensive understanding of what determines the expression of a particular phenotype and whether interneuronal dysfunction is cause or consequence of epileptic seizures.

Recent genetic models aimed to study the development of cortical interneurons have given us further cues to draw this picture (Fig. 2.7). They constitute a unique tool because in most cases changes of subtype proportions precede pathological manifestations (Fig. 2.7B). Mice lacking the transcription factor Dlx1 suffer from an apoptotic loss of SST+, CR+ and NPY+ subtypes, whereas PV+ interneurons were spared. This reduction was associated with decreased GABAergic synaptic activity, distorted theta oscillations and generalized spontaneous seizures suggesting that less SST-, CR- and NPY-expressing subtypes alone can account for seizures when the number of PV+ cells remains constant. Interestingly, Sox6 mutants, which have a reduction of PV+ and SST+ interneurons and a constant number of the VIP+ and CR+ subtypes, exhibit pathological oscillations in the delta and beta bands and an early epileptic phenotype onset, that is not compensated by increased number of NPY+ interneurons (Azim, 2009; Batista-Brito, 2009). This critical role of PV+ and SST+ subtypes is confirmed by early loss-of-function experiments of Nkx2.1 in which an excess of VIP+ and CR+ cells are generated at the expense of PV- and SST-expressing interneuronal populations (Butt et al., 2008). As a consequence, juvenile mice exhibit generalized seizures. A late (E12.5) loss of Nkx2.1 function leaves SST+ cells unaffected and causes the same interneuronal shift exclusively at the upper layers. Remarkably, although their seizure susceptibility was not directly tested, these mice did not exhibit spontaneous seizures (Butt et al., 2008).

Very interestingly, mice lacking cyclinD2, which have reduced density of PV+ interneurons but normal density of SST+ and other CGE-derived interneurons, display decreased inhibitory synaptic activity and enhanced cortical excitability, although no spontaneous seizures were recorded (Glickstein et al., 2007b). In contrast, mice with mutation of the gene encoding urokinase plasminogen activator receptor (uPAR) display a large reduction of PV+ cells exclusively, and have spontaneous generalized seizures, being also more susceptible to PTZ-induced seizures (Powell et al., 2003).

All these mouse models argue for a differential role of diverse interneuronal types in controlling cortical excitability and seizures. Our study moves forward and demonstrates that in the presence of a higher number of PV+ and NPY+ interneurons, COUP-TFI mutants show no discernible cortical EEG abnormalities, but on the contrary are more resistant to pharmacologically induced seizures. Such a resistance is dependent on GABAergic signaling because it is abolished by blockage of GABAa and GABAb receptors. Surprisingly, we found no changes in the gamma region of the spectrum in spite of the increased number of PV+ interneurons. However, we must keep in mind that coarse wire EEG recordings are not well suited to look at the local organization of cortical gamma rhythms, and probably our recordings remained too superficial to detect changes caused by increased numbers of PV+ cells at deep layers in mutant mice. Obviously, the cortical microcircuit is extremely complex and other factors, such as the layer specificity of interneuronal loss and the total number of affected cells can constraint the emergence of epileptic phenotypes and rhythm distortion. Future detailed studies of the local field potentials using multi-site recordings would help to look at the finest spatial scale of the neocortex.

Another potential source of enhanced inhibition in our *COUP-TFI CKO-Dlx5/6* mice is the reduction of the control exerted by fewer CR+ and VIP+ interneurons acting over other superficial layer interneurons. CR+ and VIP+ interneurons are known to preferentially target other interneurons (Staiger et al., 2004). Thus, under conditions of reduced number of CR+ and VIP+ interneurons, pyramidal cells would not be relieved from inhibition, being less excitable in *COUP-TFI* mutant mice. However, this is unlikely because: 1) similar decrease of CR+ interneurons in the *Dlx1* mutants results in hyperexcitability and seizures, probably aided by concomitant reduction in the number of NPY+ and SST+ cells, and 2) increased CR+ and VIP+ cells, in the presence of reduced number of PV+ interneurons, failed to rescue the epileptic phenotype of *Nkx2.1* mutants

(Butt et al., 2008). Indeed, synaptic potentials elicited by CR+ multipolar and bipolar interneurons upon their few cortical pyramidal targets are weaker than potentials initiated by PV+ interneurons, which dominate thalamocortical and intralaminar feedforward inhibition (Caputi et al., 2009; Sun et al., 2006; Xu and Callaway, 2009).

We also detected an increase of NPY+ interneurons in the deep neocortical layers of COUP-TFI mutants. This probably reflects a population of NPY+ interneurons, which derive from the dorsal MGE (Fogarty et al., 2007). NPY+ interneurons constitute a heterogeneous group, as this protein has been detected in a variety of cortical interneurons (Karagiannis et al., 2009), although a more homogeneous fraction appears to be generated from the pre-optic area (Gelman et al., 2009). Interestingly, NPY+ interneurons known to co-express NOS (nitric oxide synthase) can be morphologically and physiologically identified as neurogliaform cells and share mainly an MGE origin, although a subpopulation of NPY+ neurogliaform cells do not express NOS and derive from the CGE (Tricoire et al., 2010). Neurogliaform interneurons are a unique source of GABAb-mediated inhibition for pyramidal cells (Tamas et al., 2003). If some of the exceeding NPY+ interneurons detected in the lower cortical layers of COUP-TFI conditional mutants correspond with neurogliaform cells, their possible role in controlling cortical excitability is intriguing. Indeed, we found that removal of GABAb inhibition in the presence of a GABAa-antagonist was required in order to abolish differences of seizure onset between *COUP-TFI* mutants and WT mice. Although other sources of GABAb-mediated inhibition operate at both pre- and post-synaptic levels, the specific role of this recently discovered interneuron population remains unknown. Future studies will be essential to overcome the origin, identity and function of this miscellaneous interneuronal subtype.

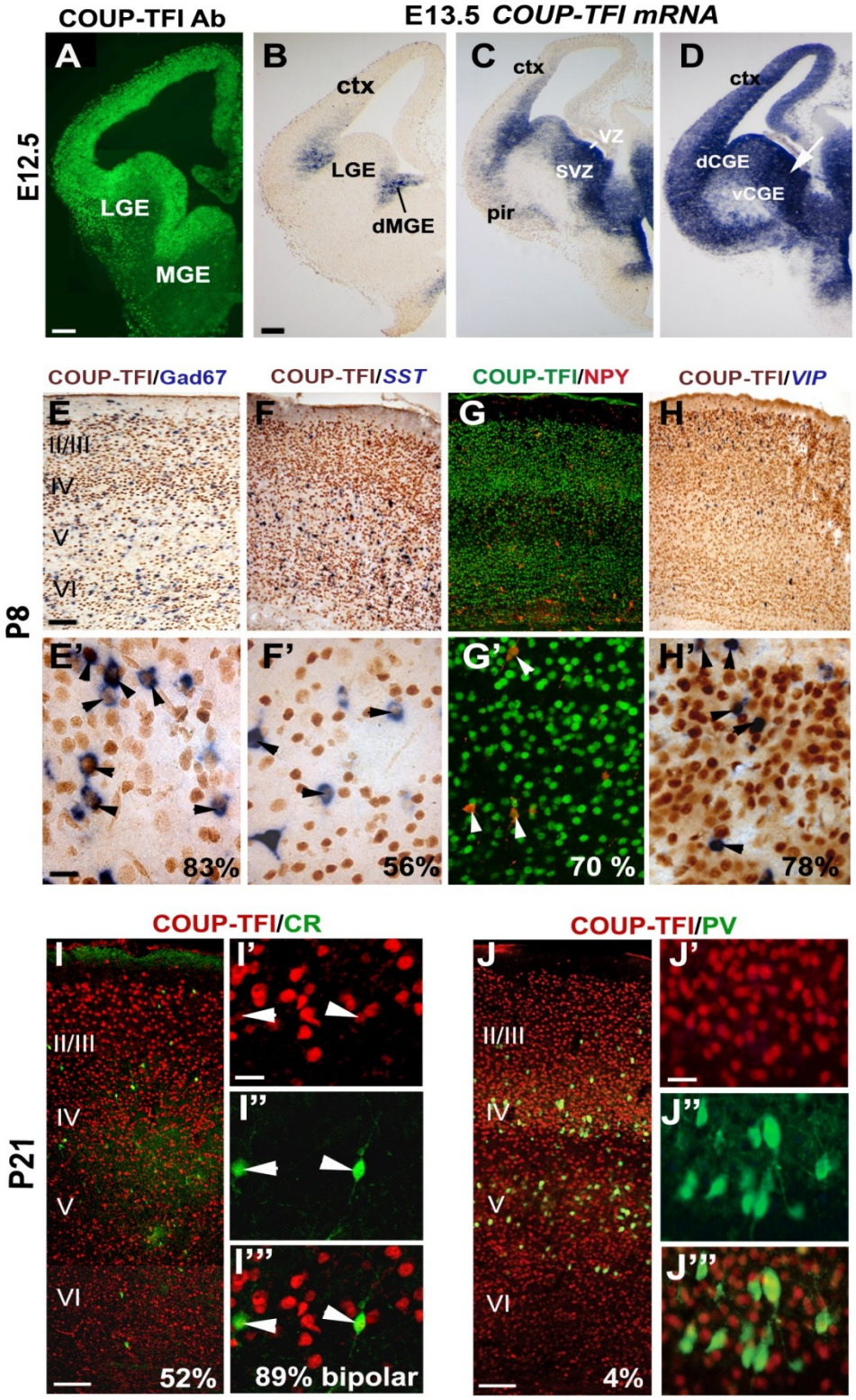
COUP-TFI Ab
E13.5 COUP-TFI mRNA
E12.5
A
LGE
MGE
B
ctx
LGE
dMGE
C
ctx
VZ
SVZ
pir
D
ctx
dCGE
vCGE
COUP-TFI/Gad67
COUP-TFI/SST
COUP-TFI/NPY
COUP-TFI/VIP
P8
E
II/III
IV
V
VI
F
G
H
E'
F'
G'
H'
83%
56%
70 %
78%
COUP-TFI/CR
COUP-TFI/PV
P21
I
I'
I''
I'''
II/III
IV
V
VI
52%
89% bipolar
J
J'
J''
J'''
II/III
IV
V
VI
4%

Figure 2.1

Figure 2. 1 COUP-TFI becomes gradually restricted to the dorsal MGE and CGE and is highly expressed in CGE-derived cortical interneurons.

(A) Coronal section of E12.5 wild-type embryo at intermediate level showing localization of COUP-TFI protein in the telencephalon. Note high expression in the LGE and dorsal half of the MGE. (B-D) Rostral to caudal sequential coronal sections of E13.5 wild-type embryos hybridized with *COUP-TFI* indicate regionalized expression in the dorsal (d) MGE (B) and in the ventricular (VZ) and subventricular (SVZ) zones of caudalmost dorsal and basal telencephalon (C), including the CGE (D). Arrow in (D) indicates highest COUP-TFI expression levels in ventral (v)CGE. (E, F, H) Double immunostaining for COUP-TFI protein and *in situ* hybridization for *Gad67*, *SST* and *VIP* and (G) double immunofluorescence for COUP-TFI and NPY in P8 somatosensory cortices. Roman numerals denote cortical layers. (E'-H') High magnification views of a representative detail from (E-H) indicate double-positive cells (arrowheads) and the different percentage of COUP-TFI-positive cells expressing *Gad67* (83%), *SST* (56%), NPY (70%) and *VIP* (78%). (I-J'") Double immunofluorescence for COUP-TFI and CR (I), and COUP-TFI and PV in P21 somatosensory cortices (J). High magnification views indicate highest co-localization of COUP-TFI with bipolar CR-positive cells (arrowheads in I'-I'"), and lowest co-localization of COUP-TFI with PV-positive cells (J'-J'"). Abbrevations: ctx, cortex; LGE, lateral ganglionic eminence; dMGE, dorsal medial ganglionic eminence; pir, piriform cortex. Scale bars: 200 μm (A-D); 100 μm (E-J); 50 μm (E'-J'").

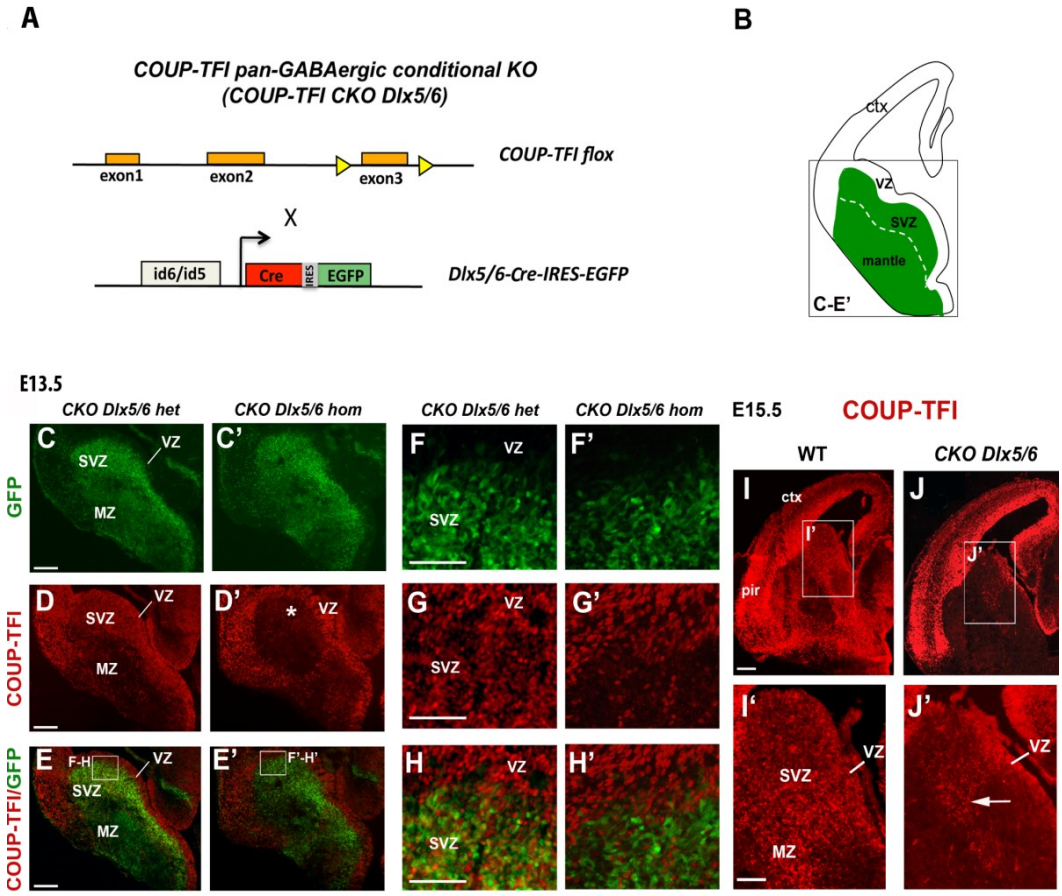
A
COUP-TFI pan-GABAergic conditional KO
(COUP-TFI CKO Dlx5/6)
exon1
exon2
exon3
COUP-TFI flox
X
id6/id5
Cre
IRES
EGFP
Dlx5/6-Cre-IRES-EGFP
B
ctx
VZ
SVZ
mantle
C-E'
E13.5
CKO Dlx5/6 het
CKO Dlx5/6 hom
CKO Dlx5/6 het
CKO Dlx5/6 hom
E15.5
COUP-TFI
WT
CKO Dlx5/6
GFP
COUP-TFI
COUP-TFI/GFP
C
C'
F
F'
D
D'
G
G'
E
E'
H
H'
I
J
I'
J'
SVZ
MZ
pir
F-H
F'-H'

Figure 2.2

Figure 2. 2. Conditional loss of COUP-TFI in cortical interneurons affects SVZ progenitors in the basal telencephalon.

(A) Schematic of the genetic strategy for examining COUP-TFI conditional loss-of-function by using the *Dlx5/6-Cre-IRES-EGFP* mouse active in the SVZ progenitors and post-mitotic interneurons of the basal telencephalon (Stenman et al., 2003). (B) Schematic of a E13.5 coronal hemisection indicating the position of panels (C-E'). Green indicates the expression of the EGFP upon Cre-mediated recombination. (C-E') Coronal sections of E13.5 *COUP-TFI CKO-Dlx5/6* (*CKO Dlx5/6*) heterozygotes and homozygotes immunostained with anti-GFP (C, C', F, F'), anti-COUP-TFI (D, D', G, G'), and merge sections (E, E', H, H'). Note that GFP is expressed in the subventricular (SVZ) and mantle (MZ) zones, but absent in the ventricular zone (VZ), whereas COUP-TFI is expressed in the VZ, SVZ and MZ of the basal telencephalon. (F-H') High magnification views of a region in the basal telencephalon indicated in (E, E'). (E', H') In *COUP-TFI CKO-Dlx5/6* homozgotes no double-labeled cells are detected, confirming loss of COUP-TFI function in SVZ and MZ (Dlx5/6-positive domains), but not in progenitors located in VZ (Dlx5/6-negative domain). (I-J') Immunostaining of anti-COUP-TFI in E15.5 WT and *CKO Dlx5/6* embryos confirms specific inactivation of COUP-TFI in the SVZ and MZ of the basal telencephalon. (I', J') High magnification views of a region in the basal telencephalon indicated in (I, J). Note that expression of COUP-TFI in the VZ and in the ventrally migrating stream is not affected in COUP-TFI conditional mutants (arrow in J'). Scale bars: 200µm (C-E', I, J); 50µm (F-H'); 100µm (I', J').

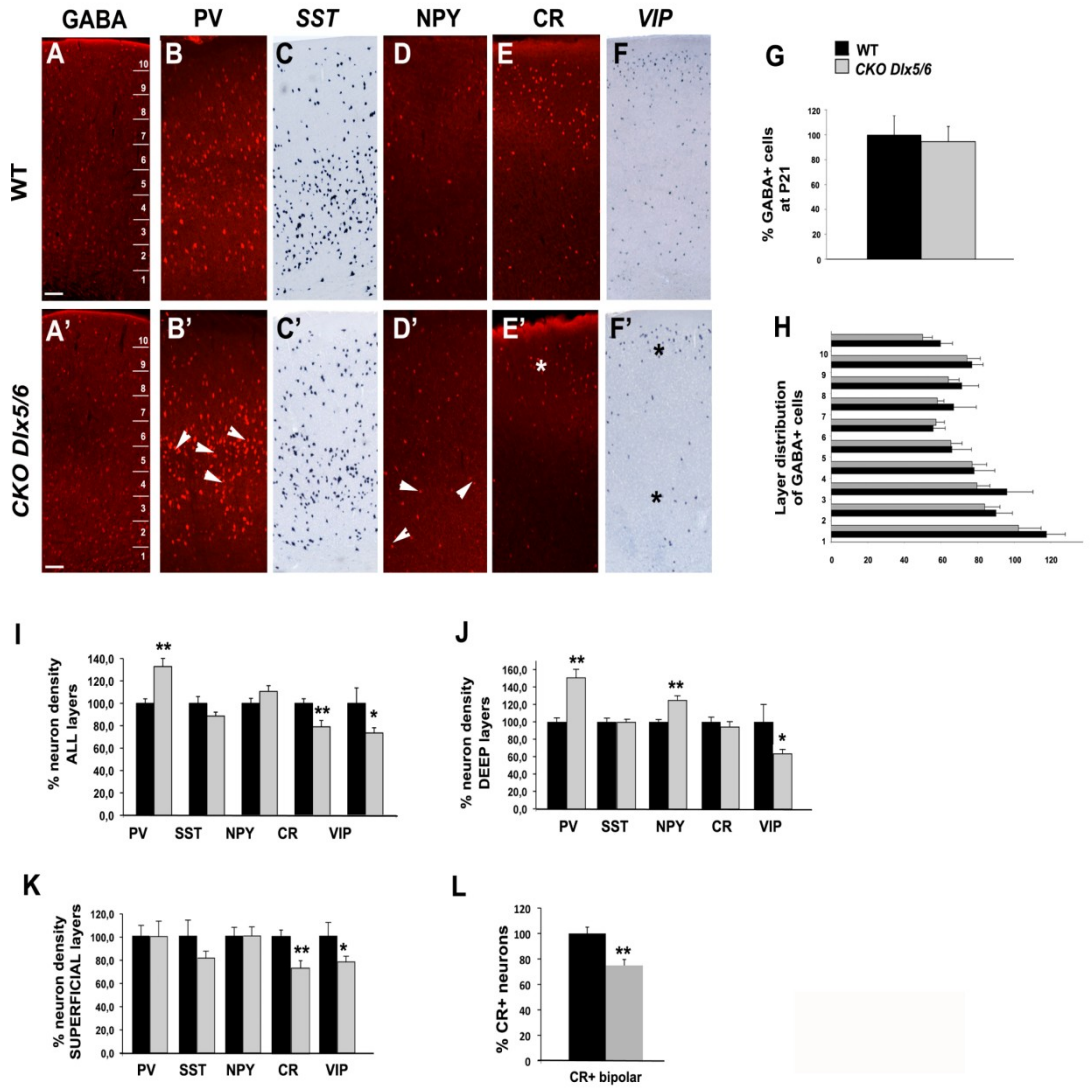
GABA
PV
SST
NPY
CR
VIP
WT
CKO Dlx5/6
A
B
C
D
E
F
A'
B'
C'
D'
E'
F'
G
WT
CKO Dlx5/6
% GABA+ cells at P21
H
Layer distribution of GABA+ cells
I
% neuron density ALL layers
PV
SST
NPY
CR
VIP
J
% neuron density DEEP layers
K
% neuron density SUPERFICIAL layers
L
% CR+ neurons
CR+ bipolar

Figure 2.3

Figure 2. 3. Altered balance between PV- and bipolar VIP- and CR-expressing cortical interneurons in the absence of COUP-TFI function.

(A-F') Representative coronal sections of P21 WT and *CKO Dlx5/6* cortices within the P21 sensorimotor cortex of WT (A-F) and *CKO Dlx5/6 (COUP-TFI CKO-Dlx5/6*) (A'-F') immunostained with anti-GABA (A-A') and with different cortical interneuron subtypes, as indicated (B-F'). (C, C', F, F') *In situ* hybridization of *SST* and *VIP* on adjacent sections. (G, H) The number and distribution of GABA+ cells were quantified by subdividing the cortex into 10 bins along the ventricular (bin 1) to pial (bin 10) axis of equivalent areas of the sensorimotor cortex from WT and *CKO Dlx5/6* animals. No significative difference in the total amount of GABA+ cells (G) and in the distribution of cells in each bin (H) was detected between WT and mutant cortices. Arrowheads in (B') and (D') point to an increased number of PV- and NPY-expressing cells, respectively, in deep layers. Asterisk in (E') denotes a reduction of CR-expressing cells in superficial layers, whereas asterisks in (F') indicate a reduction of VIP-expressing cells in both superficial and deep layers. (I-L) Graphical representation of the percentage of density of the different cortical interneuron subpopulations in the *COUP-TFI CKO* relative to WT, as indicated. (I) Along the whole radial extent of the cortex the number of the PV+ subpopulation increased significantly by 33% (WT: 165.3±6.7, *CKO*: 219±12.4; $p<0.01$; n=3), whereas the total number of bipolar VIP+ and CR+ interneurons decreased significantly by 26% (VIP; WT: 208.2±28.6, *CKO*: 153.1±9.8; p=0.03; n=3) and by 21% (CR; WT: 130.9±5.4, *CKO*: 103.5±7.1; p=0.01; n=3), respectively. (J) In deep layers the PV+ (WT: 85.9±4.5, *CKO*: 130.1±8.4; $p<0.001$; n=3) and NPY+ (WT: 42.8±1.4, *CKO*: 53.71±2.3; p=0.003; n=3) cohorts increased significantly, whereas the VIP+ subpopulation decreased significantly (WT: 64.1±13.3, *CKO*: 40.8±3.3; p=0.02; n=3) in *CKO Dlx5/6* mutants. (K) In superficial layers the CR+ (WT: 94.7±5.1, *CKO*: 69.2±5.8; p=0.003; n=3) and VIP+ (WT: 144.1±16.8, *CKO*: 112.3±6.9; p=0.04; n=3) subpopulations are decreased

significantly in *CKO Dlx5/6* mice. (L) Graphical representation of the percentage of bipolar-shaped CR+ interneurons indicates a statistically significant decrease of 25% in *CKO Dlx5/6* cortices (WT: 21.8±1.2, *CKO*: 16.3±1.4; p=0.008; n=3). Scale bars: 100μm (A-F').

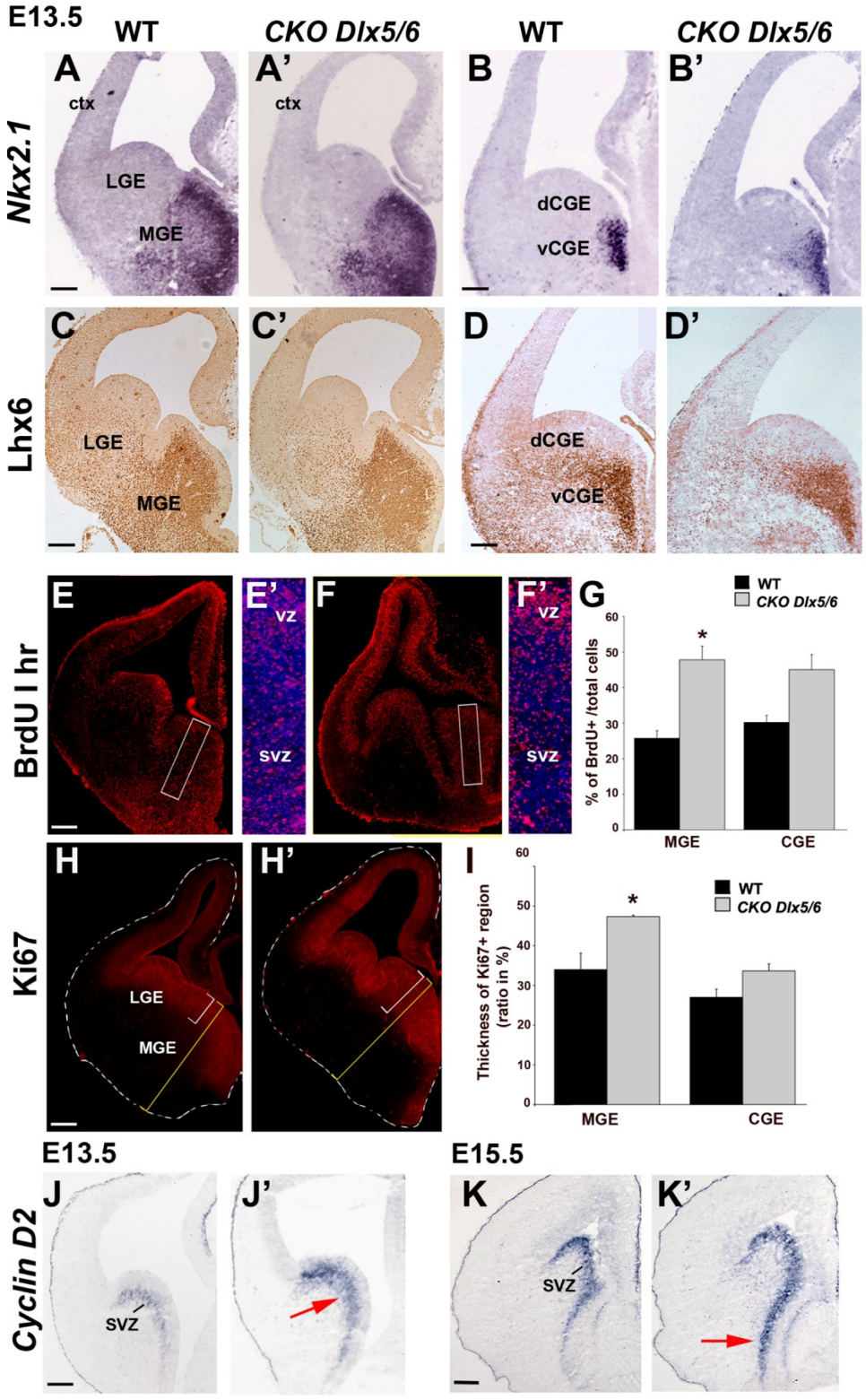
E13.5
WT
CKO Dlx5/6
WT
CKO Dlx5/6
Nkx2.1
A
A'
B
B'
ctx
ctx
LGE
MGE
dCGE
vCGE
Lhx6
C
C'
D
D'
LGE
MGE
dCGE
vCGE
BrdU I hr
E
E'
VZ
SVZ
F
F'
VZ
SVZ
G
WT
CKO Dlx5/6
% of BrdU+ /total cells
60
50
40
30
20
10
0
*
MGE
CGE
Ki67
H
H'
LGE
MGE
I
Thickness of Ki67+ region (ratio in %)
60
50
40
30
20
10
0
*
WT
CKO Dlx5/6
MGE
CGE
E13.5
E15.5
Cyclin D2
J
J'
SVZ
K
K'
SVZ

Figure 2.4

Figure 2. 4. Normal molecular identity of the MGE in *COUP-TFI* conditional mutants.

(A-B') *In situ* hybridization of *Nkx2.1* and (C-D') immunohistochemistry of Lhx6 on E13.5 coronal sections on medial (A, A', C, C') and caudal (B, B', D, D') levels indicate no relevant changes in the expression profiles of *Nkx2.1* and Lhx6 in *CKO Dlx5/6* embryos. Abbrevations: dCGE, dorsal caudal ganglionic eminence; vCGE, ventral caudal ganglionic eminence; ctx, cortex. Scale bars: 200µm. (E, F) BrdU immunofluorescence on DAPI-stained coronal sections indicate increased proliferation in the MGE of E13.5 *CKO Dlx5/6* embryos. (E', F') High magnification views on the boxes depicted on (E, F). (G) Graphical representation demonstrates a significative increase of BrdU-positive cells in the MGE (p=0.04), but not CGE (p=0.097). (H, H') Ki67 immunofluorescence labels highly proliferating cells in coronal sections of E13.5 of WT and *CKO Dlx5/6* embryos. (I) Graphical representation indicates a significative increase in the size of the Ki67-positive region of the MGE with respect to the total ventricular to pial thickness in mutant embryos (p=0.03), as indicated by an arrow in H'. (J'-K') Expression of the cell cycle protein *cyclinD2* is upregulated in the subventricular zone (SVZ) of E13.5 (arrow in J') and E15.5 *CKO Dlx5/6* embryos (arrow in K'). Abbrevations: dCGE, dorsal caudal ganglionic eminence; vCGE, ventral caudal ganglionic eminence; ctx, cortex. Scale bars: 200µm.

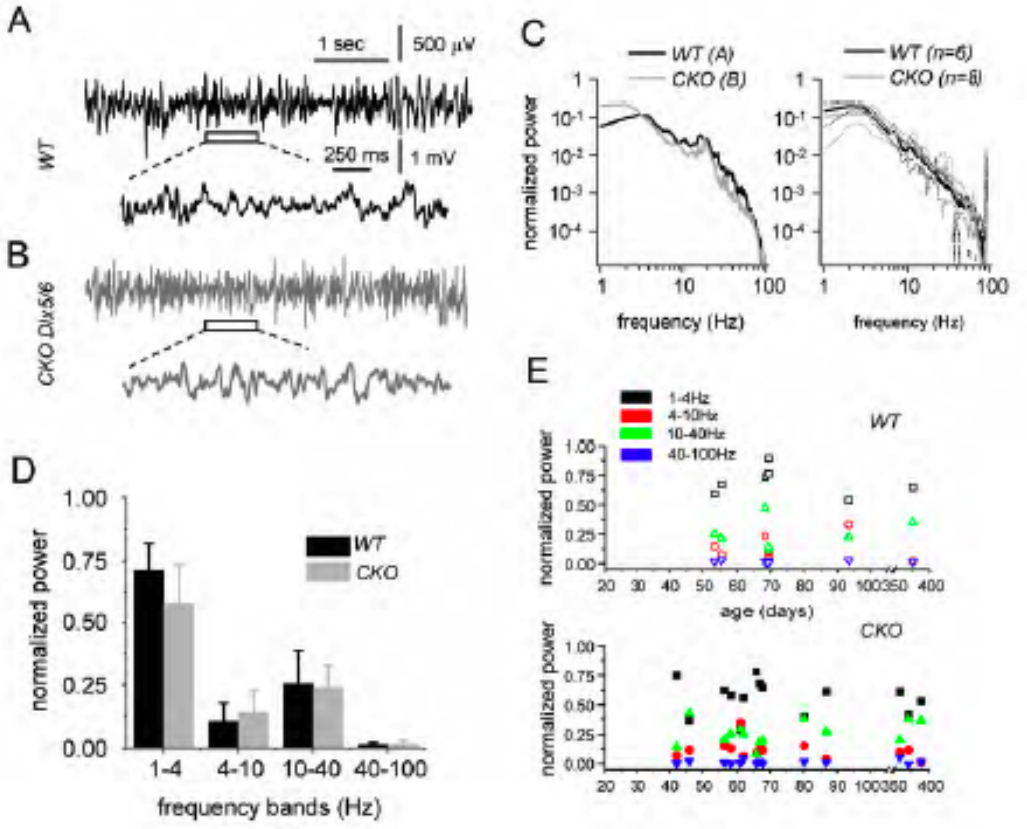
A
1 sec
500 µV
WT
250 ms
1 mV
B
CKO Div5/6
C
WT (A)
CKO (B)
WT (n=6)
CKO (n=6)
normalized power
frequency (Hz)
frequency (Hz)
D
normalized power
WT
CKO
1-4
4-10
10-40
40-100
frequency bands (Hz)
E
1-4Hz
4-10Hz
10-40Hz
40-100Hz
WT
normalized power
age (days)
CKO
normalized power

Figure 2.5

Figure 2. 5 Normal basal EEG recordings in *COUP-TFI* conditional mutants.

(A) Cortical EEG recorded from awake wild-type (WT) mice shows normal activity at 3-7Hz with episodes of beta activity at 15-20 Hz. Higher resolution trace shows details from the upper traces. (B) EEG recordings from awake *COUP-TFI CKO-Dlx5/6* mice exhibit roughly similar features than WT animals. (C) Normalized power spectra from the representative examples shown in A and B (left) and for the population means (right). No differences were found between groups. A 95% confidence interval is represented with dotted lines for each group. (D) Mean spectral power per frequency bands were not different between groups. (E) Age dependence of the spectral content at the different frequency bands.

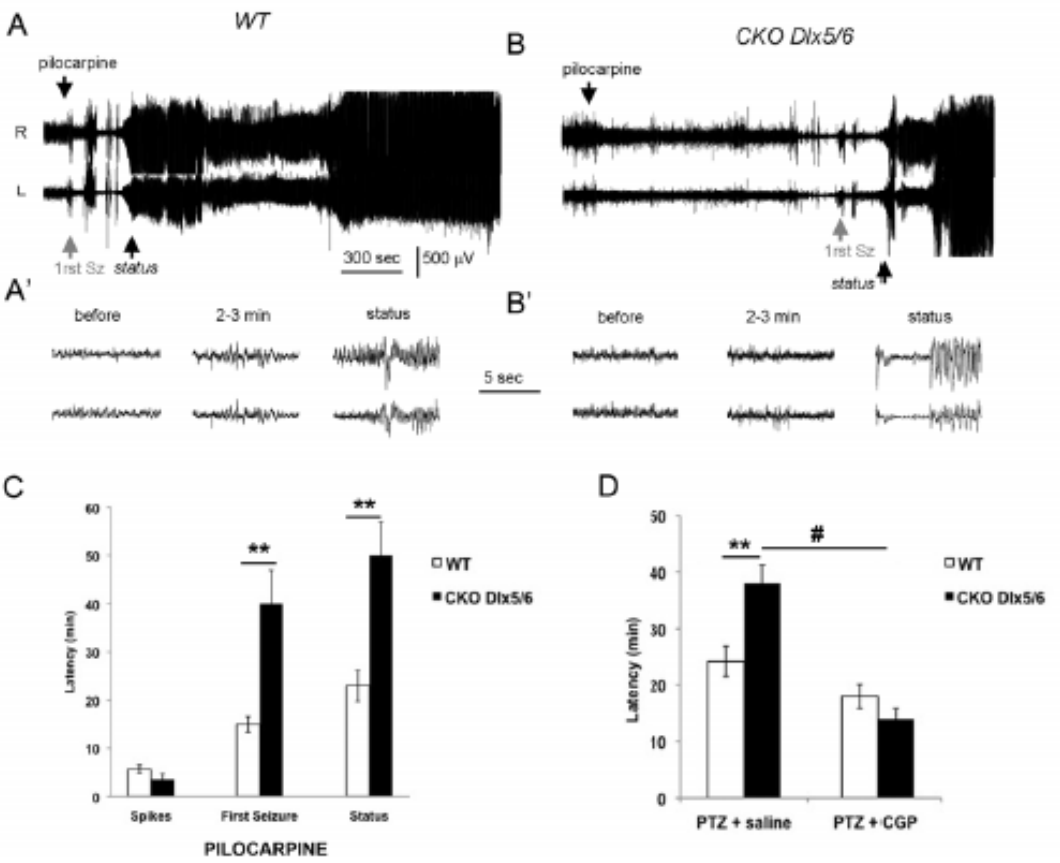
A
WT
pilocarpine
R
L
1rst Sz
status
300 sec
500 µV
B
CKO Dlx5/6
pilocarpine
1rst Sz
status
A'
before
2-3 min
status
5 sec
B'
before
2-3 min
status
C
Latency (min)
**
**
WT
CKO Dlx5/6
Spikes
First Seizure
Status
PILOCARPINE
D
Latency (min)
**
#
WT
CKO Dlx5/6
PTZ + saline
PTZ + CGP

Figure 2.6

Figure 2. 6 Seizure resistance of *COUP-TFI CKO-Dlx5/6* mice.

(A) Bilateral cortical EEG recordings obtained from a representative wild-type (WT) mouse during the progression to a *status epilepticus* induced by intraperitoneal injection of the muscarinic receptor agonist pilocarpine. Arrows indicate the timing of pilocarpine injections; the first generalized tonic-clonic seizure (1^{st} Sz) and the onset of *status epilepticus*, as defined by electroclinical information. (A') Expanded traces highlight EEG epochs recorded before, after 2-3 minutes of pilocarpine injection and at the *status* onset. (B) Bilateral cortical EEG from a representative *COUP-TFI CKO-Dlx5/6* mouse. Note the long latency to the first generalized tonic-clonic seizure (1^{st} Sz) and the onset of the *status epilepticus*. (B') Expanded traces similar to that showed in A' for *COUP-TFI CKO-Dlx5/6* (*CKO Dlx5/6*) mice. (C) Mean latency to first spikes recorded after pilocarpine injections. Note latency difference to the first generalized tonic-clonic seizure (1^{st} Sz) and the *status epilepticus* between groups. (D) Latency difference to the first tonic-clonic seizure induced by subcutaneous injection of the GABAa receptor antagonist pentylenetetrazol (PTZ). Pre-treatment with the GABAb receptor antagonist CGP 35348 significantly reduces the latency to the first tonic-clonic seizures and eliminates latency difference between WT and mutants. ** $p<0.01$ CKO Dlx5/6 versus WT, within treatment; #$p<0.0001$ CGP 35348 versus Saline pre-treatment, within genotype.

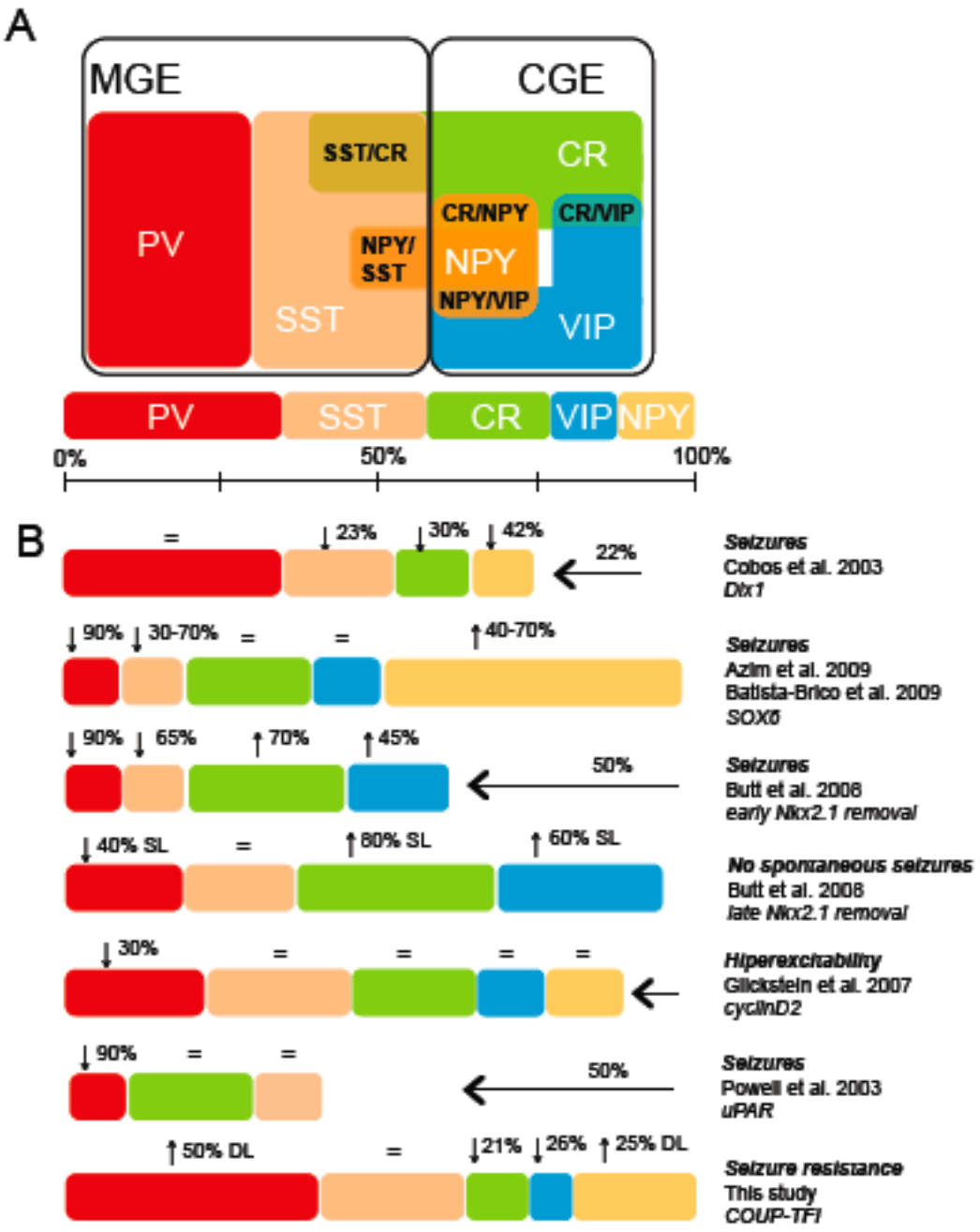
A
MGE
CGE
PV
SST/CR
SST
NPY/
SST
CR
CR/NPY
CR/VIP
NPY
NPY/VIP
VIP
PV
SST
CR
VIP
NPY
0%
50%
100%
B
=
23%
30%
42%
22%
Seizures
Cobos et al. 2003
Dlx1
90%
30-70%
=
=
40-70%
Seizures
Azim et al. 2009
Batista-Brito et al. 2009
SOX6
90%
65%
70%
45%
50%
Seizures
Butt et al. 2008
early Nkx2.1 removal
40% SL
=
80% SL
60% SL
No spontaneous seizures
Butt et al. 2008
late Nkx2.1 removal
30%
=
=
=
=
Hiperexcitability
Glickstein et al. 2007
cyclinD2
90%
=
=
50%
Seizures
Powell et al. 2003
uPAR
50% DL
=
21%
26%
25% DL
Seizure resistance
This study
COUP-TFI

Figure 2.7

Figure 2. 7 Summary on the relationship between different interneuronal subpopulations and epileptic phenotypes.

(A) Schematic showing the proportion of the different cortical interneuronal subpopulation classified according to their molecular expression profiles. In the normal mouse neocortex, parvalbumin (PV)-positive interneurons represent about 40% of the total numbers of interneurons, which together with somatostanine (SST) positive cells (~18%) mainly derive from the medial ganglionic eminence (MGE). Instead, calretinin (CR) and vasoactive intestinal peptide (VIP)-expressing interneurons originate from the caudal ganglionic eminence (CGE) and together contribute about 25% to the total number of cortical interneurons. Interneurons expressing the neurotransmitter peptide NPY are known to derive from both the MGE and the CGE and constitute about 9%. Many interneuronal markers colocalize, with SST/CR, SST/NPY, VIP/CR and VIP/NPY being the most common. Data from (Gonchar and Burkhalter, 1999; Xu and Callaway, 2009). (B) Schematic showing the percentage of interneuron subtypes affected by different genetic manipulations in the different papers cited at right and the corresponding clinical phenotype.

= indicates similar proportions compared with control;

↑, indicates an increased proportion and ↓ indicates decrease.

Chapter 3

Excitatory Projection Neuron Subtypes Differentially Control the Distribution of Local Inhibitory Interneurons in the Cerebral Cortex

Publication:

This work is in press (to be published on February, 24th 2011 *Neuron* issue) as Lodato S., Rouaux C., Quast K. B., Jantrachotechatchawan C., Studer M., Hensch T. K. and Arlotta P. (2011).
Excitatory Projection Neuron Subtypes Differentially Control the Distribution of Local Inhibitory Interneurons in the Cerebral Cortex.

Preface

In the second part of my thesis project, I focused on the effect of the cortical environment on microcircuitry development, by asking whether cortical projection neurons have an influence on the laminar distribution of cortical interneurons. Interestingly, although generated from distant germinal zones, projection neurons and interneurons synchronically born are juxtaposed within the same cortical laminaee (Fairen et al., 1986; Miller, 1985; Pla et al., 2006; Valcanis and Tan, 2003). The establishment of correct reciprocal positioning and interactions between these two broad neuronal classes is critical for balanced electrical activity and normal cortical function.

In this chapter, I report that different subtypes of projection neurons uniquely and differentially determine the laminar distribution of cortical interneurons. I find that in *Fezf2*$^{-/-}$ cortex, the exclusive absence of subcerebral projection neurons and their replacement by callosal projection neurons cause distinctly abnormal lamination of interneurons and altered GABAergic inhibition. In addition, experimental generation of either corticofugal neurons or callosal neurons below the cortex is sufficient to recruit cortical interneurons to these ectopic locations. Strikingly, the identity of the projection neurons generated, rather than strictly their birthdate, determines the specific types of interneurons recruited. These data demonstrate that in the neocortex individual populations of projection neurons cell-extrinsically control the laminar fate of interneurons and the assembly of local inhibitory circuitry.

Fezf2: the master gene for one population of cortical projection neurons

Fezf2 is a six-zinc finger domain-containing transcription factor that is conserved from *Drosophila* to human (Hashimoto et al., 2000; Matsuo-Takasaki et al., 2000; Yang et al., 2001). In mouse it has been shown that *Fezf2* is expressed at a constant level in CSMN and other subcerebral projection neurons from E18.5 to P14 (Arlotta et al., 2005). In

addition, during earlier stages of development *Fezf2* is first expressed as early as E8.5 in the dorsal telencephalic wall (Hirata et al., 2004; Matsuo-Takasaki et al., 2000). Between E12.5 and E14.5, when subcerebral projection neurons are born, *Fezf2* is detected in the ventricular zone in a pattern consistent with the location of neural progenitors and in the developing cortical plate (Hirata et al., 2004; Inoue et al., 2004), consistent with the position of newborn subcerebral projection neurons.

Initial analysis of *Fezf2* null-mutants suggested that cortical layers, including the subplate, are generated normally, but that the subplate exhibits abnormalities in maturation (Hirata et al., 2004). These studies did not investigate the development of CSMN or other subcerebral projection neurons. Therefore, it remained unclear if any neuronal populations of the cortex are affected in *Fezf2-/-* mice. Thank to a very elegant study aimed at the molecular identification of subtype-specific genes for different populations of projection neurons of the cortex, Fezf2 has been recently identified as a candidate molecular determinant of the subcerebral projection neuron subtype, located in layer V of the cortex (Arlotta et al., 2005). Then, it has been discovered that in the absence of *Fezf2,* no subcerebral projection neurons are born, and no cortical projections to the brainstem or the spinal cord ever develop (Molyneaux et al., 2005). In contrast, other populations of neurons, i.e. upper layers callosal neurons, are unaffected. The absence of subcerebral projection neurons suggested that *Fezf2* might be required for the initial fate specification of this neuronal lineage. However, two alternative possibilities could explain this phenotype: 1) *Fezf2* might control subcerebral projection neuron survival; or 2) subcerebral projection neurons could be initially born, but fail to migrate to the appropriate laminar location. In the above-mentioned study, both possibilities were carefully analyzed and it was found that neither neuronal death nor a migrational abnormality accounts for the absence of subcerebral projection neurons strongly supporting the hypothesis that *Fezf2* is involved in the initial fate specification of these

neurons. By using different tracing approaches, it has been determined that the subcerebral projections towards subcortical targets was truly absent from the *Fezf2* mutant mouse (Molyneaux et al., 2005).

All these data together pointed at *Fezf2* as a transcription factor required for the birth and specification of a specific subpopulation of projection neurons in cortical development. Gain-of-function experiments highlighted also its sufficient role in generating subcerebral projection neurons from neural precursors destined to acquire a dramatically different fate. Overexpression of *Fezf2*, by using in utero electroporation, into the ventricular zone during late embryonic development results in the ectopic production of deep layer neurons, defined by molecular properties and anatomical connectivity as subcerebral projection neurons (Molyneaux et al., 2005).

Introduction

High-level cortical function including cognition, sensory perception and motor function relies on the coordinated assembly of local microcircuitry between glutamatergic projection neurons and GABAergic interneurons (Hensch and Fagiolini, 2005). Excitatory projection neurons represent the largest portion of all cortical neurons. They are born from neural progenitors in the dorsal telencephalon and are classified into numerous subtypes based on their location within different cortical layers and areas; their axonal projections to distinct intracortical, subcortical and subcerebral targets; and the combinatorial expression of different neuron type-specific genes (Bayer and Altman, 1991). Among them, corticofugal projection neurons include corticothalamic projection neurons, which are found in layer VI and project to the thalamus, as well as corticospinal motor neurons (CSMN), corticotectal projection neurons and several other types of subcerebral projection neurons, which are located in different areas of layer V and project to the spinal cord, the superior culliculus and other targets in the brainstem and below the brain, respectively (Molyneaux et al., 2007). In addition, the cortex includes several types of callosal projection neurons (CPN), which are located in layers II/III and V (and in small numbers in layer VI) and connect to targets in the contralateral hemisphere (i.e. *via* the corpus callosum), the striatum and the frontal cortex (Lindwall et al., 2007; Mitchell and Macklis, 2005; Molyneaux et al., 2009; Richards et al., 2004).

The firing activity of these projection neuron types is modulated locally by populations of GABAergic inhibitory interneurons. Although the classification of cortical interneurons remains an open challenge (Ascoli et al., 2008), cortical interneurons are currently defined at the intersection of diverse molecular, electrophysiological and morphological properties, and based on their connections to the soma, axonal initial segment or dendritic tree of their projection neuron partners (Ascoli et al., 2008; Markram et al., 2004). As already discussed in the previous chapters, contrary to the dorsal

telencephalic origin of projection neurons, in rodents, cortical interneurons are mostly generated from neural progenitors located in the medial and caudal ganglionic eminences (MGE and CGE) and in the preoptic area (POA) in the ventral forebrain (Gelman et al., 2009; Wonders and Anderson, 2006). MGE progenitors give rise to Parvalbumin (PV)- and Somatostatin (SST)-expressing interneurons, which distribute at higher densities in deep cortical layers V and VI (Butt et al., 2005; Butt et al., 2008; Cobos et al., 2006; Fogarty et al., 2007). In contrast, Vasoactive Intestinal Peptide (VIP)- and Calretinin (CR)-expressing interneurons originate in the CGE and preferentially populate the superficial layers II/III (Miyoshi and Fishell, 2010; Miyoshi et al., 2010; Nery et al., 2002).

Even if projection neurons and interneurons are born from distal germinal zones, they ultimately coexist in the cortex, where they assemble into local microcircuitry. This requires coordinated migration and development of these two broad neuronal populations. The migration of interneurons to the cortex is particularly extensive (Corbin et al., 2001; Marin and Rubenstein, 2001). Following tangential migration through the ventral forebrain, interneurons enter the cortex where they disperse along migratory routes in the marginal zone (MZ) and the intermediate zone (IZ)/subventricular zone (SVZ) (Kriegstein and Noctor, 2004; Lavdas et al., 1999). Later, they change their mode of migration to radially invade the cortical plate (Ang et al., 2003; Polleux et al., 2002; Tanaka et al., 2003b), a process that is at least in part timed by chemokine signaling involving the CXCL12 and CXCR4 and CXCR7 pathway (Elias et al., 2008; Li et al., 2008; Lopez-Bendito et al., 2008; Sanchez-Alcaniz et al., 2011; Tanaka et al., 2003a; Tiveron et al., 2006; Wang et al., 2011).

The cellular and molecular events that direct interneurons to position precisely within specific cortical layers are much debated and poorly understood. Correct cell-autonomous development of cortical interneurons is a critical factor for the radial

positioning of GABAergic interneurons, since defective laminar distribution is often observed in mutant mice that have abnormal interneuronal differentiation (Alifragis et al., 2004; Azim et al., 2009; Batista-Brito et al., 2009; Butt et al., 2008; Cobos et al., 2006; Liodis et al., 2007). In addition, interneurons are cell-intrinsically programmed to modulate expression of the KCC2 co-transporter in order to sense extracellular GABA levels and arrest radial migration (Bortone and Polleux, 2009).

However, several lines of evidence indicate that the environment of the cortex also plays instructive roles in directing interneuron cortical distribution, pointing at a possible involvement of projection neurons in this process. For example, synchronically generated GABAergic interneurons and projection neurons preferentially pair, suggesting linked mechanisms of layer distribution (Fairen et al., 1986; Miller, 1985; Peduzzi, 1988; Pla et al., 2006; Valcanis and Tan, 2003). Additionally, interneurons invade the cortical plate only after their projection neuronal partners, possibly reflecting a need for signals originating from appropriately located projection neurons (Lopez-Bendito et al., 2008). Finally, interneurons distribute abnormally in the cortex of the *reeler* mice, in which projection neuron lamination is nearly inverted (Hammond et al., 2006; Hevner et al., 2004; Pla et al., 2006; Yabut et al., 2007). The investigation of the mechanisms that mediate the influence of projection neurons on interneuronal location, migration and their integration in the cortex is notoriously complicated by the fact that (1) the abnormal birth and specification of the interneurons themselves within the ventral telencephalon, could account for any observed interneuronal abnormalities, making it a challenge to establish cause and effect in most of these animal models; and, (2) most *in vivo* models available to study these events have broad-spread defects in more then one type of projection neuron types, making the analysis of any interneuronal phenotype very confusing.

To overcome these issues, we decided to take advantage of a genetic mouse model, the *Fezf2* null mutant, in which a specific population of cortical projection neurons is

exclusively absent from the cortex, the subcerebral projection neurons (including the CSMN); this subtype fails to develop and is replaced by another population of excitatory neurons, the callosal projection neurons (Chen et al., 2005a; Chen et al., 2008; Chen et al., 2005b; Molyneaux et al., 2005). This occurs without overall loss of projection neurons or changes in the total thickness of the cortex. Such a unique model allowed us to analyze the cortical distribution of inhibitory interneurons that results abnormal in the *Fezf2*$^{-/-}$cortex, with a concomitant aberrant cortical activity due to defective GABAergic inhibition across layers. The defect is projection neuron type-specific, since the generation of CPN in place of the missing subcerebral projection neurons cannot compensate for the observed interneuron abnormalities in the *Fezf2*$^{-/-}$ cortex.

In addition to the loss-of-function analysis, we performed gain-of-function experiments that further indicated that different types of projection neurons can affect interneuron positioning. Indeed, we experimentally generated either corticofugal projection neurons or layer II/III CPN in proximity to the cortex and we found ectopic presence of cortical interneurons within those clusters of projection neurons. In line with the loss-of-function results, the types of interneurons recruited by each projection neuron population are appropriate for the subtype-specific identity of the projection neurons generated, rather than strictly their experimental day of birth.

Therefore, we show that projection neurons are required for the laminar distribution of interneurons and, further, that distinct subtypes of projection neurons provide different interneuron populations with specific positional information. The data suggest that “circuit-pairing” of excitatory and inhibitory cortical neurons may be pre-defined at the time when both populations acquire their subtype-specific identity. In conclusions, individual types of projection neurons play critical roles in governing the radial distribution of GABAergic interneurons, a process that is critically important for the development of balanced cortical circuitry.

Materials and Methods

Mice

Fezf2$^{-/-}$ mice were generated by Hirata and colleagues (Hirata et al., 2004). Gad67::GFP mice were generated by Yanagawa and colleagues (Tamamaki et al., 2003) and crossed to *Fezf2*$^{+/-}$ to generate *Fezf2*$^{+/-}$/Gad67::GFP mice. Timed-pregnant CD-1 mice for *in utero* electroporation were obtained from Charles River Laboratories (Wilmington, MA). *Lhx6*-GFP BAC transgenic mice were obtained from GENSAT (Gong et al., 2003). SV129S1/SvImj strain mice were obtained from Jackson Laboratories (Bar Harbor, ME). The day of the vaginal plug was designated embryonic day 0.5 (E0.5). The day of birth was designated postnatal day 0 (P0). All mouse studies were approved by the Massachusetts General Hospital IACUC and were performed in accordance with institutional and federal guidelines.

CPN Retrograde labeling

Mice were anesthetized by hypothermia at P2 and injected with FG in the contralateral cortex (Arlotta et al., 2005). Six injections per pup were performed, with a total of 60–80 nl of FG per injection site. Pups were returned to the care of their mother and deeply anesthetized at P6 before perfusion and collection of the cortex for immunocytochemistry.

Immunocytochemistry, *in situ* hybridization and Cresyl Violet staining

Brains for immunocytochemistry were fixed by transcardial perfusion with PBS followed by 4% paraformaldehyde, and post fixed overnight at 4˚C in 4% paraformaldehyde. 40 μm coronal floating sections were blocked in 0.3% BSA (Sigma), 8% goat or donkey serum, and 0.3% Triton X-100 (Sigma) for 1 hour at room temperature, before incubation in primary antibody ((Arlotta et al., 2005). Primary

antibodies and dilutions were as follows: rabbit anti-TBR1 antibody, 1:2500 (gifts of R. Hevner); goat anti-SOX5 antibody, 1:500 (Santa Cruz); rat anti-CTIP2 antibody, 1:1000 (Abcam); rabbit anti-GFP, 1:500 (Invitrogen); chicken anti-GFP, 1:500 (Chemicon); rabbit anti-GABA, 1:1000 (Sigma); mouse anti-PV, 1:1000 (Chemicon); rabbit anti-CR, 1:1000 (Chemicon); mouse anti-SATB2, 1:50 (Santa Cruz); rat anti-BrdU, 1:400 (Accurate Chemical); rabbit anti-TLE4, 1:1000 (Santa Cruz); rabbit anti-CUX1, 1:100 (Santa Cruz); rabbit anti-NPY, 1:3000 (Immunostar); mouse anti-Reelin, 1:1000 (gift from A. Goffinet); rabbit anti-Caspase 3, 1:1000 (Pharmigen); chicken anti-betagalactosidease, 1:500 (Gentaur). Appropriate secondary antibodies were from the Molecular Probes Alexa series. Biotinylated secondary antibodies goat anti-rabbit and goat anti-chicken 1:200 (Vector Laboratories, Burlingame, CA) were used with standard avidin-biotin-diaminobenzidine visualization according to the manufacturer's protocol (Vector Laboratories, Burlingame, CA). Tissue sections were imaged using a Nikon 90i fluorescence microscope equipped with a Retiga Exi camera (Q-IMAGING) and analyzed with Volocity image analysis software v4.0.1 (Improvision). Cresyl violet staining was processed as previously described (Arlotta et al., 2005; Macklis, 1993). Fluorojade-C (Histo-Chem Incorporation, Jefferson, AR) staining was performed according to Schmued and Hopkins (2000) on 40μm-thick sections cut on a vibrating microtome. Nonradioactive *in situ* hybridization and combined *in situ* hybridization with immunohistochemistry were performed following published methods and using 40μm-thick sections cut on a vibrating microtome and mounted on superfrost slides (Fisher) (Tiveron et al., 1996). Riboprobes were generated by using the standard digoxigenin (DIG)-labeled cRNA probes method. cDNA template clones for: *Fezf2, Lpl, Inhba* and *Limch1*, were gifts of J. Macklis; *SST* and *VIP*, were gifts of J. Rubenstein; *Lhx6* was a gift of V. Pachnis; the *GAD67* probe was generated from cDNA using the following primers: 5'-CCTTCGCCTGCAACCTCCTCGAAC, 3'- GCGCAGTTTGCTCCTCCCCGTTCTT,

and cloned into the EcoRI site of pCR II-TOPO (Invitrogen) (Arlotta et al., 2005). To minimize the chance that more than one transcript might be recognized by the same probe, whenever possible, we designed the PCR primers to amplify the same gene-specific regions that were used as targets in oligo design by Affymetrix and compared them to the GenBank database by BLAST to exclude the possibility of selecting cDNA regions shared by more than one gene. Each clone was sequenced on both strands.

Cell quantification

For quantification of interneuron numbers in *Fezf2*$^{-/-}$ and wild type cortex, anatomically matched sections spanning motor, somatosensory and visual cortex were selected from littermate mice and processed by *in situ* hybridization to detect the *Gad67* transcript (n = 3 *Fezf2*$^{-/-}$; n = 3 wild type, 8-10 hemispheres per area, for each mouse at P28). Boxes of 300 pixels in width and spanning the entire thickness of the cortex were superimposed at matched locations on each section and divided into 10 equally-sized bins. *Gad67*-positive interneurons were quantified in each bin, and bin-distribution was defined as the percentage of interneurons in each bin relative to the total number of interneurons in all bins. *A priori* criteria were defined for analysis. All counts were performed by an investigator who was blinded to genotype and the paired, two-tailed t test was used for statistical analysis. All results are expressed as the mean ± s.e.m.

In order to assign bins to specific cortical layers, *Gad67 in situ* hybridization was combined with β-galactosidase immunostaining in the *Fezf2*$^{-/+}$ cortex, across all three areas sampled. Layer V spanned bins 4-5 in the motor and somatosensory cortex and bins 3-4 in the visual cortex. Layers VI and IV-II/III were defined as spanning bins located below and above layer V, respectively. For quantification of interneuron subtypes, anatomically matched sections spanning the somatosensory cortex were selected and processed by *in situ* hybridization to detect *SST* transcript (n=3 *Fezf2*$^{-/-}$; n=3 wild type, 8-

10 hemispheres per mouse at P28), or by immunocytochemistry to detect PV (*n*=3 *Fezf2*$^{-/-}$; *n*=3 wild type, 8-10 hemispheres per mouse at P28) and CR (*n*=3 *Fezf2*$^{-/-}$; *n*=3 wild type, 8-10 hemispheres per mouse at P28). Bin and layer distribution was calculated as described above.

For the quantification of interneuron-projection neuron ratio within layer V, 2 to 3 anatomically matched sections spanning the somatosensory area were selected from wild type mice (n=4) at P14 and immunostained for CTIP2, SATB2 and GABA. 850μm square boxes were superimposed at matched locations on each section and layer V was subdivided in Va (identified by high level SATB2-expressing nuclei) and Vb (identified by high level CTIP2-expressing nuclei). The number of GABA-positive interneurons was quantified in Va and Vb and divided by the total number of projection neurons located in each sublayer, respectively.

For quantification of *SST*-positive interneurons in the SV129S1/SvImJ strain, anatomically matched sections spanning the somatosensory area from littermate female mice were selected and processed by *in situ* hybridization to detect *SST* transcript (*n* = 3 with Pb; *n* = 3 with normal cc, 6 hemispheres per mouse at P28). Bin and layer distribution was calculated as described above.

For cell death quantification, anatomically matched sections spanning somatosensory cortex from littermate wild type and *Fezf2*$^{-/-}$ mice at P0, P7 and P14 were selected and processed for FluoroJade-C staining. All the results are expressed as the mean ± s.e.m. The paired, two-tailed *t* test was used for statistical analysis.

Voltage-sensitive dye imaging (VSDI)

Mice were decapitated under brief isoflurane anesthesia, then the brains were removed and placed into ice-cold ACSF (119 mM NaCl, 2.5 mM KCl, 1.0 mM NaH_2PO_4, 2.5 mM $CaCl_2$, 1.3 mM $MgCl_2$, 26.2 mM $NaHCO_3$, 20 mM glucose). Coronal slices (400

μm thick) were cut on a Microm HM 650 V vibratome and incubated in ACSF (35°C, 15 min). Slices were then transferred to ACSF containing the voltage-sensitive dye di-4-ANEPPS (0.25mM, Invitrogen) for 90 min at room temperature. Continuous oxygenation (95%) was applied throughout the entire cutting, incubation and imaging period.

Slices were imaged on an Olympus MVX10 microscope. A stimulating pulse (1 ms) was delivered through an ACSF-filled patch pipette to the white matter in V1. The resultant change in emitted dye fluorescence, corresponding to a change in membrane potential, was recorded using a MiCam Ultima (Brain Vision, SciMedia) camera (at 1 frame/ms). Changes in fluorescence were averaged across ten 512 ms trials using the MiCam Ultima analysis software. Regions of interest (125 μm^2) in the upper (150 μm below the pia) and lower layers (300 μm above the white matter) "on beam" to the stimulating electrode were analyzed for maximum change in intensity normalized to the resting intensity (ΔF/F).

***In utero* electroporation**

For control experiments, a vector containing IRES-EGFP under the control of a constitutively active CMV/beta actin promoter was used (*control*^{GFP}; generous gift of C. Lois, MIT). *Fezf2* was cloned into this vector to create the construct *Fezf2*^{GFP} for overexpression (Molyneaux et al., 2005). 750 nl of purified DNA (0.5-2.0 μg/μl) mixed with 0.005% Fast Green in sterile PBS was injected *in utero* into the lateral ventricle of CD1 embryos at E14.5 under ultrasound guidance (Vevo 660, VisualSonics) and electroporated into the neocortical ventricular zone essentially according to (Saito and Nakatsuji, 2001). Five 40 volt pulses of 50 ms duration at 1 second intervals were delivered in appropriate orientation across the embryonic head using 1 cm diameter platinum electrodes and a CUY21EDIT square wave electroporator (Nepa Gene, Japan). Similar conditions were used to inject and electroporate the U6 *APP* shRNA-2 construct, kindly provided by T. Young-Pearse (Young-Pearse et al., 2007). For characterization of

the *APP*-shRNA phenotype 0.5µg/µl of CAG-*GFP* vector was coeletroporated. Injected embryos were collected for analysis and tissue processing at P5-P6.

***In vitro* migration assay**

E12.5 MGE from *Lhx6*-GFP BAC were microdissected and cultured in three-dimensional matrigel matrix (Bekton-Dickinson, Billerica, MA) either alone or in close proximity to *Fezf2*-expressing aggregates of corticofugal neurons microdissected at E18.5 (electroporations at E14.5). Cocultures were incubated for 4 DIV in Neurobasal Medium (Invitrogen, San Diego, CA). All explants were cultured on glass coverslips coated with Poly-D-Lysine (Sigma-Aldrich, St. Louis, MO). For quantification, each MGE explant was divided into two subdivisions, proximal (P) and distal (D), and the ratio between the number of interneurons in P over that in D (P/D) was calculated to estimate polarized migration of interneurons towards the *Fezf2*-expressing neuronal explants (P/D>1), away from them (P/D<1) or unbiased growth in all directions (P/D=1).

BrdU birthdating

Timed pregnant CD-1 females received a single intraperitoneal injection of BrdU (50 mg/kg) at E12.5 or E14.5. Embryos were electroporated at E14.5, allowed to develop to P6 and then were perfused and processed for BrdU, GABA and GFP or SATB2 immunocytochemistry (Magavi and Macklis, 2001). Birthdating of interneurons within the experimental neuronal aggregates was done by counting the number of first-generation BrdU-positive cells that co-expressed GABA and that were localized within the perimeter of each GFP-positive or SATB2-positive aggregate. Numbers were expressed as a percentage of the total number of GABA-positive cells within each aggregate. The percentages of first-generation, Brdu- and GABA-positive interneurons in the deep and superficial layers of the overlying cortex were quantified using the same methods.

Results

Subcerebral projection neurons are selectively absent from the cortex of Fezf2$^{-/-}$ mice and are substituted by neurons with deep layer callosal projection neuron identity

It has been previously reported that loss of the transcription factor *Fezf2* results in the selective absence from the cortex of all subcerebral projection neurons, which fail to develop while other projection neuron types across all cortical layers are generated normally (Chen et al., 2005a; Chen et al., 2005b; Molyneaux et al., 2005). Importantly, loss of subcerebral neurons in this mutant is accompanied by the expansion of a different population of projection neurons with callosal projection neuron properties (Chen et al., 2008) without overall loss of neurons, defective migration or changes in cortical thickness (Molyneaux et al., 2005). Despite the developmental failure to generate subcerebral neurons, *Fezf2*$^{-/-}$ mice are viable and motile (Molyneaux et al., 2005). However, I observed that they are prone to develop seizures upon handling or exposure to auditory stimuli.

To determine whether the abnormal development of projection neurons in this mutant is sufficient to affect the distribution of cortical interneurons and, most importantly, whether specific subtypes of projection neurons play different roles, we first defined the precise nature of the CPN that replace subcerebral projection neurons in layer V of *Fezf2*$^{-/-}$ cortex. As expected, CTIP2, a central gene for subcerebral projection neurons was not expressed in layer V of the mutant cortex (Molyneaux et al., 2005). In contrast, TBR1, a marker of layer VI and layer II/III neurons, and SATB2, a protein important for CPN development, were both expanded (Chen et al., 2005b; Molyneaux et al., 2005)(and Fig. 3.1A-F) and were co-expressed in a new population of projection neurons that is located in layer Vb of the *Fezf2*$^{-/-}$ cortex (Fig. 3.1G-P).

To determine whether this exact population projects through the corpus callosum, we retrogradely labeled CPN of the mutant mice using FluoroGold (FG) injections in the contralateral hemisphere. Despite the fact that most CPN form Probst bundles (Pb) in this

mutant, making retrograde labeling from the contralateral cortex very inefficient, FG-labeled CPN were clearly visible within layer V. The FG-labeled neurons co-expressed TBR1 and SATB2, defining this expanded population as CPN (Fig. 3.2A-E). These data extend prior electrophysiological analysis and characterization of these neurons in chimeric mice by demonstrating that the neurons project through the corpus callosum (Chen et al., 2008). These CPN are distinct from the CPN of layer Va, which expressed SATB2 but not TBR1 (data not shown). CPN are a very heterogeneous population of neurons (Koralek and Killackey, 1990; Molyneaux et al., 2009; Reiner et al., 2003)

To precisely define the subtype-specific identity of CPN present in the mutant layer V, we analyzed the expression of three CPN-specific genes among several that were recently shown to label subpopulations of CPN in different layers (Molyneaux et al., 2009). *Lpl* labels CPN in layers V, VI and in the deeper part of layer II/III; *Inhba* selectively labels CPN of layer II/III; and *Limch1* is expressed in subpopulations of CPN within the upper part of layer II/III. In the *Fezf2*$^{-/-}$ cortex, *Lpl* expression was increased in layer V (Fig 3.2F,G; arrows), whereas expression of *Inhba* and *Limch1* remained unchanged (Fig. 3.2H-K; arrowheads). This molecular and hodological analysis indicates that CPN from layers Vb/VI, but not from layers Va or II/III, replace subcerebral projection neurons within layer V of the *Fezf2*$^{-/-}$ cortex.

GABAergic interneurons acquire abnormal radial distribution in the *Fezf2*$^{-/-}$ cortex

Fezf2$^{-/-}$ mice represent a unique mutant model in which a single projection neuron population fails to develop and is substituted by glutamatergic projection neurons of a different subtype-specific identity. This motivated us to use this mouse line to determine whether projection neurons control the laminar distribution of GABAergic interneurons, and, further, whether different types of projection neurons have different roles. we found both of these hypotheses to be correct. We used *in situ* hybridization for *GAD67* to

visualize the vast majority of cortical interneurons at P28 in wild type and *Fezf2*$^{-/-}$ littermates (Fig. 3.3A,B). First, we quantified the total number of *GAD67*-positive interneurons across the dorso-ventral extent of the cortex in serial matched sections representing three cortical areas: motor, somatosensory and visual cortex (n=3 wt; n=3 *Fezf2*$^{-/-}$). The total number of *GAD67*-positive interneurons did not differ between the wild type and mutant cortex (Fig. 3.3C), but the distribution of *GAD67* interneurons was distinctly abnormal in the *Fezf2*$^{-/-}$, with a larger percentage of interneurons in the superficial layers and reduced interneuron percentages in the deep layers (Fig. 3.3).

To precisely determine the radial distribution of *GAD67*-positive interneurons, we divided the cortex into 10 bins of equal size spanning the entire cortical thickness. Calculation of the percentage of interneurons located in each bin demonstrated a clear reduction of *GAD67*-positive interneurons within lower bins across the three cortical areas of the *Fezf2*$^{-/-}$ cortex. This difference was particularly prominent for bins 4-5 in the motor and somatosensory areas, and bins 3-4 for the visual area. The interneuron reduction in the lower bins was accompanied by an increase of interneurons in more superficial bins (Fig. 3.3 D-F,I-K,N-P). Double staining for *GAD67* and β−galactosidase (labeling subcerebral projection neurons) in heterozygote *Fezf2*$^{+/-}$ mice showed that bins with reduced percentages of interneurons mostly corresponded to layer V (Fig. 3.3G,L,Q). This anatomical information on layer positioning allowed me to assign bins to three groups spanning layers VI, V and II-III/IV. Analysis of interneuron distribution within each of these layers highlighted acute phenotypic abnormalities within layer V, which in the *Fezf2*$^{-/-}$ cortex showed a clear reduction in interneuron percentages (Fig. 3.3H,M,R). Reduced percentages of interneurons in *Fezf2*$^{-/-}$ layer V were observed across all cortical areas sampled and it was in agreement with the previously demonstrated lack of subcerebral projection neurons across medio-lateral and rostro-caudal positions of layer V in this mutant (Molyneaux et al., 2005). This was accompanied by increased interneuron

percentages in the *Fezf2*$^{-/-}$ superficial layers II-III/IV, a phenotype particularly evident in the somatosensory and visual areas (with a similar trend in the motor area). In contrast, layer VI remained unaffected (Fig. 3.3H,M,R).

To understand whether the reduced number of interneurons in layer V of the *Fezf2*$^{-/-}$ cortex might reflect a smaller number of interneurons normally associated with CPN compared to subcerebral projection neurons, we also quantified the number of GABA-positive interneurons surrounding these two projection neuron subpopulations within wild type layer V (Fig. 3.4). Indeed, we found that the number of interneurons associated with SATB2-expressing CPN in layer Va was significantly smaller than the number of interneurons associated with CTIP2-positive subcerebral projection neurons in layer Vb (n=3; p value=0.001). This suggests that the reduced numbers of interneurons observed in layer V of the mutant cortex (where CPN substitute subcerebral projection neurons) is in line with a typically lower number of cortical interneurons distributed around deep layer CPN.

Together, these data indicate that upon reaching the cortex, interneurons require projection neurons in order to acquire proper lamination. Furthermore, given that there is no overall loss of projection neurons in the *Fezf2*$^{-/-}$ cortex, but rather a precise replacement of one population of excitatory projection neurons (subcerebral projection neurons) with another (CPN), these findings demonstrate that different types of projection neurons differentially affect the distribution of cortical interneurons.

Fezf2$^{-/-}$ mice exhibit unbalanced cortical activity due to defective GABAergic inhibition

To determine whether the observed changes in interneuron distribution results in unbalanced cortical activity and physiology, with the expert help of Dr. Hensch's laboratory, we used voltage-sensitive dye imaging (VSDI) (Grinvald and Hildesheim,

2004) to examine spatio-temporal dynamics of functional connections in the *Fezf2*$^{-/-}$ mice. The spread of activity through coronal slices of the visual cortex in response to a current pulse delivered to the white matter was quantified. As expected, wild type and heterozygous *Fezf2*$^{+/-}$ mice exhibited a strong response that propagated rapidly to the upper layers "on beam" with the stimulating electrode, spreading only weakly along the deep layers even at threshold stimulating strengths (Fig. 3.5B). In contrast, the response in *Fezf2*$^{-/-}$ slices at threshold rarely reached the upper layers, and remained largely confined to the lower layers (Fig. 3.5A,C).

Maximum fluorescence intensity was quantified within two 125 mm^2 regions in-line with the stimulating electrode, one in upper layers (Fig. 3-5B,C; black box) and one in lower layers (Fig. 3.5B,C; white box). Input-output curves revealed an increase in upper layer response with increasing stimulus intensity, however the response failed to reach wild-type levels in the upper layers of *Fezf2*$^{-/-}$ mice across all stimuli (Fig. 3.5D,F). Conversely, lower layer responses were consistently stronger in *Fezf2*$^{-/-}$ mice compared to wild type (Fig. 3.5F). These differences were significant for both upper and lower layers at half maximal stimulation (Fig. 3.5E,G).

Physiological imbalance of excitation across cortical layers in *Fezf2*$^{-/-}$ cortex may be explained by abnormal excitatory networks, altered inhibitory GABAergic interneurons, or both. To distinguish among these possibilities, we performed VSDI measurements in the presence of the $GABA_A$ receptor antagonist bicuculline. Strikingly, the laminar differences between genotypes above were eliminated under these conditions, indicating that the excitatory network scaffold is intact in the *Fezf2*$^{-/-}$ mutant cortex. Taken together, an increased GABAergic tone in the superficial layers of the mutant cortex (without defects in excitatory network function) provides physiological support for our histological findings that interneuron numbers are reduced in layer V and increased in the upper layers II-III/IV of the *Fezf2*$^{-/-}$ cortex.

Fezf2 does not affect the fate specification of cortical GABAergic interneurons

Defects of interneuron fate specification or tangential migration could account for laminar abnormalities of interneuron function. Therefore we investigated whether *Fezf2* plays a cell-autonomous role in the fate specification or migration of GABAergic interneurons in the ventral forebrain, as this could potentially explain the abnormal lamination of interneurons observed in the mutant. Our laboratory, among others, has previously defined the expression pattern of *Fezf2* in the forebrain at E12.5, E13.5 (peak birth date of most MGE-derived interneurons), E15.5 (peak birth date of most CGE-derived interneurons), E18.5 (when interneurons are invading the cortical plate) and P7 (when interneurons have already positioned in cortex). We find that with the exception of a small area in the developing amygdala, *Fezf2* is absent from the entire ventral telencephalon, and is clearly not expressed in the MGE and CGE, where the majority of cortical GABAergic interneurons are born. In contrast, in the dorsal telencephalon, *Fezf2* was expressed in progenitors, and within the cortical plate at high levels in subcerebral projection neurons and at low levels in layer VI projection neurons (Chen et al., 2005a; Chen et al., 2005b; Hirata et al., 2004; Molyneaux et al., 2005; Rouaux and Arlotta, 2010).

Similarly, we found that *Fezf2* was not expressed in interneurons within the cortex, as assessed by crossing GAD67::GFP mice, in which interneurons are visualized by GFP reporter expression, with *Fezf2*$^{-/+}$ mice that carry a *LacZ* reporter gene inserted into the *Fezf2* locus. GFP-positive interneurons did not colocalize with β-galactosidase-positive and CTIP2-positive subcerebral neurons (Fig. 3.6A-F). In agreement with the absence of *Fezf2* expression in interneurons and their progenitors, expression levels of *Mash1* and *Nkx2.1,* which normally label and control the specification of early-born interneuron progenitors in the MGE, and *Lhx6,* which labels their postmitotic interneuronal progeny, were unchanged in the mutant (Fig. 3.6G-L). In addition, we used *COUPTF-II* to label

late-born interneuron progenitors within the CGE and found that wild type and mutant mice display comparable levels and distribution of this transcription factor (Fig. 3.6M,N).

Taken together, these data demonstrate that in the telencephalon *Fezf2* expression is excluded from GABAergic interneurons and does not affect expression of genes that are critical for interneuron fate specification. Therefore, the defective laminar distribution of *GAD67*-interneurons is not due to an intrinsic role of *Fezf2* in interneuron specification.

Subcerebral projection neurons are required for the proper distribution of SST- and PV-expressing interneurons, but not CR-expressing interneurons

Despite the fact that cortical interneuron subtype identities are diverse and it is not currently possible to precisely associate specific interneuron subtypes with strict layer locations, it is known that early-born, SST- and PV-expressing interneurons preferentially populate the deep layers of the cortex (Butt et al., 2008; Cobos et al., 2006; Fogarty et al., 2007). In contrast, mostly late-born, CR-expressing interneurons are present in higher numbers in the superficial cortical layers (Miyoshi et al., 2010; Nery et al., 2002; Xu et al., 2008). To define whether the absence of subcerebral projection neurons affects the distribution of all interneurons equally or exerts selective control over interneuronal populations that normally occupy the same deep layers of the cortex, we investigated the distribution of SST-, PV-, and CR-expressing interneurons in the *Fezf2*$^{-/-}$ mutant and wild type cortex.

Given that the distribution of *GAD67*-positive interneurons was abnormal in layer V across all areas sampled, we concentrated the analysis of interneuron subpopulations on one representative area: the somatosensory cortex. First, we studied the distribution of *SST*-expressing interneurons, since in the wild type cortex these interneurons are present in high numbers within layer V (Fig. 3.7A). We used *in situ* hybridization to detect *SST* in serial sections spanning the somatosensory cortex at P28 (n=3 wt; n=3 *Fezf2*$^{-/-}$). In

agreement with the *GAD67* data, the total number of *SST*-expressing neurons was unchanged in the mutant cortex compared to wild type (Fig. 3.7C), indicating that *SST*-interneurons are born correctly and migrate to the cortex. However, the appropriate laminar distribution of SST seen in layer V of the wild type cortex was strikingly altered in the mutant (Fig. 3.7A,B). The percentage of *SST*-interneurons was clearly decreased in layer V (corresponding to bins 4-5, as indicated by β-galactosidase expression in *Fezf2*$^{+/-}$) and increased in layers II-III/IV (bins 6-10) (Fig. 3.7D-F).

PV-expressing interneurons also showed abnormal radial distribution comparable to that of *SST*-interneurons (n=3 wt; n=3 *Fezf2*$^{-/-}$). The percentage of PV-expressing interneurons in the somatosensory cortex at P28 was decreased in layer V and increased in the upper layers II-III/IV, without a change in the total PV-positive interneuron number (Fig. 3.7G-L).

In stark contrast to the abnormal distribution of *SST*- and PV-expressing interneurons, CR-expressing interneurons, which are normally preferentially found in the superficial layers, were not affected by the absence of subcerebral projection neurons and were distributed normally in the P28 *Fezf2*$^{-/-}$ somatosensory cortex (n=3 wt; n=3 *Fezf2*$^{-/-}$) (Fig. 3.8A-F). These findings strongly suggest that distinct projection neuron subpopulations selectively and preferentially affect the distribution of cortical interneuron subtypes that are normally destined to populate the same cortical layers.

Interneuron reduction in layer V of *Fezf2*$^{-/-}$ cortex is not due to abnormal connectivity by CPN or interneuron cell death.

The reduced percentages of cortical interneurons in *Fezf2*$^{-/-}$ layer V suggest that CPN affect interneurons differently from the subcerebral projection neurons that they replace. However, factors independent from the subtype-specific identity of projection neurons may have influenced interneuron distribution in this mutant. Firstly, it is possible

that the presence of Probst bundles (Pb) and thus the altered connectivity by CPN across the corpus callosum may have affected their ability to interact with interneurons in the *Fezf2*$^{-/-}$ cortex. In order to understand whether development of Pb *per se* could cause the observed abnormalities, we analyzed the distribution of *SST*-expressing interneurons (the most affected population in the *Fezf2* mutant) in SV129S1/SvImJ wild type mice, a strain where females sporadically develop very large Pb without concomitant changes in other cerebral commisures or projection neuron fate specification (Wahlsten et al., 2003).

Quantification of the total number and dorso-ventral, binned distribution of *SST*-expressing interneurons in somatosensory areas of SV129S1/SvImJ female mice with Pb compared to matched female littermates with a normal corpus callosum (cc), showed no differences (total interneuron numbers, Pb mice: 125.93+/-6.23, n=3; control mice: 135.08+/-10.96, n=3; p value= 0.51) (Fig. 3.9A-E). This strongly suggests that abnormal connectivity by CPN to contralateral targets is not sufficient to influence interneuron layer positioning. In addition, our VSDI data show that projection neurons in the mutant cortex were excitable, a finding supported by prior electrophysiological recordings in mutant layer V (Chen et al., 2008). The data supports the hypothesis that CPN identity rather than connectivity primarily influenced interneuron distribution.

Secondly, increased interneuron cell death, either secondary to interneuron mispositioning, or due to reduced trophic support from projection neurons, among others, could have accounted for the reduced percentage of interneurons present in *Fezf2*$^{-/-}$ layer V (Cobos et al., 2006; Seah et al., 2008). To investigate this possibility, we performed staining for FluroJade-C, which broadly labels dying neurons, in wild type (n=3) and *Fezf2*$^{-/-}$ (n=3) cortex at 3 postnatal ages: P0, P7 and P14, by which time interneuronal abnormalities are already distinctly evident (data not shown). Comparison of the number of FluoroJade-C positive neurons in wild type and mutant somatosensory areas showed no differences at any of the ages sampled (Figure 3.9F-J). In addition, we did not detect any

increase in Caspase-3 staining in *GAD67*-expressing interneurons (Fig. 3.9K-N), a result that confirms and extends prior prenatal analysis of cell death in this mutant (Molyneaux et al., 2005). Together with the finding that the total number of interneurons is unchanged in the *Fezf2*$^{-/-}$ cortex at P28, these data demonstrate that increased cell death did not account for the abnormal distribution of cortical interneurons in this mutant.

De novo generation of corticofugal projection neurons is sufficient to recruit deep layer cortical interneurons to a new ectopic location

Loss-of-function data demonstrate that a fate switch between two specific populations of projection neurons in the cortex leads to a change in the distribution of specific subtypes of cortical interneurons. This suggests that different subtypes of projection neurons provide distinct signals to radially migrating interneurons, directing them to position in the correct layer. Signaling between projection neuron and interneuron subtypes may be a mechanism by which projection neuron classes instruct the recruitment of specific interneuron partners.

To investigate this possibility, we performed *in utero* electroporation to overexpress *Fezf2* within cortical progenitors at E14.5, a stage at which projection neurons of the superficial layers, mostly CPN of layer II/III, are normally generated. In agreement with previously published data (Molyneaux et al., 2005), elevated levels of *Fezf2* in late-stage neural progenitors instructed a fate switch resulting in the heterochronic generation of virtually pure populations of deep layer corticofugal projection neurons (including subcerebral projection neurons) instead of superficial layer CPN. Importantly, *Fezf2*-induced corticofugal projection neurons did not migrate radially into the cortex, likely due to accelerated differentiation into postmigratory neurons. Instead, they clustered ectopically within the germinal zone and developed immediately below the corpus callosum (Fig. 3-10C, arrow).

Despite their ectopic subcortical location, these neurons extend corticofugal axonal projections to the thalamus and the pons (Molyneaux et al., 2005). They expressed TBR1, TLE4 and SOX5, three markers of corticofugal projection neurons and CTIP2, which is expressed at high levels in subcerebral projection neurons (Fig. 3.10B-E,G-P). In addition, none of the *Fezf2*-induced neurons expressed SATB2 or CUX1, molecular markers of CPN (Fig. 3.10D,F,G,Q-S). Therefore, overexpression of *Fezf2* results in the generation of a new population of corticofugal projection neurons outside of (yet in close proximity to) the cortex. We examined expression of GABA in this system to visualize interneurons and to determine if any might be present within these ectopic neuronal clusters.

In contrast to contralateral matched locations, we found that many GABAergic interneurons invaded the aggregates of corticofugal projection neurons and were distinctly located within and around them (Fig. 3.11B-F). This finding was confirmed using *in situ* hybridization to detect ectopic *GAD67*-positive cells within these clusters (Fig. 3.11G-H'). We quantified the number of GABA-positive interneurons within each projection neuron aggregate and normalized it to the area covered by the GFP-positive corticofugal neurons. This area is proportional to the number of corticofugal projection neurons generated. Interestingly, the number of interneurons present in each aggregate directly correlated with the size of the aggregate (Fig. 3.12; Pearson's correlation coefficient r=0.8653; p value=0.0006, n=11), suggesting that projection neurons recruit cortical interneurons in proportion to their own numbers.

Strikingly, ectopic corticofugal projection neurons appear to play an attractive role upon cortical interneurons in an *in vitro* migration assay (Fig. 3.13). *Fezf2* was electroporated *in utero* in cortical progenitors at E14.5 as described above, and the induced clusters of corticofugal neurons were microdissected at E18.5 and cultured in proximity to explants of MGE derived from *Lhx6*-GFP positive, E12.5 embryos (Fig. 3.13D). As control explants, we cultured E12.5 MGE explants alone (Fig. 3.13A). As expected, MGE

explants cultured in isolation displayed unbiased outgrowth of GFP-positive interneurons in all directions around and away from the explant (Fig. 3.13B,C). In contrast, interneurons showed polarized migration towards the cluster of *Fezf2*-expressing corticofugal neurons (Fig. 3.13E,F). These results indicate that experimentally generated corticofugal projection neurons can attract cortical interneurons, a finding in agreement with prior data demonstrating that cortical plate neurons attract interneurons in a similar *in vitro* assay (Lopez-Bendito et al., 2008).

We then asked whether the ectopic clusters of corticofugal neurons recruit interneurons that are characteristic of the deep layers of the cortex. Remarkably, many *Lhx6*-positive and *SST*-positive interneurons, which normally populate primarily the deep cortical layers, were distinctly found within the corticofugal neuron aggregates (Fig. 3.14A-D'). In contrast, interneuron populations that are preferentially found in upper cortical layers were mostly absent from the aggregates. Among these, NPY-expressing interneurons, normally restricted to the superficial layers were not present in these clusters (Fig. 3.14G-J). Similarly, *VIP*-expressing interneurons, which show a less restricted, yet still preferential distribution in the upper layers, were only present in very low numbers, likely corresponding to those normally located in the deep layers (Fig. 3.14E-F'). Remarkably, Reelin, a gene that among interneurons labels those located in layers II/III and Va, the portion of layer V where CPN are located (Alcantara et al., 1998) (Fig. 3.14K") was absent from the corticofugal neuron aggregates (Fig. 3.14K-O).

Together with our earlier loss-of-function data indicating projection neuron influence on subtype-specific interneuron populations, these gain-of-function results support a model by which deep layer corticofugal projection neurons selectively affect the distribution of interneuron subtypes that normally localize to the same layers.

Ectopically positioned upper layer II/III callosal projection neurons can recruit cortical interneurons

The ability to recruit interneurons could be a unique property of deep layer corticofugal projection neurons or might be applicable, more broadly, to other types of projection neurons. To investigate this possibility directly, we experimentally induced ectopic clusters of a different population of cortical projection neurons - layer II/III callosal neurons and tested their ability to affect interneuron positioning. It has previously been shown that knock-down of the β–Amyloid Precursor Protein (*APP*) gene in rat cortical progenitors results in abrupt arrested migration of projection neurons (Young-Pearse et al., 2007). We took advantage of this system to focally arrest layer II/III CPN below the corpus callosum (Fig. 3.15).

A construct carrying an *APP* shRNA (referred to as U6-*APP* shRNA-2) was electroporated *in utero* together with a reporter CAG-*GFP* construct at E14.5, when upper layer CPN are normally generated. Mice were sacrificed at P6, by which time distinct clusters of neurons were visible below the corpus callosum (Fig. 3.15C). The location of these neuronal clusters corresponded precisely to that of the *Fezf2*-induced corticofugal neuron aggregates. Molecular characterization of neuronal subtype-specific identity showed that despite their ectopic position, these neurons expressed SATB2 and CUX1, and did not express CTIP2 (Fig. 3.15C-E), confirming that they differentiated appropriately into upper layer CPN. GABA immunocytochemistry on these CPN clusters (highlighted by the expression of SATB2) showed the distinct presence of GABA-positive interneurons within the aggregates, compared to matched positions in the contralateral hemisphere, which were virtually free of GABA-positive cells (n=9; Fig. 3.15B-F). The experiment was also performed in the rat with identical results (n=3).

These results demonstrate that layer II/III CPN are also able to recruit interneurons and further support a model by which projection neurons are generally able to affect

interneuron lamination.

Projection neurons recruit interneurons that are appropriate for their projection neuron subtype-specific identity and not strictly their birthdate

It is intriguing that cortical projection neurons and interneurons that are synchronically born preferentially populate the same cortical layers (Fairen et al., 1986; Miller, 1985; Peduzzi, 1988; Pla et al., 2006; Valcanis and Tan, 2003). Early-born (peak at E13), largely MGE-derived interneurons localize in deep layers, whereas late-born (peak at E15), largely CGE-derived interneurons occupy the superficial layers (Angevine and Sidman, 1961; Fairen et al., 1986; Miller, 1985; Peduzzi, 1988; Pla et al., 2006). Our finding that ectopic corticofugal projection neurons specifically recruit large numbers of *Lhx6*- and *SST*-expressing deep layer interneurons despite being born synchronically with superficial layer CPN led us to investigate whether the projection neuron-type identity, rather than strictly the projection neuron birth date, affects the choice of interneurons recruited.

We examined whether the *Fezf2*-induced corticofugal projection neurons heterochronically generated two days after the bulk production of endogeneous corticofugal neurons has ended (a stage when CPN of the superficial layers II/III are normally born) preferentially recruit either interneurons that are appropriate for their projection neuron-type identity (i.e. interneurons born at E12-E13) or, rather, interneurons appropriate for their heterochronic day of birth (i.e. interneurons born the day of the electroporation, at E14.5). In complementary experiments, we investigated whether upper layer II/III CPN that were synchronically born with *Fezf2*-induced corticofugal neurons at E14.5 and that were similarly positioned below the corpus callosum (due to *APP* knock-down), recruited interneurons born at the same time.

In separate animals, we administered intraperitoneally BrdU to timed-pregnant

females at either E12.5 or E14.5, combined with either *Fezf2* overexpression or *APP* downregulation in cortical progenitors at E14.5 (Fig. 3.16A). Mice were all sacrificed at P6. Quantification of BrdU-labeled, GABA-positive interneurons showed that heterochronic, late-born corticofugal projection neurons preferentially recruited interneurons that were born early, at E12.5 (Fig. 3.16A, C-H). These are appropriate for the deep-layer identity of the corticofugal projection neurons generated, but not for their heterochronic experimental birthdate (E14.5). In agreement with the E14.5 experimental birthdate of the corticofugal projection neurons generated, we found that neuronal aggregates contained high numbers of Brdu-labeled cells at E14.5 (Fig. 3.16H). These cells did not express GABA, however, and most corresponded to the corticofugal neurons generated that day. Confirming the specificity of this effect, we found that upper layer II/III CPN populations born the same day as the experimentally generated corticofugal neurons specifically attracted late-born interneurons (Fig. 3.16A,I-N). This is noteworthy, since in this experimental system, corticofugal neurons and layer II/III CPN shared the same day of birth and were similarly located below the cortex, giving them access to comparable pools of cortical interneurons.

To precisely determine whether the relative distribution of early- and late-born interneurons found in these aggregates corresponded to the distribution normally present in the deep or superficial layers of the cortex, we quantified the number of E12.5- and E14.5-born interneurons within the deep and superficial layers of the cortex overlying the aggregates. As expected, we found an "inside-out" distribution of cortical interneurons depending on their respective birthdates. Strikingly, *Fezf2*-corticofugal aggregates had similar relative proportions of early- and late-born interneurons as found in the deep layers of the cortex (Fig. 3.16A,B). In a complementary trend, *APP* shRNA-layer II/III CPN showed the same distribution of early- and late-born interneurons as present in the superficial layers (Fig. 3.16A,B). We conclude that cortical projection neurons select

interneuron partners that are appropriate for their specific projection neuron identity and not strictly based on synchronic birthdates.

Discussion

One of the most prominent traits of the mammalian cerebral cortex is its complex cellular architecture, which relies on the development of a diversity of neurons extensively interconnected into functional networks. Cortical excitation and inhibition are executed by highly heterogeneous populations of glutamatergic excitatory projection neurons and GABAergic inhibitory interneurons, respectively. Remarkably, although generated from distally-located germinal zones, projection neurons and interneurons are juxtaposed within cortical laminae (Fairen et al., 1986; Miller, 1985; Peduzzi, 1988; Pla et al., 2006). The establishment of correct reciprocal positioning and interactions between these two broad neuronal classes is critical for balanced electrical activity and normal cortical function. Here, we demonstrate that projection neurons are necessary to determine the laminar positioning of interneurons during cortical development, ultimately affecting the function of the local inhibitory microcircuitry. This effect is dependent on the subtype-specific identity of projection neurons, which selectively and preferentially affect the lamination of the subclasses of interneurons normally located in their same layers. The data support a model by which the molecular identity of projection neuron and interneuron subtypes ultimately determines their pairing in the cortex.

Projection neurons control interneuron positioning in the cerebral cortex

Many factors have the potential to affect the laminar distribution of interneurons, including cell fate-specification and their tangential and radial migration. Defining the independent contribution of each of these developmental events has been problematic. In particular, the inability to uncouple cell-intrinsic determinants of interneuron development from cell-extrinsic guidance by the environment of the cortex has constrained studies aimed at defining the roles of projection neurons in this process. Our finding that loss of *Fezf2* does not affect the birth, early specification or ventral migration of interneurons

allows us now to overcome this hurdle. We find that projection neurons are cell-extrinsically required for the normal lamination of cortical interneurons, an effect that is not secondary to interneuron fate specification.

These findings are consistent with observations made for the *reeler* mouse, in which cortical projection neurons are abnormally distributed in the cortex and interneurons demonstrate defective radial distribution (Hevner et al., 2004; Pla et al., 2006; Yabut et al., 2007). This conclusion is also supported by our gain-of-function experiments, which demonstrate that projection neurons are not only required for proper interneuron positioning, but are also sufficient to recruit appropriate interneurons to ectopic locations. It is remarkable that the clusters of projection neurons generated ectopically by either overexpression of *Fezf2* or by *APP* knock-down are populated by GABAergic interneurons. The fact that ectopic clusters of both corticofugal neurons and layer II/III callosal neurons contain interneurons indicates that the ability to recruit GABAergic interneurons may be a general property of all projection neuron subpopulations of the cortex.

Mechanistically, projection neurons might affect interneuron positioning in different ways, by attracting, arresting or stabilizing them at specific locations, for example. In these regards, our *in vitro* data indicate that isolated corticofugal neurons can indeed attract interneurons, a finding that is in agreement with earlier work showing that explants of cortical plate can also attract interneurons in similar conditions (Lopez-Bendito et al., 2008). In addition, the role of projection neurons over interneuron lamination could be strictly local or also rely on a population-level contribution.
In the future, it will be important to investigate these mechanistic questions.

Distinct types of projection neurons uniquely affect interneuron lamination

Within the broader role of projection neurons in cortical interneuron lamination, it

is an open question whether individual subtypes of projection neurons provide interneurons with different signals. Finding an answer to this fundamental question of cortical development is complicated by several factors, not the least of which is the fact that cortical projection neurons and interneurons are among the most diverse and heterogenous classes of neurons in the central nervous system (Markram et al., 2004; Molyneaux et al., 2007). The *Fezf2* mutant cortex provides a first model with which to directly address the function of projection neuron subtypes.

Loss of *Fezf2* results in a precise fate-switch between two types of projection neurons: subcerebral projection neurons, which fail to develop, and are replaced by deep layer CPN, in the same layer (Chen et al., 2005a; Chen et al., 2005b; Molyneaux et al., 2005). We find that this simple switch of fate between projection neuron types in layer V is sufficient to affect interneuron radial distribution, indicating that CPN possibly produce different guidance or arrest cues for interneurons compared to subcerebral projection neurons. This occurs despite the fact that the two highly related projection neuron populations normally occupy the same cortical layer and are synchronically generated. Notably, CPN cannot compensate for subcerebral projection neurons in the recruitment of appropriate numbers of *SST*- and PV- interneurons despite the fact that CPN are normally present within wild type layer V, where both SST- and PV-interneurons are located.

This could be due to different mechanisms of interneuron sorting used by subcerebral projection neurons compared to CPN, a possibility supported by our finding that CPN of layer V are normally surrounded by fewer interneurons. It is also possible that they interact with different subpopulations of *SST*- and PV-interneurons. Indeed it is well known that both *SST* and PV populations are very diverse at the cytological, electrophyisiological and molecular levels (Batista-Brito and Fishell, 2009; Markram et al., 2004). The implications of these findings therefore extend beyond the conclusion that different layers produce different signals, and argue that even within the same layer not all

projection neuron subtypes act identically. Individual populations of projection neurons affect interneurons in a unique manner.

SST- and PV-positive interneurons are specifically affected in the *Fezf2* null-mutant

The classification of interneuron subtypes is extremely complex, with different subclasses defined based on molecular, morphological and electrophysiological characteristics (Ascoli et al., 2008). Within the limits of this partial classification, it is known that MGE-derived, early-born SST-positive and PV-positive (both *Lhx6*-positive) interneurons preferentially populate the deep layers of the cortex, whereas CR-positive, late-born, interneurons preferentially populate the superficial layers. Here, we find that *SST*- and PV-positive populations are sensitive to the absence of subcerebral projection neurons, but the CR-positive interneurons are unaffected.

Given that cell-cell interactions typically rely on the expression of complementary sets of molecules by the cells involved, it follows that populations of interneurons might express different surface molecules, which enable them to respond differently to projection neurons. Intriguingly, this may explain why a recently identified population of Reelin-positive CGE-derived interneurons preferentially locate within the upper layers even if they are born early, at E12.5 (Miyoshi and Fishell, 2010). These early-born CGE-derived interneurons might not be molecularly capable of responding to arrest signals provided by deep layer projection neurons and are exclusively sensitive to cues presented by superficial layer projection neurons. Indeed, our ectopic, deep layer corticofugal neurons do not recruit these early-born Reelin-positive interneurons. It is noteworthy that even CR-interneurons located in layer V are not affected by the fate-switch of subcerebral projection neurons into CPN, and position themselves normally in the *Fezf2*$^{-/-}$ cortex. This is in stark contrast to *SST*- and PV-interneurons of the same layer, suggesting that CR-interneurons in layer V might respond equally well to subcerebral projection neurons and

CPN within this layer.

The data support a model of selective interaction among projection neuron and interneuron subtypes, a conclusion in agreement with our gain-of-function results that *Lhx6*- and *SST*-positive interneurons (which normally populate the deep layers) are recruited by corticofugal neurons, while *VIP*-, NPY- and Reelin-positive interneurons of the superficial layers are not. Taken together, these data offer a picture of the striking precision with which different subtypes of projection neurons in the neocortex can affect the radial distribution of selected classes of interneurons.

Cortical projection neurons selectively recruit local interneurons based on subtype-specific identity rather than strictly by birthdate

Projection neurons and interneurons that share similar birthdates preferentially populate the same cortical layers (Fairen et al., 1986; Miller, 1985; Peduzzi, 1988; Pla et al., 2006; Valcanis and Tan, 2003). This may be explained by different mechanisms, including the possibility (supported by our data) that pairing of synchronically-born projection neurons and interneurons relies on the expression of complementary molecules, which may have evolved to ensure the coordinated positioning of populations born at the same time. Should this model be correct, then the "molecular identity" of projection neurons, rather than strictly their date of birth, would affect interactions with the correct types of interneurons.

In our gain-of-function experiments, we tested this hypothesis by changing the birth date of a projection neuron subpopulation, without affecting its molecular identity. We demonstrated that the ectopic generation of deep layer corticofugal projection neurons at the wrong time (when superficial layer neurons are normally born) is sufficient to preferentially recruit early-born interneurons, which are appropriate for the deep layer identity of the projection neurons generated and not for their experimentally-imposed time

of birth. This finding is reinforced by the fact that the recruited interneurons expressed *Lhx6* and *SST*, two markers of early-born interneurons that normally locate in the deep cortical layers. Notably, this selection-based mechanism of differential interneuron sorting is directly supported by the data that layer II/III CPN born at the same time as the *Fezf2*-induced corticofugal neurons (and occupying similar subcortical locations) select late-born interneurons, as appropriate for their upper layer CPN identity.

This implies that the pairing into circuitry of cortical projection neuron and interneuron partners might be "pre-programmed" during early stages of fate-specification of each neuron type, possibly days before interneurons acquire their final position in the appropriate cortical layers. This study provides a new conceptual framework for exploration of the mechanisms controlling subtype-specific interactions between selected populations of projection neurons and interneurons. In light of our findings, future strategies to identify the molecular mechanisms controlling precise laminar positioning of interneurons may require the purification and molecular comparison of the correct subtypes of "interacting" projection neurons and interneurons, rather than a more general analysis of the two broad neuronal populations independently.

Understanding the developmental events that regulate subtype-specific interactions between projection neurons and interneurons in the cerebral cortex will provide further insights into the basic developmental processes that establish local cortical microcircuitry (Hensch and Fagiolini, 2005) and may inspire tools with which to modulate these circuits in epileptic and psychiatric diseases.

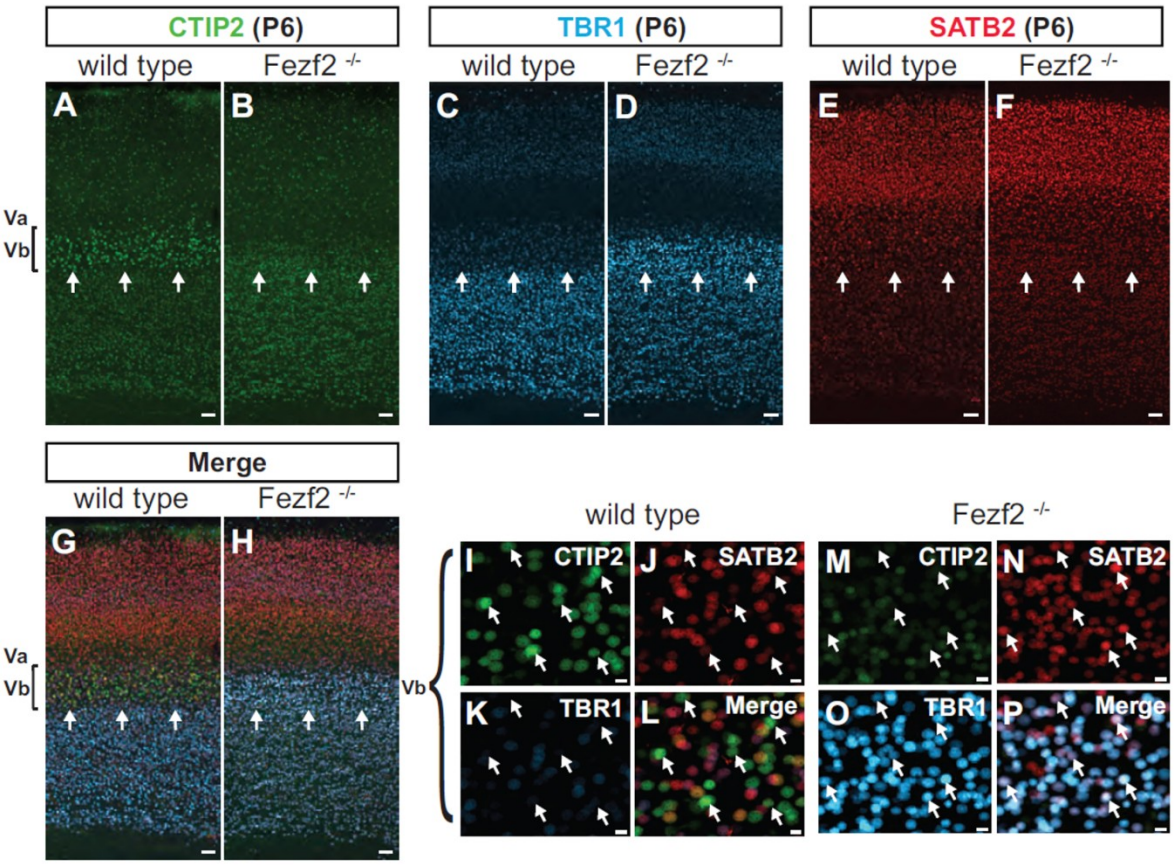
CTIP2 (P6)
wild type
Fezf2 -/-
TBR1 (P6)
wild type
Fezf2 -/-
SATB2 (P6)
wild type
Fezf2 -/-
A
B
C
D
E
F
Va
Vb
Merge
wild type
Fezf2 -/-
G
H
Va
Vb
wild type
Fezf2 -/-
I CTIP2
J SATB2
K TBR1
L Merge
M CTIP2
N SATB2
O TBR1
P Merge
Vb

Figure 3.1

Figure 3. 1. Loss of *Fezf2* results in the absence of all subcerebral projection neurons and the expansion in layer V of a new population of TBR1- and SATB2-positive projection neurons.

(A-P) Immunocytochemical analysis of projection neuron type-specific markers in *Fezf2*$^{-/-}$ and wild type cortex showing that all CTIP2-positive subcerebral projection neurons are absent from the mutant (A,B, arrows), and a population of neurons expressing TBR1 and SATB2 has expanded to take the place of the missing subcerebral projection neurons (CP, arrows). (I-P) High-magnification images in layer Vb of wild type (I-L) and *Fezf2*$^{-/-}$ (M-P) cortex showing that TBR1-positive neurons in mutant layer V co-express SATB2 and do not express CTIP2. Scale bars, 100 μm (A-H), 20μm (I-P).

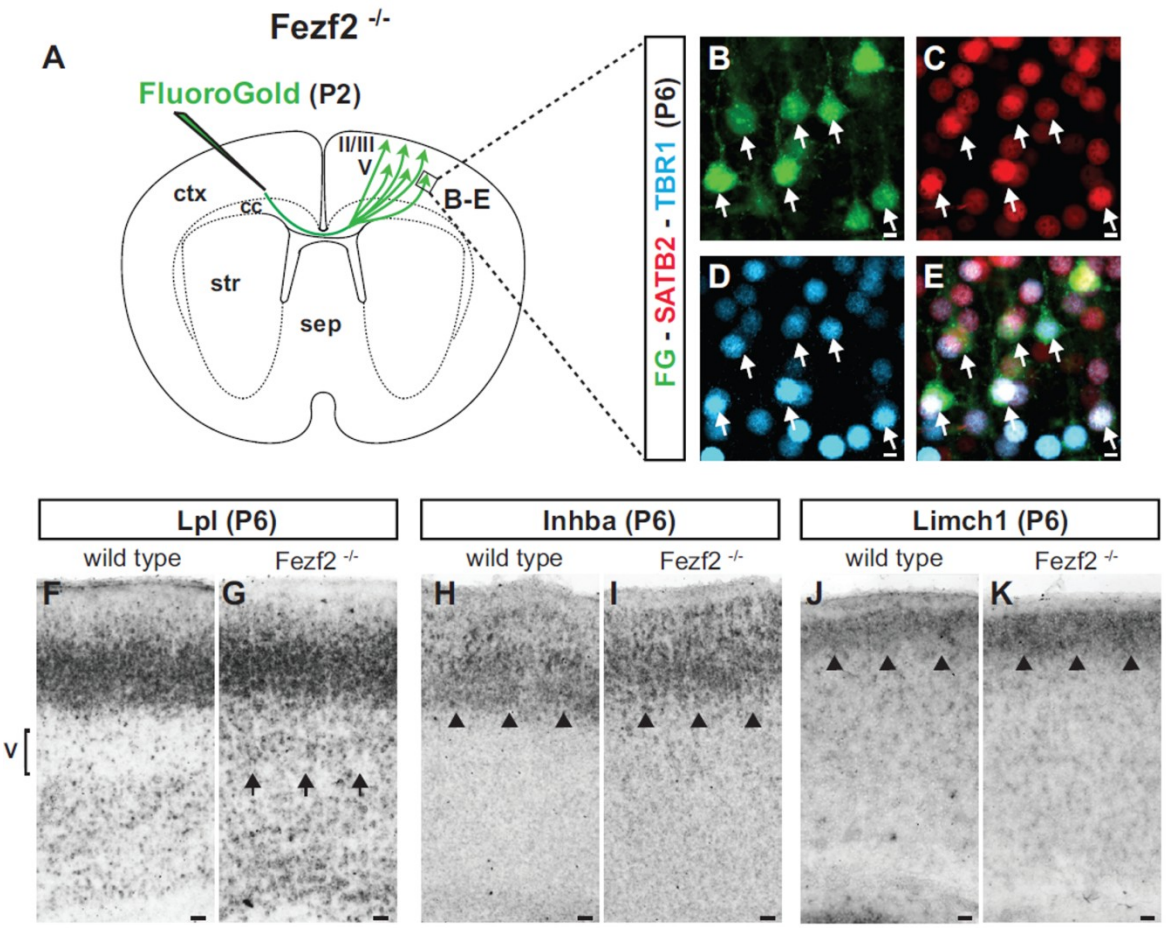
A
Fezf2 -/-
FluoroGold (P2)
ctx
cc
II/III
V
B-E
str
sep
FG - SATB2 - TBR1 (P6)
B
C
D
E
Lpl (P6)
Inhba (P6)
Limch1 (P6)
wild type
Fezf2 -/-
F
G
H
I
J
K
V

Figure 3.2

Figure 3. 2. Neurons that replace subcerebral projection neurons in *Fezf2*$^{-/-}$ cortex are CPN of deep layer identity.

(A-E) Retrograde labeling of CPN in contralateral *Fezf2*$^{-/-}$ cortex shows colocalization of FG with the expanded population of TBR1- and SATB2 -positive neurons in layer V. (F-K) *In situ* hybridizations at P6 for *Lpl, Inhba* and *Limch1* (CPN markers), showing that the expanded population of CPN in *Fezf2*$^{-/-}$ layer V are of deep layer identity. Scale bars, 100 μm (F-K), 20 μm (B-E). (See also Figure 3.1)

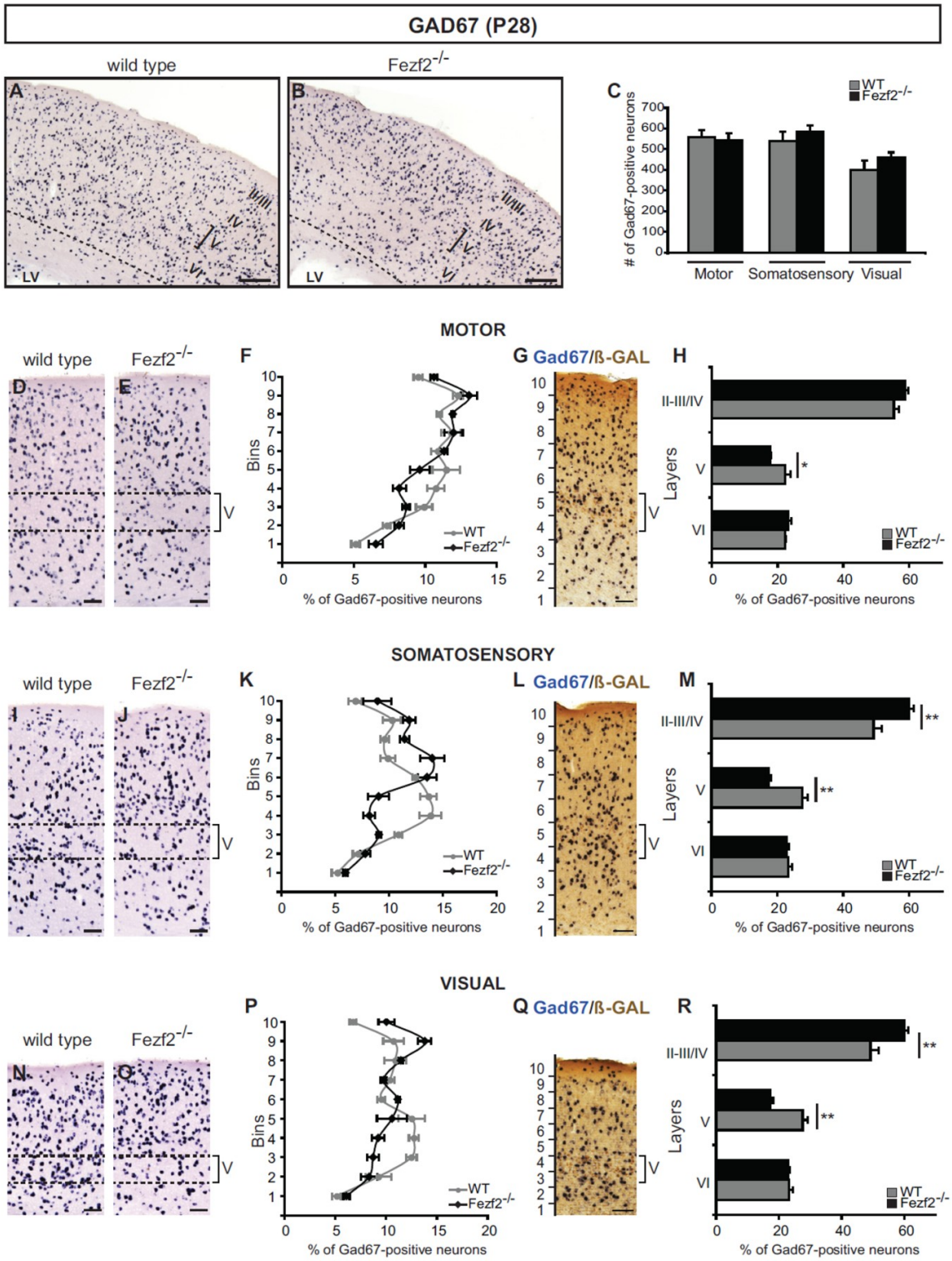
GAD67 (P28)
wild type
Fezf2-/-
A
B
LV
C
WT
Fezf2-/-
# of Gad67-positive neurons
Motor
Somatosensory
Visual
MOTOR
wild type
Fezf2-/-
D
E
V
F
Bins
% of Gad67-positive neurons
G Gad67/ß-GAL
H
II-III/IV
V
VI
Layers
*
SOMATOSENSORY
I
J
K
L Gad67/ß-GAL
M
**
VISUAL
N
O
P
Q Gad67/ß-GAL
R

Figure 3.3

Figure 3. 3. The *Fezf2*$^{-/-}$ cortex has abnormal radial distribution of GABAergic interneurons.

(A,B) *In situ* hybridization for *Gad67* in wild type (A) and *Fezf2*$^{-/-}$(B) cortex at P28 shows reduced numbers of interneurons in layer V and increased numbers in superficial layers of the *Fezf2*$^{-/-}$ cortex. (C) Total number of *Gad67*-interneurons is unchanged between wild type and *Fezf2*$^{-/-}$ cortex. (D-R) Quantification of the layer distribution of *Gad67*-interneurons across motor (D-H), somatosensory (I-M) and visual (N-R) cortex. (D,E,I,J,N,O) Representative sections of wild type and *Fezf2*$^{-/-}$ cortex. (F,K,P) Unbiased binned distribution of *Gad67*-interneuron percentages shows decreased percentages in deep bins and increased percentages in superficial bins of the mutant. (G,L,Q) β-galactosidase immunocytochemistry in *Fezf2*$^{+/-}$ heterozygote mice demonstrates that layer V corresponds to bins 4-5 (in motor and somatosensory cortex) and bins 3-4 (in visual cortex). (H,M,R) Quantification of interneurons within layers demonstrates a specific reduction in interneuron percentages in mutant layer V across all cortical areas, and an increase in interneuron percentages in layers II/III-IV. All results are expressed as the mean ± s.e.m.. LV, lateral ventricle. Scale bars, 500 μm (A,B); 200 μm (D,E,G,I,J,L,N,O,Q).

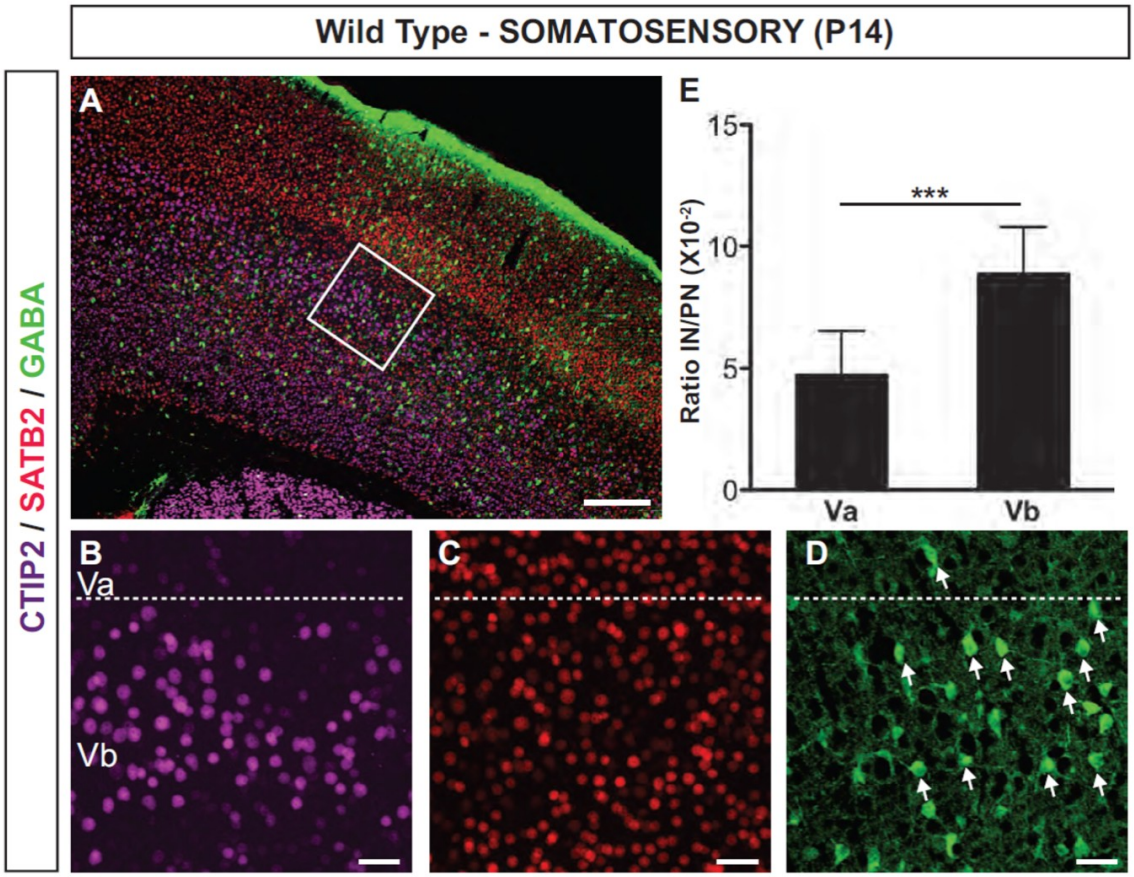
Wild Type - SOMATOSENSORY (P14)
CTIP2 / SATB2 / GABA
A
B
Va
Vb
C
D
E
Ratio IN/PN (X10-2)
15
10
5
0
***
Va
Vb

Figure 3.4

Figure 3. 4. A different ratio between interneurons and projection neurons is found in layer Va compared to Vb.

(A-D) Immunocytochemistry for CTIP2, SATB2 and GABA on coronal section of P14 wild-type cortex shows that a higher number of GABA-positive neurons are found in layer Vb compared to layer Va. (E) Quantification of the number of interneurons within cortical layers Va or Vb per 100 projection neurons (defined as CTIP2- and or SATB2-positive neurons). Scale bars, 500 μm (A) and 100 μm (B-D).

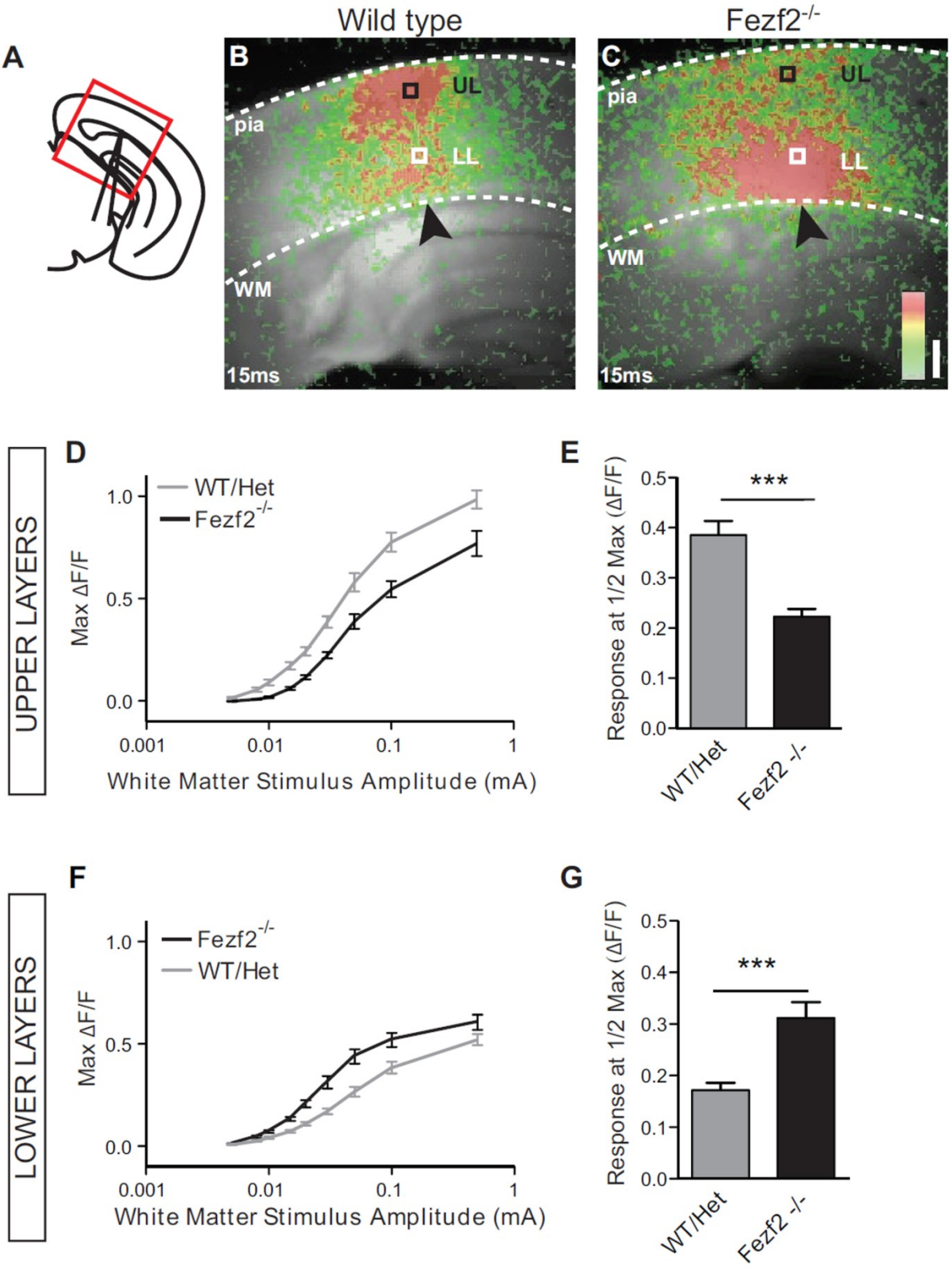
Wild type
Fezf2-/-
A
B
C
UL
LL
pia
WM
15ms
UPPER LAYERS
D
E
WT/Het
Fezf2-/-
Max ΔF/F
White Matter Stimulus Amplitude (mA)
Response at 1/2 Max (ΔF/F)
***
WT/Het
Fezf2 -/-
LOWER LAYERS
F
G

Figure 3.5

Figure 3. 5. Spread of neuronal activity is restricted to the deep layers in *Fezf2*$^{-/-}$ cortex.

(A) Schematic of recording area (red box) indicating the position of the stimulating electrode in the white matter (WM). (B,C) Pseudocolor peak response frames from VSDI movies of wild type (B) and *Fezf2*$^{-/-}$ (C) slices 15 ms after the stimulus (arrowhead), showing that wild type mice exhibit a strong stimulus response that propagates rapidly to the upper layers (B); whereas, the response in *Fezf2*$^{-/-}$ slices rarely reaches the upper layers, remaining largely confined to the lower layers (C). Black and white squares indicate quantified regions of interest in the upper (UL) and lower layers (LL), respectively. Scale bars, 250 μm. (D,F) Stimulus response curve in the regions of interest for upper (D) and lower (F) layers. (E, G) Response at half max. *** $p<0.001$, t-test. (See also Movies S1, S2, S3 and S4).

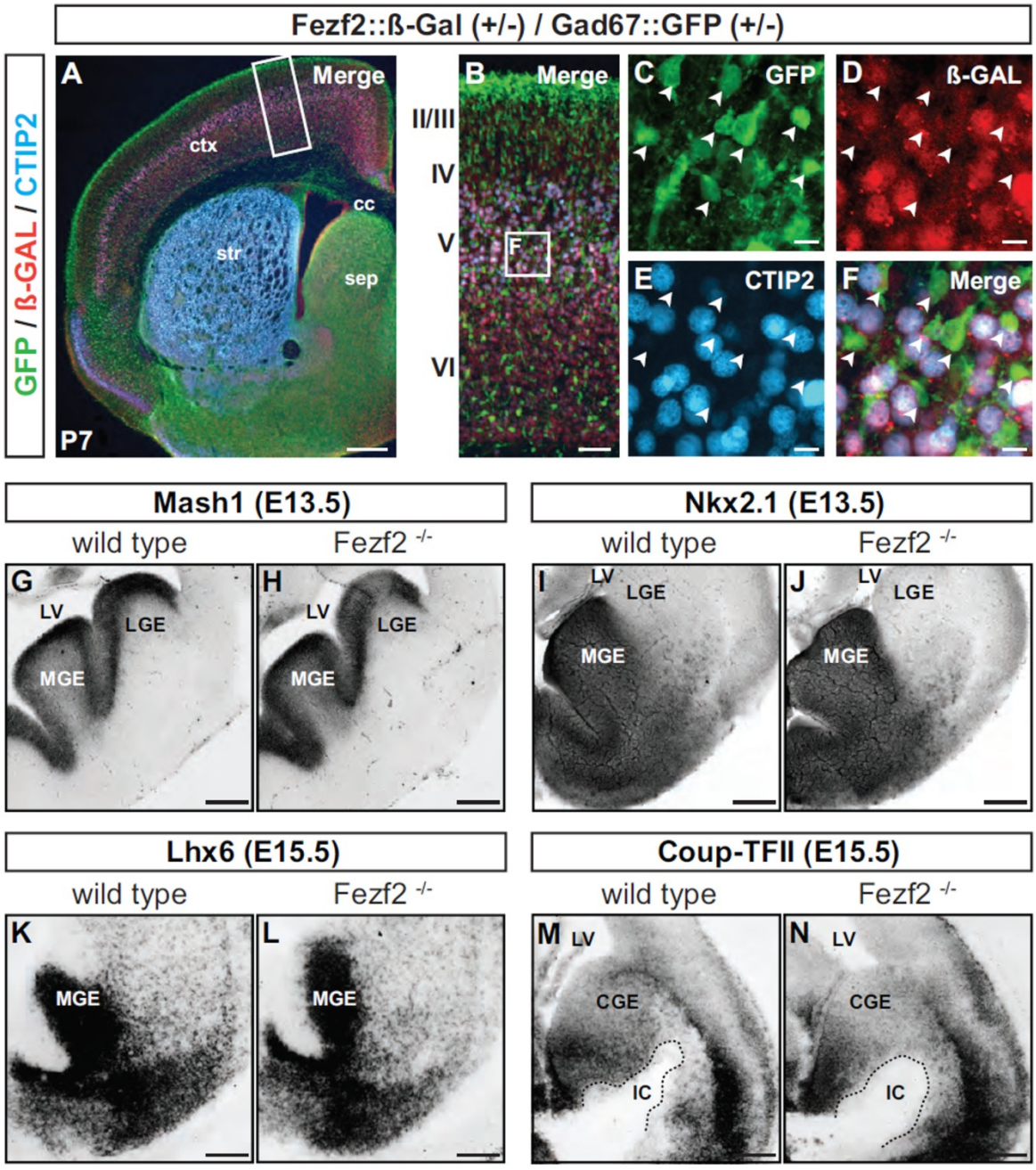
Fezf2::ß-Gal (+/-) / Gad67::GFP (+/-)
GFP / ß-GAL / CTIP2
A
Merge
ctx
cc
str
sep
P7
B
Merge
II/III
IV
V
VI
F
C
GFP
D
ß-GAL
E
CTIP2
F
Merge
Mash1 (E13.5)
wild type
Fezf2 -/-
G
LV
LGE
MGE
H
LV
LGE
MGE
Nkx2.1 (E13.5)
wild type
Fezf2 -/-
I
LV
LGE
MGE
J
LV
LGE
MGE
Lhx6 (E15.5)
wild type
Fezf2 -/-
K
MGE
L
MGE
Coup-TFII (E15.5)
wild type
Fezf2 -/-
M
LV
CGE
IC
N
LV
CGE
IC

Figure 3.6

Figure 3. 6. *Fezf2* is excluded from GABAergic cortical interneurons and loss of *Fezf2* does not affect the birth and specification of cortical interneurons in the ventral telencephalon.

(A-F) Mice resulting from a cross of *Fezf2*$^{+/-}$::*LacZ* to GAD67-GFP mice display colocalization of β-galactosidase with CTIP2 in subcerebral projection neurons but not with GABAergic interneurons. (G-N) *In situ* hybridization for *Mash1* (G,H) and *Nkx2.1* (I,J) on coronal sections of the wild type and *Fezf2*$^{-/-}$ forebrain at E13.5 showing no difference in expression levels or distribution of the transcription factors in the MGE. (K,L) *In situ* hybridization for *Lhx6* on coronal sections of wild type and *Fezf2*$^{-/-}$ forebrain at E15.5 showing no differences in expression in postmitotic interneurons of the MGE. (M,N) *In situ* hybridization for *Coup-TFII* on coronal sections of the wild type and *Fezf2*-/- forebrain at E15.5 showing no differences in expression or distribution in the CGE. cc, corpus callosum; ctx, cortex; str, striatum; sep, septum; LV, lateral ventricle; LGE, lateral ganglioning eminence; MGE, medial ganglionic eminence; CGE, caudal ganglionic eminence; ic, internal capsule. Scale bars, 500 μm (A,G-N); 100 μm (B); 20 μm (C-F).

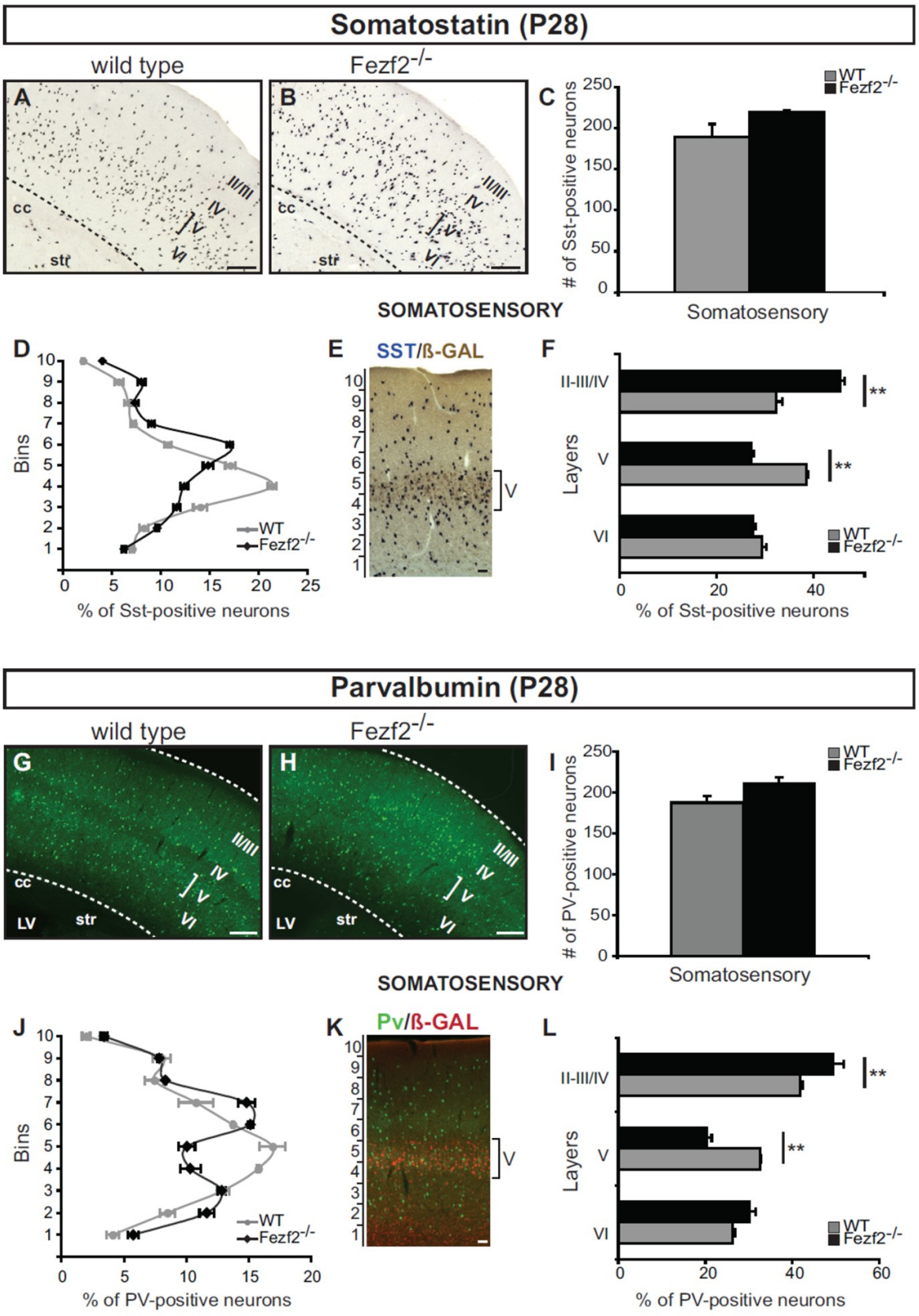
Somatostatin (P28)
wild type
Fezf2-/-
A
B
cc
str
I/II/III
IV
V
VI
C
WT
Fezf2-/-
# of Sst-positive neurons
250
200
150
100
50
0
Somatosensory
SOMATOSENSORY
D
Bins
% of Sst-positive neurons
WT
Fezf2-/-
E
SST/ß-GAL
V
F
II-III/IV
V
VI
Layers
**
Parvalbumin (P28)
G
H
LV
I
# of PV-positive neurons
J
K
Pv/ß-GAL
L
% of PV-positive neurons

Figure 3.7

Figure 3. 7. *SST*- and PV-interneuron subtypes are reduced in layer V and increased in the superficial layers of the *Fezf2*$^{-/-}$ cortex.

(A,B,G,H) *In situ* hybridization for *SST* (A,B) and immunocytochemistry for PV (G,H) in wild type and *Fezf2*$^{-/-}$ somatosensory cortex at P28 show reduction of both interneuron populations in layer V and increase in upper layers. (C,I) Total number of *SST*- (C) and PV- (I) interneurons is unchanged between wild type and *Fezf2*$^{-/-}$ cortex. (D,J) Unbiased binned distribution of *SST*- and PV-interneuron percentages shows decreased numbers in deep bins and increased numbers in superficial bins of the mutant. (E,K) β-galactosidase immunocytochemistry in *Fezf2*$^{+/-}$ heterozygote mice highlights layer V in bins 4-5. (F,L) Quantification of *SST*- (F) and PV- (L) interneurons within layers demonstrates a reduction in the percentages of both interneuronal subpopulations in mutant layer V and an increase in layers II/III-IV. All results are expressed as the mean ± s.e.m.. LV, lateral ventricle; str, striatum; cc, corpus callosum. Scale bars, 500 μm (A,B,G,H); 100 μm (E,K).

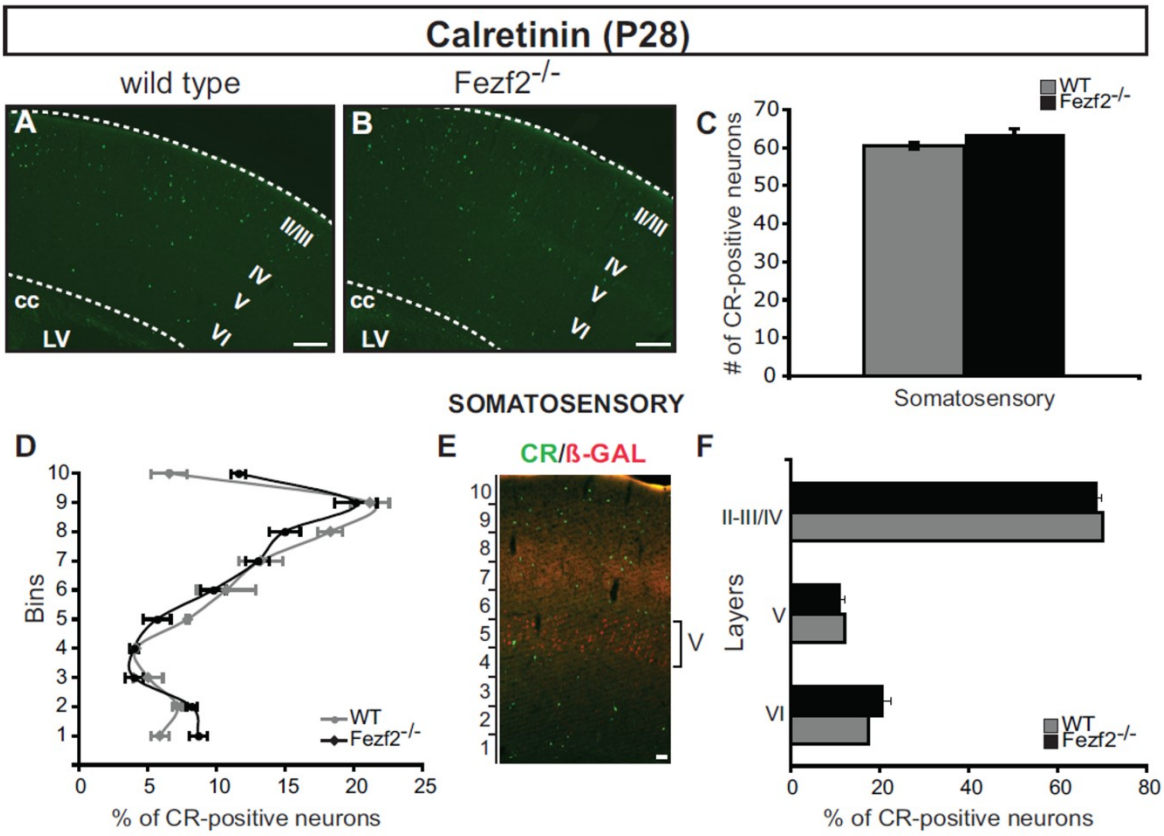
Calretinin (P28)
wild type
Fezf2-/-
A
B
cc
LV
II/III
IV
V
VI
C
WT
Fezf2-/-
# of CR-positive neurons
Somatosensory
SOMATOSENSORY
D
Bins
% of CR-positive neurons
E
CR/ß-GAL
F
II-III/IV
Layers
V
VI
% of CR-positive neurons

Figure 3.8

Figure 3. 8. Radial distribution of CR-positive interneurons is not affected in *Fezf2*$^{-/-}$ cortex

(A,B) Immunocytochemistry for CR on coronal sections of wild type and *Fezf2*$^{-/-}$ somatosensory cortex at P28 shows similar distributions for CR-positive interneurons. (C) Quantification of the total number of CR-interneurons showing no differences between wild type and *Fezf2*$^{-/-}$ cortex. (D) Unbiased binned distribution of CRinterneuron percentages along the dorso-ventral axis of wild type and *Fezf2*$^{-/-}$ cortex shows no differences. (E) β-galactosidase immunocytochemistry in *Fezf2*$^{+/-}$ heterozygote mice highlights the bins spanning layer V (4-5) and enables assignment of layer location to different groups of bins. (F) Quantification of CR-interneurons within layer VI, V and II/III-IV of wild type and *Fezf2*$^{-/-}$ cortex confirms that there are no differences in layer distribution for CR-interneurons. All results are expressed as the mean ± s.e.m. Roman numerals indicate cortical layers. LV, lateral ventricle; cc, corpus callosum. Scale bars, 500 μm (A,B); 100 μm (E).

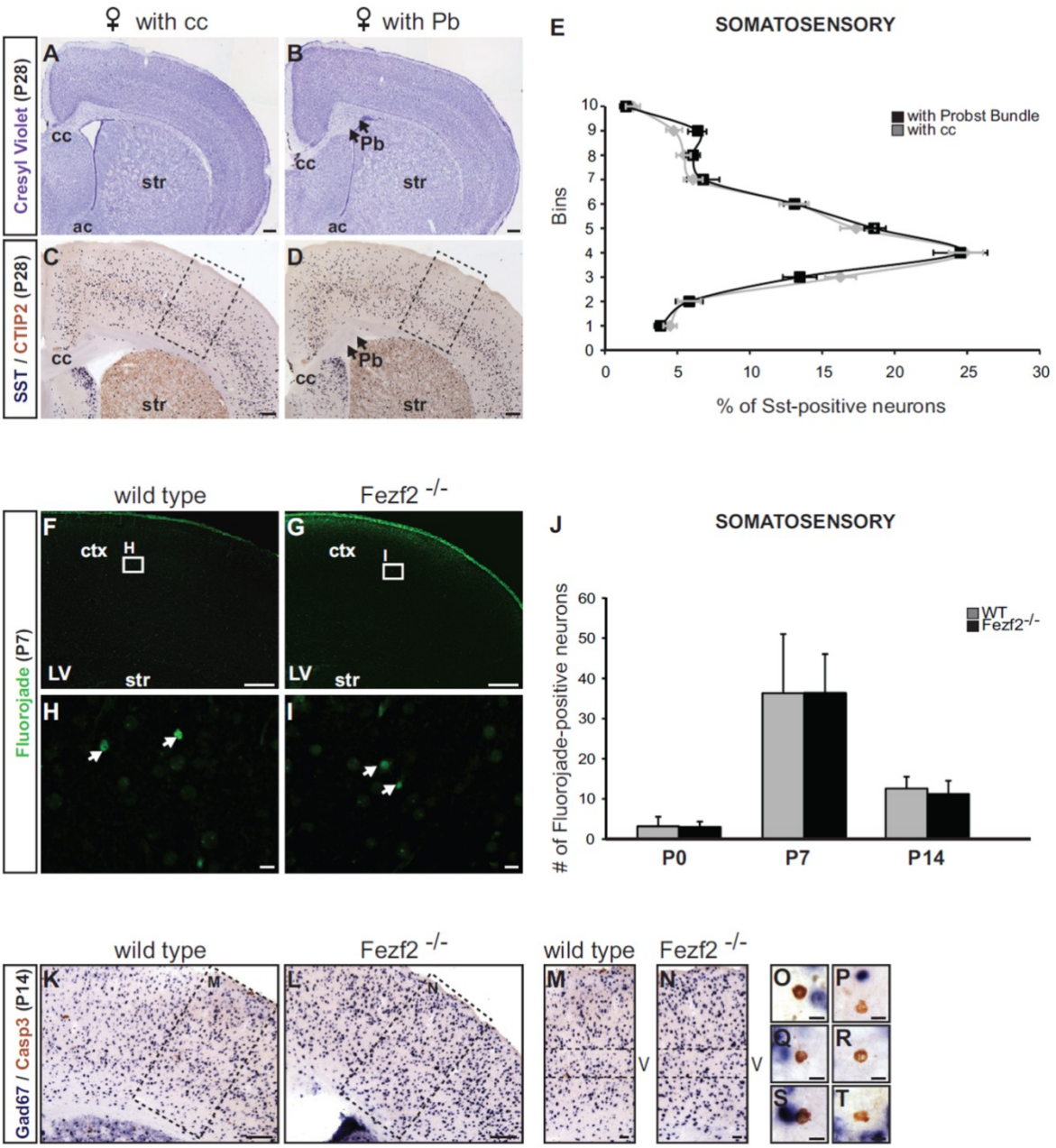
SV129S1/SvImJ strain
♀ with cc
♀ with Pb
Cresyl Violet (P28)
SST / CTIP2 (P28)
A
B
C
D
cc
str
ac
Pb
E
SOMATOSENSORY
with Probst Bundle
with cc
Bins
% of Sst-positive neurons
wild type
Fezf2 -/-
Fluorojade (P7)
F
G
H
I
ctx
LV
J
SOMATOSENSORY
WT
Fezf2-/-
# of Fluorojade-positive neurons
P0
P7
P14
Gad67 / Casp3 (P14)
K
L
M
N
O
P
Q
R
S
T
V

Figure 3.9

Figure 3. 9. Abnormal distribution of interneurons in the *Fezf2*$^{-/-}$ cortex is not due to abnormal connectivity of CPN or increased cell death

(A,B) Cresyl Violet staining of coronal sections from P28 wild type females of the SV129S1/SvlmJ strain shows that some animals develop Probst bundles (Pb) (B, arrows) that are similar to those observed in the *Fezf2*$^{-/-}$ cortex, while other animals have a normal corpus callosum (cc) (A). (C,D) *In situ* hybridization for SST combined with immunocytochemistry for CTIP2 shows no difference in the cortical radial distribution of SST-positive interneurons between mice with Probst bundles and with a normal corpus callosum (C,D). (E) Unbiased binned distribution of SST-interneuron percentages along the dorso-ventral axis of SV129S1/SvlmJ wild type females with Probst bundles and with a normal corpus callosum. (F-I) FluoroJade-C staining on coronal sections from P7 wild type (F,H) and *Fezf2*$^{-/-}$ (G,I) animals show no increase in cell death in the Fezf2-/- cortex. (J) Quantification of the number of Fluorojade-C-positive neurons in the somatosensory areas of wild type and *Fezf2*$^{-/-}$ cortex at P0, P7 and P14. (K-N) *In situ* hybridization for *Gad67* combined with immunocytochemistry for Caspase-3 shows no major differences in apoptotic interneurons between wild type (K,M) and *Fezf2*$^{-/-}$ (L,N) cortex. (O-T), Representative Caspase-3 positive cells. Scale bars, 500 μm (A-D,F,G,K,L); 100 μm (M,N) 20 μm (H,I,O,P,Q, O-T).

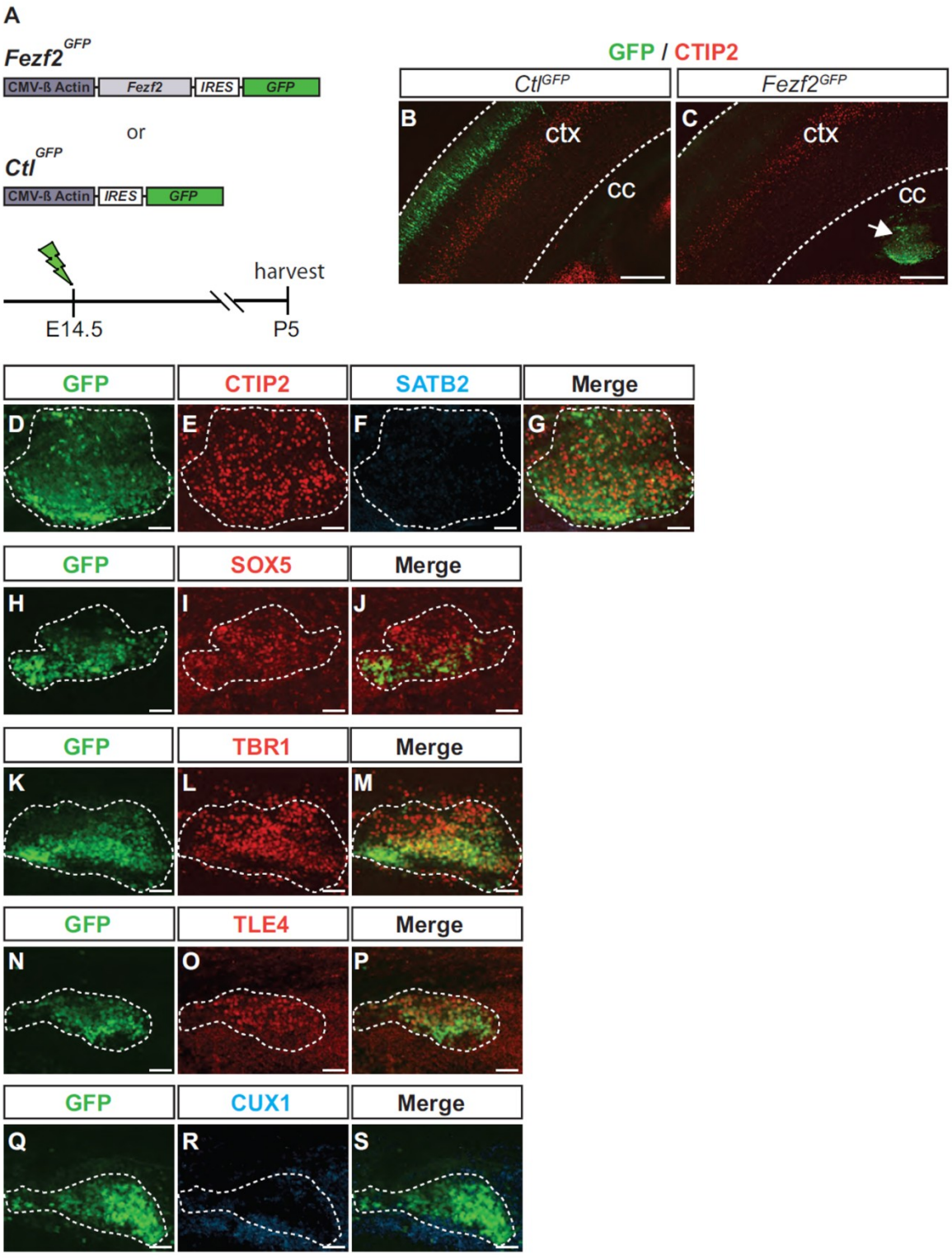
A
Fezf2GFP
CMV-ß Actin
Fezf2
IRES
GFP
or
CtlGFP
CMV-ß Actin
IRES
GFP
harvest
E14.5
P5
GFP / CTIP2
CtlGFP
Fezf2GFP
B
ctx
cc
C
ctx
cc
GFP
CTIP2
SATB2
Merge
D
E
F
G
GFP
SOX5
Merge
H
I
J
GFP
TBR1
Merge
K
L
M
GFP
TLE4
Merge
N
O
P
GFP
CUX1
Merge
Q
R
S

Figure 3.10

Figure 3. 10. Overexpression of *Fezf2* in progenitors of superficial layer neurons instruct the ectopic generation of corticofugal projection neurons

(A) Schematic of the experimental design. (B,C) coronal sections of P5 brain electroporated *in utero* at E14.5 with a control construct (B) or $Fezf2^{GFP}$ (C), showing that control-electroporated neurons populate the superficial cortical layers whereas $Fezf2^{GFP}$-electroporated neurons develop within ectopic clusters below the corpus callosum (cc). (D,E, G-P) High-magnification images showing that $Fezf2^{GFP}$-electroporated neurons express molecular markers of corticofugal projection neurons. (F,Q-S) High-magnification images showing that $Fezf2^{GFP}$-electroporated neurons do not express molecular markers of superficial layer projection neurons. Scale bars, 500 μm (B,C); 100 μm (D-S).

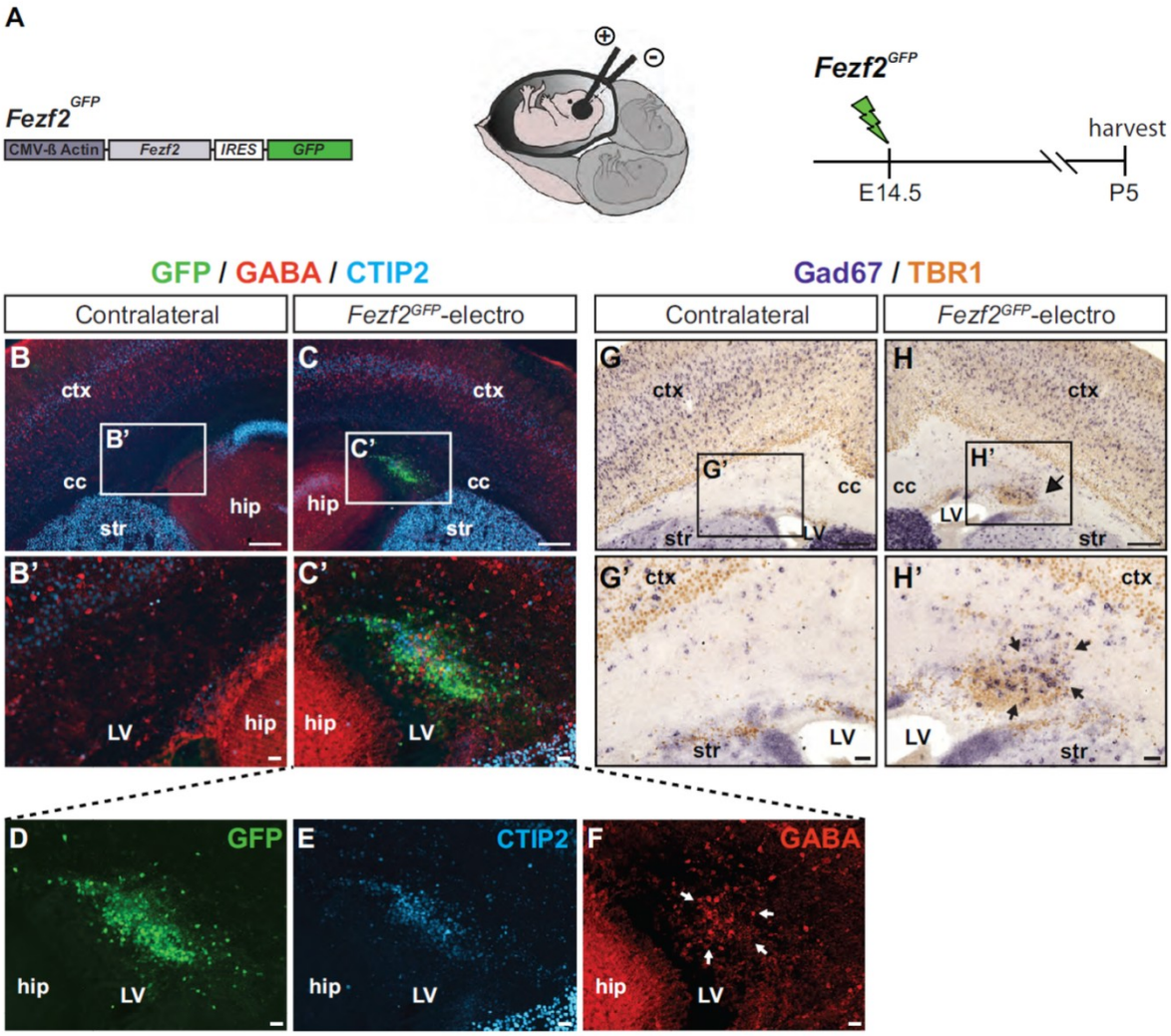
A
Fezf2GFP
CMV-ß Actin
Fezf2
IRES
GFP
Fezf2GFP
harvest
E14.5
P5
GFP / GABA / CTIP2
Gad67 / TBR1
Contralateral
Fezf2GFP-electro
Contralateral
Fezf2GFP-electro
B
ctx
B'
cc
hip
str
C
ctx
C'
cc
hip
str
G
ctx
G'
cc
str
LV
H
ctx
H'
cc
LV
str
B'
LV
hip
C'
hip
LV
G' ctx
str
LV
H' ctx
LV
str
D
GFP
hip
LV
E
CTIP2
hip
LV
F
GABA
hip
LV

Figure 3.11

Figure 3. 11. Experimentally-generated aggregates of corticofugal projection neurons recruit cortical interneurons to new ectopic locations.

(A) Schematic of experimental approach. (B-C') *In utero* overexpression of *Fezf2* in cortical progenitors at E14.5 causes a switch of fate to corticofugal projection neurons, which develop as ectopic aggregates below the corpus callosum. (C'-F) GFP- and CTIP2-positive aggregates of corticofugal neurons contain GABA-positive interneurons (arrows). (G-H') *In situ* hybridization for *Gad67* and immunocytochemistry for TBR1 demonstrates that TBR1-positive aggregates of corticofugal neurons contain *Gad67*-interneurons (arrows). Scale bars, 500 μm (B,C,G,H); 100 μm (B',C',D-F,G',H'). (See also Figures S6, S7 and S8).

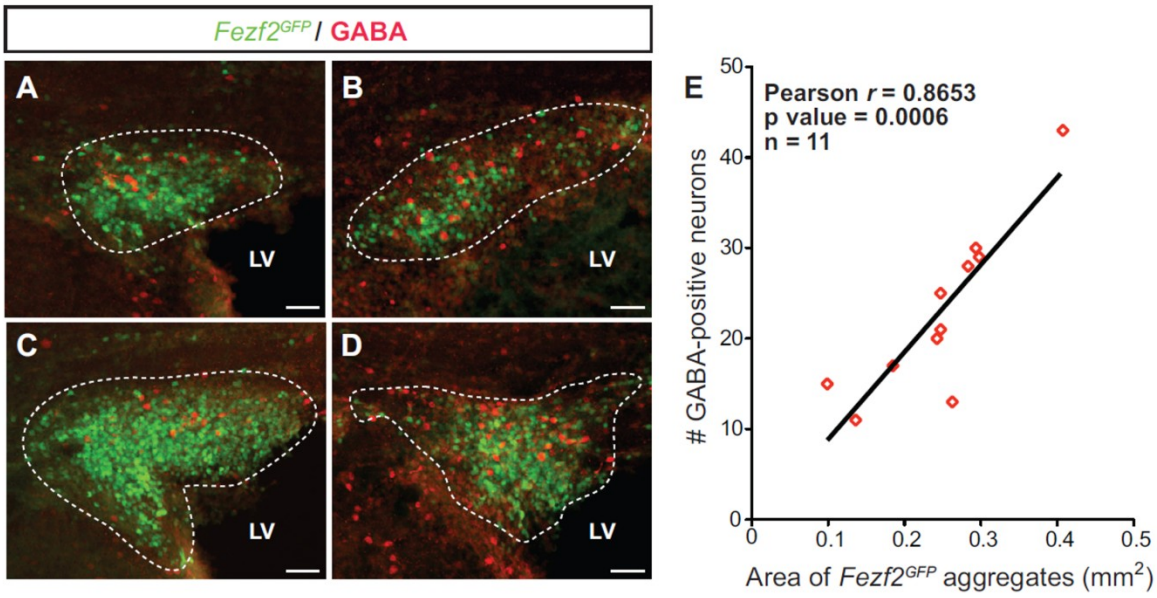
Fezf2GFP / GABA
A
B
C
D
LV
LV
LV
LV
E
Pearson r = 0.8653
p value = 0.0006
n = 11
# GABA-positive neurons
Area of Fezf2GFP aggregates (mm2)
0
10
20
30
40
50
0
0.1
0.2
0.3
0.4
0.5

Figure 3.12

Figure 3. 12. The number of GABAergic interneurons recruited to the ectopic aggregates of corticofugal projection neurons is linearly correlated to the size of the aggregates.

(A-D). Immunocytochemical analysis of four exemplary aggregates showing GABApositive interneurons within GFP aggregates of corticofugal projection neurons. Dotted lines indicate the perimeter of each aggregate. (E) Quantification of GABA-positive interneurons found in each aggregate relative to the aggregate area shows a linear correlation (Pearson's correlation coefficient r=0.8653). Scale bars, 100 μm.

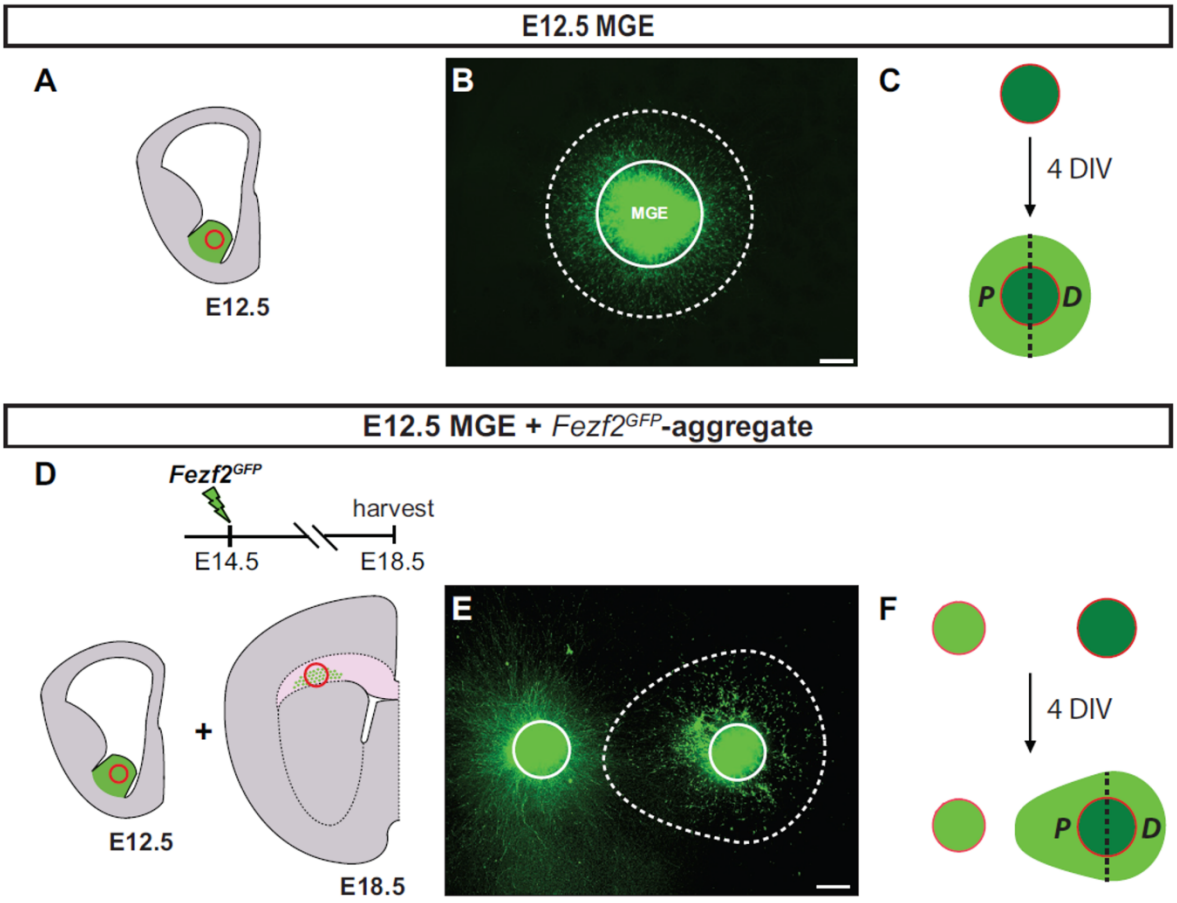
E12.5 MGE
A
E12.5
B
MGE
C
4 DIV
P
D
E12.5 MGE + Fezf2GFP-aggregate
D
Fezf2GFP
harvest
E14.5
E18.5
E12.5
+
E18.5
E
F
4 DIV
P
D

Figure 3.13

Figure 3. 13. *Fezf2*^{GFP}-positive aggregates of corticofugal projection neurons attract MGE-derived interneurons *in vitro*.

(A,D) Schematic of the experimental design. (B,E) Low magnification images of a representative *Lhx6::GFP*-positive MGE explant (B), and of cocultures of a *Lhx6::GFP*-positive MGE explant with a *Fezf2*^{GFP}-positive corticofugal neuron aggregate (E) at 4 days *in vitro* (4DIV). Solid lines demarcate the original limits of the explants at DIV0 and dotted lines indicate the front of migration by interneurons around the MGE explant at DIV4. (C-F) Schematic of the results. P and D indicate the proximal and distal halves of the MGE explant, respectively, relative to the position of the *Fezf2*^{GFP}-positive corticofugal neuron aggregate. Scale bars, 500 μm.

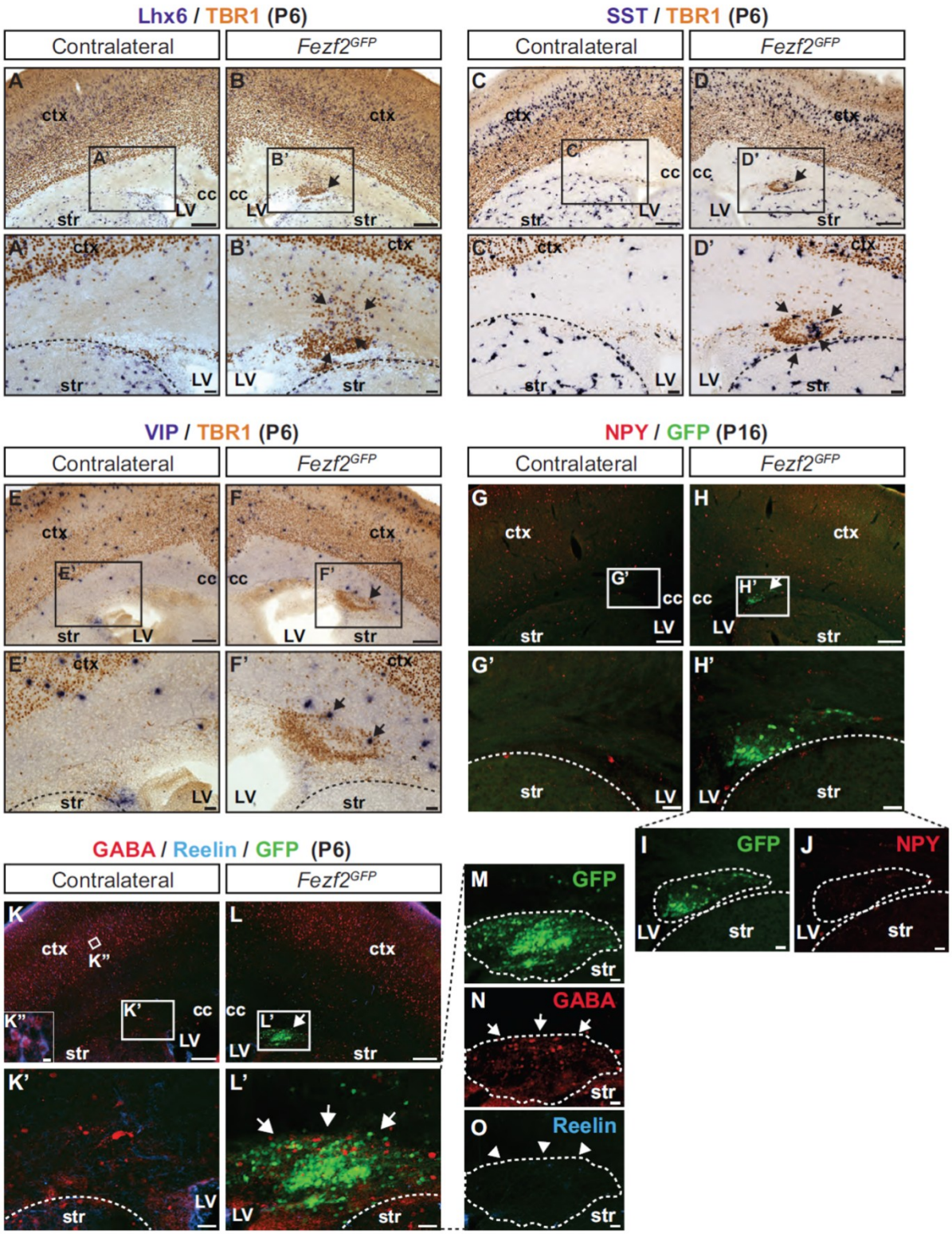
Lhx6 / TBR1 (P6)
Contralateral
Fezf2GFP
SST / TBR1 (P6)
Contralateral
Fezf2GFP
VIP / TBR1 (P6)
Contralateral
Fezf2GFP
NPY / GFP (P16)
Contralateral
Fezf2GFP
GABA / Reelin / GFP (P6)
Contralateral
Fezf2GFP
GFP
NPY
GFP
GABA
Reelin

Figure 3.14

Figure 3. 14. Interneurons characteristic of deep-layers are selectively found in corticofugal neuron aggregates.

(A-F') *In situ* hybridization for *Lhx6* (A-B'), *SST* (C-D') and *VIP* (E-F') combined with immunocytochemistry for TBR1 on electroporated brains demonstrates that aggregates of corticofugal neurons (B',D',F', arrows) contain deep layer *Lhx6*-positive (B,B', arrows) and *SST*-positive (D,D', arrows) interneurons and very small numbers of *VIP*-positive (F,F', arrows) interneurons. Aggregates of interneurons are absent from contralateral locations (A',C',E'). (G-O) Immunocytochemistry for NPY (G-J), GABA, Reelin and GFP (K-O) show that interneuron subpopulations that are mostly found in cortical superficial layers or layer Va are absent from the *Fezf2*-positive aggregates (H',J,L',O). (K") Coexpression of GABA and Reelin in layer Va. Scale bars, 500 μm (A,B,C,D,E,F,G,H,K,L); 100 μm (A'B',C',D',E',F',G'H',I,J,M-O).

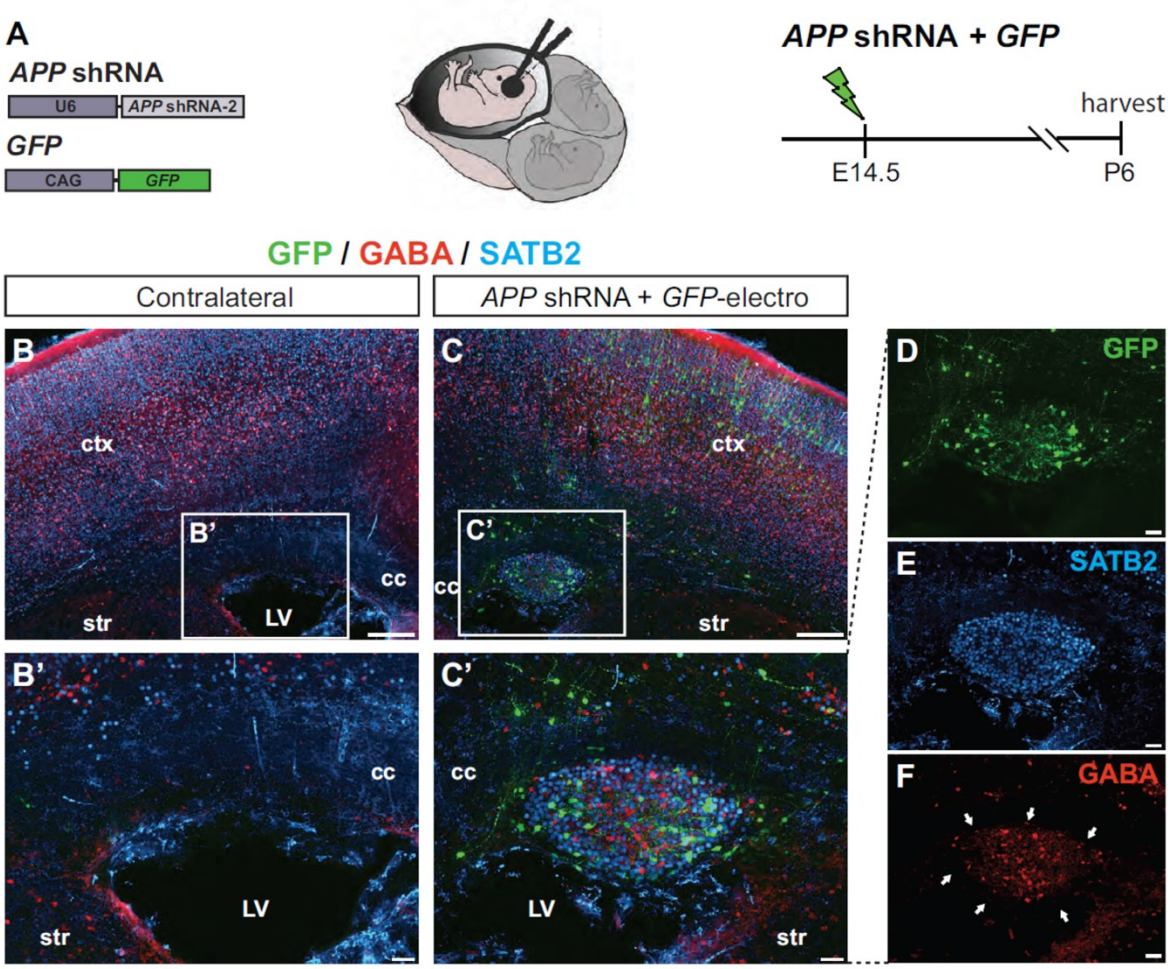
A
APP shRNA
U6
APP shRNA-2
GFP
CAG
GFP
APP shRNA + GFP
harvest
E14.5
P6
GFP / GABA / SATB2
Contralateral
APP shRNA + GFP-electro
B
ctx
B'
cc
str
LV
C
ctx
C'
cc
str
D
GFP
E
SATB2
F
GABA

Figure 3.15

Figure 3. 15. Ectopically-located aggregates of layer II/III callosal projection neurons recruit cortical interneurons.

(A) Schematic of experimental approach. (B-C') *In utero* overexpression of *APP* shRNA combined with CAG-GFP in cortical progenitors at E14.5 blocks the migration of superficial layer projection neurons, which differentiate as ectopic aggregates below the corpus callosum. (C', D-F) GFP- and SATB2-positive aggregates of upper layer CPN contain GABA-positive interneurons (arrows). Scale bars, 500 μm (B,C); 100 μm (B',C',D-F).

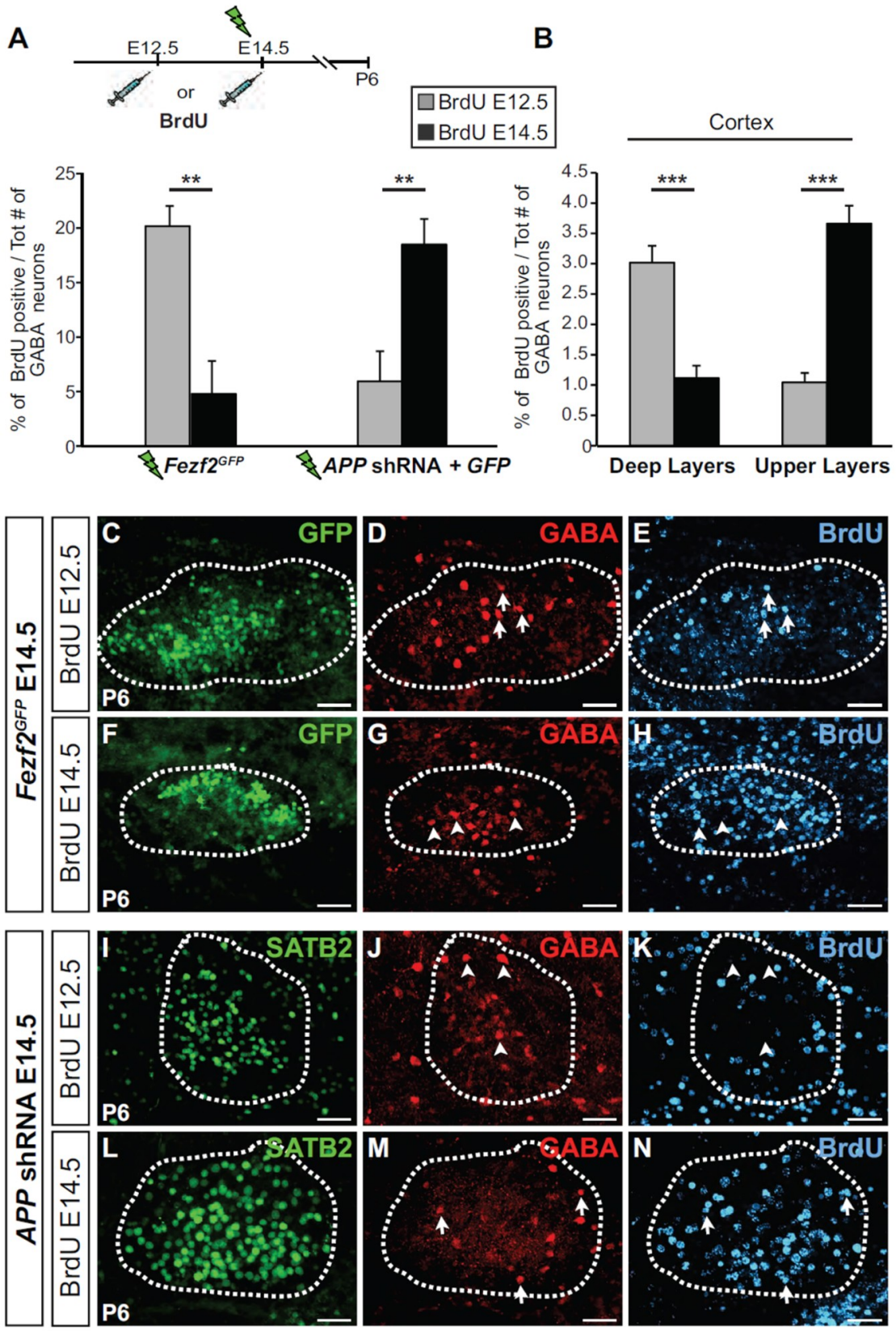
A
E12.5
E14.5
P6
or
BrdU
B
BrdU E12.5
BrdU E14.5
Cortex
% of BrdU positive / Tot # of GABA neurons
**
**
***
***
Fezf2GFP
APP shRNA + GFP
Deep Layers
Upper Layers
Fezf2GFP E14.5
APP shRNA E14.5
BrdU E12.5
BrdU E14.5
C GFP
D GABA
E BrdU
F GFP
G GABA
H BrdU
I SATB2
J GABA
K BrdU
L SATB2
M GABA
N BrdU
P6

Figure 3.16

Figure 3. 16. Ectopic aggregates of corticofugal projection neurons recruit interneurons that are appropriate for their projection neuron-type identity.

(A) Schematic of experimental design and quantification of first-generation, BrdU-positive and GABA-positive interneurons within aggregates expressing either *Fezf2*^{GFP} or *APP* shRNA. GABAergic interneurons in the corticofugal aggregates (*Fezf2*^{GFP}) are largely early-born, while those in the aggregates of layer II/III CPN (*APP* shRNA and CAG-GFP) are largely late-born. (B) Quantification of first-generation, BrdU-positive and GABA-positive interneurons within the deep and superficial layers of the cortex overlying the aggregates. Late-generated corticofugal neuron aggregates and synchronically generated CPN show distribution of E12.5- and E14.5- interneurons as observed in the deep and superficial cortical layers, respectively. (C-N) GABA-positive interneurons within *Fezf2*^{GFP} aggregates are born at E12.5 (C-E, arrows) and not at E14.5 (F-H, arrowheads), while GABA-positive interneurons within the *APP* shRNA aggregates are born at E14.5 (L-N, arrows) and not at E12.5 (I-K, arrowheads). Scale bars, 100 μm (C-N).

Chapter 4

Conclusions

CGE-derived interneurons: a new picture

In the first part of my thesis project, I have identified the role of the transcription factor COUP-TFI in generating CGE-derived interneurons of the cerebral cortex during development. Until recently, the CGE was not considered a distinct anatomical and molecular entity, mainly due to the absence of a morphologically definite sulcus demarcating the CGE from the MGE and LGE, and to the lack of CGE-restricted molecular markers (Flames et al., 2007). However, a series of experimental evidence including *in vivo* transplantation studies, *in vitro* migratory assays and preliminary fate mapping analyses have established the CGE as a separate molecular territory and confirmed that CGE-derived cortical interneurons contribute to a subset of interneuron subtypes with distinct morphological and electrophysiological interneurons (Kanatani et al., 2008; Miyoshi et al., 2010; Nery et al., 2002; Willi-Monnerat et al., 2008; Yozu et al., 2005). Still, no functional studies on genes required for the specification of CGE-derived cortical interneurons have been described to date of my report.

The discovery that COUP-TFI expression in the ventral telencephalon was restricted to the dorsal MGE and CGE at E13.5, and to CGE-derived cortical interneurons, in the adult cortex, such as VIP- and CR-expressing bipolar interneurons (appr. 80% and 90%, respectively), was a very promising starting point to hurtle this issue. Interestingly, although COUP-TFI is expressed in the MGE at early stages during the production of PV+ interneurons, its expression is not maintained in this cell type at P21 (only 4% of PV+ interneurons express COUP-TFI).

In this study, we report for the first time that COUP-TFI is required for the correct specification of the CGE-derived CR+ and VIP+ interneuron subtypes. Indeed, by the molecular and morphological analysis of the *COUP-TFI CKO-Dlx5/6* conditional mutant mice, in which the gene is inactivated COUP-TFI solely in interneuron SVZ progenitors, we observe that the two main CGE-derived populations were greatly reduced in superficial

cortical layers. Moreover, in concomitance with the reduction of CGE-derived interneurons, we report increased production of PV+ interneurons in deep cortical layers of the mature cortex of the conditional mutants. This phenotype indicates that COUP-TFI regulates the balance between distinct cortical interneuron subtypes during corticogenesis, thereby enabling proper cortical microcircuitry and functional activity.

These findings are unequivocally enhancing our understanding of the generation of interneuronal diversity in the cerebral cortex. Future work of fate-mapping the COUP-TFI lineage within the CGE will help identifying the diverse subpopulations of CGE-derived interneurons and their morphological and electrophysiological features, providing a broader picture of the CGE-derived population and its contribution to the diversity of the cerebral cortex. Identification of the COUP-TFI targets/interactors would also provide insightful information on the molecular mechanisms regulating the generation of many different subtypes of interneurons.

Interneuron subtypes and cell cycle regulation

The specification of MGE-derived interneurons has been extensively studied, providing a quite fulfilling picture of the mechanisms controlling the specification of specific cortical subtypes (Butt et al., 2005; Butt et al., 2008). Interestingly, the removal of Nkx2.1, the master gene of the MGE lineage, at distinct neurogenic time points, results in a switch in the subtypes of neurons observed at more mature ages (i.e. CGE-derived interneurons). These findings support a model in which the identity of a specific subtype of interneurons is trascriptionally determined within the progenitor population.

In our system, we showed that the imbalance between MGE- and CGE-derived interneurons induced by the loss of COUP-TFI function was not due to a change of cell fate, as observed for Nkx2.1 mutants (Butt et al., 2008). Although further mechanistic studies will be required, we suggest here an interesting alternative interpretation of the

molecular events controlling the balance between MGE- and CGE- derived interneurons occurring in absence of COUP-TFI. While the relation between the regulation of VZ/SVZ progenitors cell cycle and cell fate acquired by their progeny has been extensively investigated in the cerebral cortex, very little is known about progenitor divisions in the germinal zones.

Here, we propose that COUP-TFI plays a strict control on precursor cell divisions within the MGE, as seen by increased proliferation and expression levels of the cell cycle protein cyclinD2 in SVZ precursors (Glickstein et al., 2007a; Glickstein et al., 2007b). Of note, null mutant mice for cyclinD2 show a selective deficit in cortical PV-expressing interneurons and increased excitability, without affecting other MGE-derived subtypes, such as SST+ interneurons. Accordingly, in our model, overexpression of cyclinD2 in COUP-TFI conditional mutants results in an increase of PV+ neurons (Glickstein et al., 2007b), implying that negative control of SVZ divisions by COUP-TFI may normally limit the number of PV+ interneurons. According to this model, in the absence of COUP-TFI function, this repression is released and an excess of PV+ interneurons is produced. Since COUP-TFI is expressed in the MGE from E10.5 to E12.5 (Armentano et al., 2007; Armentano et al., 2006) (and this study), and production of PV+ interneurons occurs from E9.5 to E15.5 (Miyoshi et al., 2007), it is reasonable to assume that presumptive PV+ cells express COUP-TFI while proliferating in the SVZ and that COUP-TFI normally controls early SVZ progenitor divisions during generation of PV+ interneurons (Schematic 4.1).

We hypothesize that the overproduction of PV+ interneurons, at a time when normally VIP+ and CR+ cells are generated (from E14.5 to E18.5) (Miyoshi et al., 2010), depletes the progenitor pool in the MGE, resulting in a decrease of VIP+ and CR+ bipolar interneuron precursors in the CGE. Thus, I propose that COUP-TFI normally regulates the number of PV+ cells during generation of CR+ and VIP+ neurons by controlling sequential cell divisions in SVZ progenitors. Excessive cell divisions during the time of

PV+ interneuron generation would affect the sequential production of VIP/CR bipolar interneurons. Interestingly, increased PV+ interneurons are found in deep cortical layers (appropriately for their MGE origin), and decreased CR+ and VIP+ interneurons are still located in superficial layers (appropriate for their CGE origin) in COUP-TFI conditional mutants.

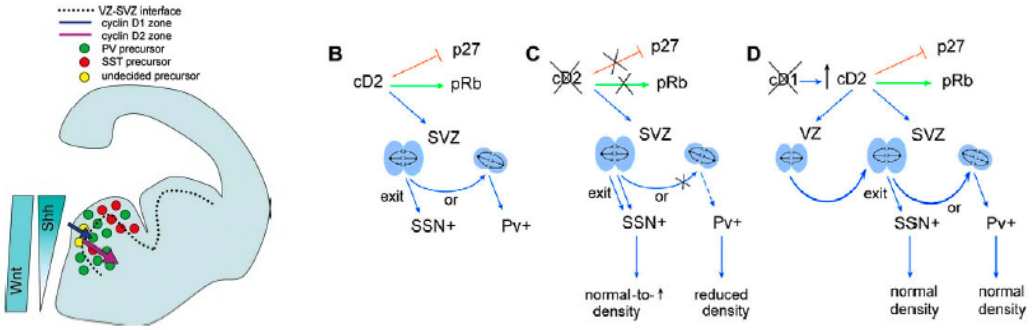

Schematic 4.1 (A) Neurogenesis in the MGE. Interneuron progenitors reflect both dorso–ventral and temporal, medial-lateral, gradients. Progenitors that generate SST+ (red) interneurons predominate in the dorsal MGE (dMGE), while PV+ (green) interneuron precursors originate mostly in the ventral MGE (vMGE). Their fate depends in part on Shh signaling that is more robust in the dMGE than vMGE. Betacatenin dependent Wnt signaling throughout the MGE is critical for progenitor proliferation. At the same time, progenitors in the VZ use G1-phase active cyclin D1 (cD1) to proliferate while symmetric SVZ neurogenic divisions use cyclin D2 (cD2), reflecting a temporal progression from radial glial to intermediate progenitor divisions. (Adapted from Ross, 2010).

(B-D) Model of D cyclin roles in the MGE. cD2 normally suppresses p27 levels more strongly than does cD1, requiring more p27 to accumulate before cells can exit the cycle. cD2 also promotes phosphorylation of Rb (pRb), facilitating progression through G1 phase and perhaps influencing downstream gene transcription. cD2 support of SVZ divisions promotes the balanced production of SST+ and PV+ interneurons. (C) In the absence of cD2, constraints on p27 are lifted and pRb levels fall, hastening cell cycle exit and leaving the proportion of SST+ neurons unchanged or slightly increased, whiledisproportionately fewer PV+ interneurons are generated. (D) Loss of cD1 induces cD2 in the VZ, which inhibits p27 and promotes pRb. Divisions continue in both the VZ and SVZ, although they may be slower overall. This leads to fewer roundsof division and reduced total neuronal numbers, but preserved SST+ and PV+ neuron densities in *cD1–/–* brains. (Adapted from Glickstein et al., 2007)

The suggested model of a temporal control over ventral progenitors is in agreement with the already reported function of COUP-TFI in the cerebral cortex, where is required to balance motor and sensory cortical areas by repressing corticospinal motor neuron

generation during production of corticofugal pyramidal neurons (Armentano et al., 2007; Tomassy et al., 2010a). Moreover, both COUP-TFs regulate the timing of the switch between neurogenesis (early corticogenesis) and gliogenesis (late corticogenesis) and in their absence, neurogenesis is sustained and the generation of early-born neurons is prolonged (Naka et al., 2008b). Finally, the *Drosophila* COUP-TF ortholog, *svp*, controls neuroblast diversity in a temporally controlled mode by regulating the balance between early- and late-born neuroblasts during neurogenesis (Kanai et al., 2005). Overall, I propose that in the basal telencephalon COUP-TFI plays a critical temporal and spatial control over the differentiation of different subtypes of cortical interneurons, thereby enabling the temporal and spatial specification of PV-, and bipolar CR- and VIP-expressing interneurons. These new findings on the relation between cell cycle and neuronal fate in the ganglionic eminence will contribute to elucidate the events controlling the generation of different subtypes of interneurons destined not only to the cortex but also to other regions of the brain.

Interneuronal "balance" and epilepsy

Functional circuits in the central nervous system depend on a delicate balance of synaptic excitation and inhibition. Defects in cortical neural circuitry formation during development are likely to underlie important neurological and psychiatric illnesses. Indeed, inherited disruption of the developmental events controlling the coordinated integration of different subtypes of interneurons and projection neurons in the cortical circuitry commonly leads to human neurological and psychiatric disorders such as epilepsy, anxiety and depression with a developmental onset during childhood or adolescence. It is now well established that GABAergic cell dysfunction is associated primarily with epilepsy, one of the most common neurological disorder affecting young people (about 1% of the population in their most productive years) (Baraban, 2007;

Cossart et al., 2005). However, we still lack a comprehensive understanding of what determines the expression of a particular phenotype and whether interneuronal dysfunction is cause or consequence of epileptic seizures. To our knowledge, this study describes for the first time an epilepsy-resistant phenotype after genetic manipulation of interneuronal subtypes, and suggests a potential role for increased PV+ and NPY+ interneurons in controlling seizures.

Recent genetic models aimed to study the development of cortical interneurons have provided further cues to draw important conclusions about cortical development and epilepsy (Fig. 2.7). They constitute a unique tool because in most cases changes of subtype proportions precede pathological manifestations (Fig. 2.7B). Although all these mouse models represent precious model for understanding the role of diverse interneuronal types in controlling cortical excitability and seizures, our study moves forward demonstrating that in the presence of a higher number of PV+ interneurons, COUP-TFI mutants show no discernible cortical EEG abnormalities, but on the contrary are more resistant to pharmacologically induced seizures. Obviously, the cortical microcircuit is extremely complex and other factors, such as the layer specificity of interneuronal loss and the total number of affected cells, can constraint the emergence of epileptic phenotypes and rhythm distortion. Future detailed studies of the local field potentials using multi-site recordings would help to look at the finest spatial scale of the cortex.

Interneurons lamination: is that matter of identity?

Ultimate function of mature cortical interneurons is to integrate into cortical microcircuitries and to modulate the firing activity of their neuronal partners, the glutamatergic projection neurons. As their "ancient" definition suggests, cortical interneurons are responsible for the "local" inhibition; therefore, it is reasonable assuming that their synaptic partners are located approximately in the same region (area/ layer) of the cortex. However, the mechanisms that control the assembly of the cortical microcircuitry are still largely unknown.

Interstingly, it has been reported that, although originated from distant germinal zones, synchronically generated interneurons and projection neurons end up occupying the same cortical layer in the mature cortex. In order to reach their final position, cortical interneurons undergo an extensive journey through the ventral and dorsal telencephalon. Upon reaching the cortical plate, interneurons generated at different time points disperse within the cortical layers already populated by their synaptic partners, the projection neurons. The precise relative distribution of these two populations is critical for balanced electrical activity and normal cortical function, and implies coordinated mechanisms of migration and lamination.

Intrinsic defects in the specification of cortical interneurons result in abnormal cortical lamination. Strikingly, several reports pointed out the role of the cortical environment in influencing the distribution of cortical interneurons. Indeed, independent studies of animal models, in which the cortical lamination of the projection neurons is severely impaired (i.e. reelin mouse), show a concomitant defective distribution of cortical interneurons (Hammond et al., 2004; Hevner et al., 2004; Pla et al., 2006; Yabut et al., 2007).

In the second part of my thesis project, I investigated the role of projection neurons in cortical interneuronal lamination, by taking advantage of the Fezf2-null mutant model

in which the subcerebral projection neurons - a subtype of projection neurons located in layer V- are replaced by another subtype, the callosal projection neurons. This defect does not affect the overall thickness of the cortex or the specification of other projection neuron types (Molyneaux et al., 2005; Chen et al., 2005). Here, I demonstrate that projection neurons control the laminar positioning of interneurons during cortical development, ultimately affecting the function of the local inhibitory microcircuitry. Remarkably, I find that not all interneuron subtypes are affected by the lack of subcerebral projection neurons in the mutant cortex; indeed, only the SST- and PV- expressing interneurons, preferentially located in the deep layers of the cortex, distribute abnormally, while CR-expressing interneurons are "insensitive" to the projection neurons defect. These findings suggest that not all the interneuronal subtypes are equally "sensitive" to potential positional cues provided by projection neurons. Moreover, the observation that in the Fezf2 null mutant the callosal population developed in place of the missing subcerebral projection neurons is not sufficient to rescue the interneuronal phenotype suggests that this effect is subtype-depend. Every subtype of projection neurons uniquely controls the lamination of different subtypes of interneurons with which are "paired" in the same cortical layer. These data together strongly support a model in which projection neuron subtypes are required for the correct distribution of GABAergic interneurons and provide cues to guide cortical interneurons to their appropriate layer.

In addition, I find that different subtypes of experimentally generated projection neurons - corticofugal and callosal projection neurons - are sufficient to recruit specific subtypes of interneurons to ectopic location below the cortex, indicating a selective mechanism of pairing between projection neurons and interneurons.

The current model, by which cortical interneurons adopt their laminar fate, includes imprints originating from the subcortical environment in which interneurons are generated, but it also takes into account the contribution from the cortical environment that

refines their final position. The observations that both fate determinants and local cues are important to specify the laminar fate of interneurons favor a model in which interneurons born at specific times during development are committed to distinct layers of the cortex in response to cues provided by projection neurons (Pla et al., 2006). Early-born (peak at E13), largely MGE-derived interneurons localize in deep layers, whereas late-born (peak at E15), largely CGE-derived interneurons occupy the superficial layers. This current interpretation greatly emphasizes on the "birth date" of cortical interneurons in intimate relation to their laminar fate. In our system, we find evidences that "molecular identity" of interneurons and projection neurons, more than strictly their birthdate, can control their final position in the cortex. To assess the validity of the "birthdate theory", we ectopically generated corticofugal projection neurons two days after which the bulk production of endogeneous corticofugal neurons has ended (a stage when CPN of the superficial layers II/III are normally born) and tested whether those preferentially recruit interneurons that are appropriate for their projection neuron-type identity (i.e. interneurons born at E12-E13) or, rather, interneurons appropriate for their heterochronic day of birth (i.e. interneurons born the day of the electroporation, at E14.5). In complementary experiments, we investigated whether upper layer II/III CPN that were synchronically born with *Fezf2*-induced corticofugal neurons at E14.5 and that were similarly positioned below the corpus callosum, recruited interneurons born at the same time. We find that heterochronic, late-born corticofugal projection neurons preferentially recruited interneurons that were born early, at E12.5, in accordance with their "molecular deep-layer identity", but not for their experimental date of birth. Confirming the specificity of this effect, we find, instead, that upper layer II/III CPN populations born the same day as the experimentally generated corticofugal neurons specifically attracted late-born interneurons. Of note, these findings are reinforced by the fact that molecular characterization of interneurons recruited by corticofugal projection neurons express SST

and Lhx6, two markers of MGE-derived, early born interneurons mainly destined to the deep layers of the cortex.

Our findings shed light on the molecular identity of interneurons and projection neurons in the coordinated process of cortical distribution. This also implies that the pairing into circuitry of cortical projection neuron and interneuron partners might be "pre-programmed" during early stages of fate-specification of each neuron type, possibly days before interneurons acquire their final position in the appropriate cortical layers. Therefore, the present study extends the current understanding on the mechanisms controlling the formation of laminar structures in the brain.

Molecular players: new prospectives

The discovery that excitatory projection neurons play a direct role in controlling interneurons position, in a subtype-specific manner, paves the way for new exploration of the mechanisms controlling subtype-specific interactions between selected populations of projection neurons and interneurons. In light of our findings, future works to identify the molecular mechanisms controlling precise laminar positioning of interneurons may require the purification and molecular comparison of the correct subtypes of "interacting" projection neurons and interneurons, rather than a more general analysis of the two broad neuronal populations independently. One study, currently in progress in our laboratory, is driven by the hypothesis that coupled cell-surface signaling mechanisms mediate the "aggregation" of the proper types of neurons to facilitate neighboring interactions. The neuronal partners that have been selected for this study are the Corticospinal Motor Neurons, a clinically relevant subtype of subcerebral projection neurons, and their interneuronal counterpart, represented by the Lhx6-expressing subtype, MGE-derived and preferentially located within the deep layers of the cortex. Specifically, we use FACS (Fluorescence Activated Cell Sorting) to purify interneurons at different stages of

integration into circuitry from the motor cortex of *Lhx6*-GFP transgenic mice that are amenable to this experiment. Upon purification, profiling of the Lhx6 populations at different time points will be perfomed by Affimetrix arrays with standard platforms. Taking advantage of previously purified and profiled CSMN at matching time points (Arlotta et al., 2005), pure populations of the exact neuron types that interact *in vivo* will be available for comparing analysis. The results of the microarrays analysis will be indeed mined in search for interacting pairs of molecules that are expressed complementarily in the two populations (i.e. excitatory neurons and interneurons). This should provide us with potential candidate genes for their ability to mediate interaction between projection neurons and interneurons.

References

Aaku-Saraste, E., Hellwig, A., and Huttner, W.B. (1996). Loss of occludin and functional tight junctions, but not ZO-1, during neural tube closure--remodeling of the neuroepithelium prior to neurogenesis. Dev Biol *180*, 664-679.

Alcamo, E.A., Chirivella, L., Dautzenberg, M., Dobreva, G., Farinas, I., Grosschedl, R., and McConnell, S.K. (2008). Satb2 regulates callosal projection neuron identity in the developing cerebral cortex. Neuron *57*, 364-377.

Alcantara, S., Ruiz, M., D'Arcangelo, G., Ezan, F., de Lecea, L., Curran, T., Sotelo, C., and Soriano, E. (1998). Regional and cellular patterns of reelin mRNA expression in the forebrain of the developing and adult mouse. J Neurosci *18*, 7779-7799.

Alifragis, P., Liapi, A., and Parnavelas, J.G. (2004). Lhx6 regulates the migration of cortical interneurons from the ventral telencephalon but does not specify their GABA phenotype. J Neurosci *24*, 5643-5648.

Anderson, D.J. (2001). Stem cells and pattern formation in the nervous system: the possible versus the actual. Neuron *30*, 19-35.

Anderson, S.A., Kaznowski, C.E., Horn, C., Rubenstein, J.L., and McConnell, S.K. (2002). Distinct origins of neocortical projection neurons and interneurons in vivo. Cereb Cortex *12*, 702-709.

Anderson, S.A., Marin, O., Horn, C., Jennings, K., and Rubenstein, J.L. (2001). Distinct cortical migrations from the medial and lateral ganglionic eminences. Development *128*, 353-363.

Anderson, S.A., Qiu, M., Bulfone, A., Eisenstat, D.D., Meneses, J., Pedersen, R., and Rubenstein, J.L. (1997). Mutations of the homeobox genes Dlx-1 and Dlx-2 disrupt the striatal subventricular zone and differentiation of late born striatal neurons. Neuron *19*, 27-37.

Ang, E.S., Jr., Haydar, T.F., Gluncic, V., and Rakic, P. (2003). Four-dimensional migratory coordinates of GABAergic interneurons in the developing mouse cortex. J Neurosci *23*, 5805-5815.

Angevine, J.B., Jr., and Sidman, R.L. (1961). Autoradiographic study of cell migration during histogenesis of cerebral cortex in the mouse. Nature *192*, 766-768.

Anthony, T.E., Klein, C., Fishell, G., and Heintz, N. (2004). Radial glia serve as neuronal progenitors in all regions of the central nervous system. Neuron *41*, 881-890.

Arlotta, P., Molyneaux, B.J., Chen, J., Inoue, J., Kominami, R., and Macklis, J.D. (2005). Neuronal subtype-specific genes that control corticospinal motor neuron development in vivo. Neuron *45*, 207-221.

Armentano, M., Chou, S.J., Tomassy, G.S., Leingartner, A., O'Leary, D.D., and Studer, M. (2007). COUP-TFI regulates the balance of cortical patterning between frontal/motor and sensory areas. Nat Neurosci *10*, 1277-1286.

Armentano, M., Filosa, A., Andolfi, G., and Studer, M. (2006). COUP-TFI is required for the formation of commissural projections in the forebrain by regulating axonal growth. Development *133*, 4151-4162.

Ascoli, G.A., Alonso-Nanclares, L., Anderson, S.A., Barrionuevo, G., Benavides-Piccione, R., Burkhalter, A., Buzsaki, G., Cauli, B., Defelipe, J., Fairen, A.*, et al.* (2008). Petilla terminology: nomenclature of features of GABAergic interneurons of the cerebral cortex. Nat Rev Neurosci *9*, 557-568.

Azim, E., Shnider, S.J., Cederquist, G.Y., Sohur, U.S., and Macklis, J.D. (2009). Lmo4 and Clim1 progressively delineate cortical projection neuron subtypes during development. Cereb Cortex *19 Suppl 1*, i62-69.

Baraban, S.C. (2007). Emerging epilepsy models: insights from mice, flies, worms and fish. Curr Opin Neurol *20*, 164-168.

Batista-Brito, R., and Fishell, G. (2009). The developmental integration of cortical interneurons into a functional network. Curr Top Dev Biol *87*, 81-118.

Batista-Brito, R., Rossignol, E., Hjerling-Leffler, J., Denaxa, M., Wegner, M., Lefebvre, V., Pachnis, V., and Fishell, G. (2009). The cell-intrinsic requirement of Sox6 for cortical interneuron development. Neuron *63*, 466-481.

Bayer, S.A., and Altman, J. (1991). Neocortical Development (New York, Raven Press).

Beato, M., Herrlich, P., and Schutz, G. (1995). Steroid hormone receptors: many actors in search of a plot. Cell *83*, 851-857.

Bellion, A., Baudoin, J.P., Alvarez, C., Bornens, M., and Metin, C. (2005). Nucleokinesis in tangentially migrating neurons comprises two alternating phases: forward migration of the Golgi/centrosome associated with centrosome splitting and myosin contraction at the rear. J Neurosci *25*, 5691-5699.

Ben-Ari, Y. (2002). Excitatory actions of gaba during development: the nature of the nurture. Nat Rev Neurosci *3*, 728-739.

Bielle, F., Griveau, A., Narboux-Neme, N., Vigneau, S., Sigrist, M., Arber, S., Wassef, M., and Pierani, A. (2005). Multiple origins of Cajal-Retzius cells at the borders of the developing pallium. Nat Neurosci *8*, 1002-1012.

Boldajipour, B., Mahabaleshwar, H., Kardash, E., Reichman-Fried, M., Blaser, H., Minina, S., Wilson, D., Xu, Q., and Raz, E. (2008). Control of chemokine-guided cell migration by ligand sequestration. Cell *132*, 463-473.

Bortone, D., and Polleux, F. (2009). KCC2 expression promotes the termination of cortical interneuron migration in a voltage-sensitive calcium-dependent manner. Neuron *62*, 53-71.

Bulfone, A., Wang, F., Hevner, R., Anderson, S., Cutforth, T., Chen, S., Meneses, J., Pedersen, R., Axel, R., and Rubenstein, J.L. (1998). An olfactory sensory map develops in the absence of normal projection neurons or GABAergic interneurons. Neuron *21*, 1273-1282.

Butt, S.J., Fuccillo, M., Nery, S., Noctor, S., Kriegstein, A., Corbin, J.G., and Fishell, G. (2005). The temporal and spatial origins of cortical interneurons predict their physiological subtype. Neuron *48*, 591-604.

Butt, S.J., Sousa, V.H., Fuccillo, M.V., Hjerling-Leffler, J., Miyoshi, G., Kimura, S., and Fishell, G. (2008). The requirement of Nkx2-1 in the temporal specification of cortical interneuron subtypes. Neuron *59*, 722-732.

Buzsaki, G., Geisler, C., Henze, D.A., and Wang, X.J. (2004). Interneuron Diversity series: Circuit complexity and axon wiring economy of cortical interneurons. Trends Neurosci *27*, 186-193.

Canty, A.J., and Murphy, M. (2008). Molecular mechanisms of axon guidance in the developing corticospinal tract. Prog Neurobiol *85*, 214-235.

Caputi, A., Rozov, A., Blatow, M., and Monyer, H. (2009). Two calretinin-positive GABAergic cell types in layer 2/3 of the mouse neocortex provide different forms of inhibition. Cereb Cortex *19*, 1345-1359.

Casarosa, S., Fode, C., and Guillemot, F. (1999). Mash1 regulates neurogenesis in the ventral telencephalon. Development *126*, 525-534.

Cavanagh, M.E., and Parnavelas, J.G. (1989). Development of vasoactive-intestinal-polypeptide-immunoreactive neurons in the rat occipital cortex: a combined immunohistochemical-autoradiographic study. J Comp Neurol *284*, 637-645.

Caviness, V.S., Jr., and Sidman, R.L. (1973). Time of origin or corresponding cell classes in the cerebral cortex of normal and reeler mutant mice: an autoradiographic analysis. J Comp Neurol *148*, 141-151.

Chen, B., Schaevitz, L.R., and McConnell, S.K. (2005a). Fezl regulates the differentiation and axon targeting of layer 5 subcortical projection neurons in cerebral cortex. Proc Natl Acad Sci U S A *102*, 17184-17189.

Chen, B., Wang, S.S., Hattox, A.M., Rayburn, H., Nelson, S.B., and McConnell, S.K. (2008). The Fezf2-Ctip2 genetic pathway regulates the fate choice of subcortical projection neurons in the developing cerebral cortex. Proc Natl Acad Sci U S A *105*, 11382-11387.

Chen, J.G., Rasin, M.R., Kwan, K.Y., and Sestan, N. (2005b). Zfp312 is required for subcortical axonal projections and dendritic morphology of deep-layer pyramidal neurons of the cerebral cortex. Proc Natl Acad Sci U S A *102*, 17792-17797.

Chenn, A., Zhang, Y.A., Chang, B.T., and McConnell, S.K. (1998). Intrinsic polarity of mammalian neuroepithelial cells. Mol Cell Neurosci *11*, 183-193.

Cobos, I., Long, J.E., Thwin, M.T., and Rubenstein, J.L. (2006). Cellular patterns of transcription factor expression in developing cortical interneurons. Cereb Cortex *16 Suppl 1*, i82-88.

Corbin, J.G., Nery, S., and Fishell, G. (2001). Telencephalic cells take a tangent: non-radial migration in the mammalian forebrain. Nat Neurosci *4 Suppl*, 1177-1182.

Cossart, R., Bernard, C., and Ben-Ari, Y. (2005). Multiple facets of GABAergic neurons and synapses: multiple fates of GABA signalling in epilepsies. Trends Neurosci *28*, 108-115.

D'Arcangelo, G., Homayouni, R., Keshvara, L., Rice, D.S., Sheldon, M., and Curran, T. (1999). Reelin is a ligand for lipoprotein receptors. Neuron *24*, 471-479.

D'Arcangelo, G., Miao, G.G., Chen, S.C., Soares, H.D., Morgan, J.I., and Curran, T. (1995). A protein related to extracellular matrix proteins deleted in the mouse mutant reeler. Nature *374*, 719-723.

Dayer, A.G., Cleaver, K.M., Abouantoun, T., and Cameron, H.A. (2005). New GABAergic interneurons in the adult neocortex and striatum are generated from different precursors. J Cell Biol *168*, 415-427.

Desai, A.R., and McConnell, S.K. (2000). Progressive restriction in fate potential by neural progenitors during cerebral cortical development. Development *127*, 2863-2872.

Du, T., Xu, Q., Ocbina, P.J., and Anderson, S.A. (2008). NKX2.1 specifies cortical interneuron fate by activating Lhx6. Development *135*, 1559-1567.

Dulabon, L., Olson, E.C., Taglienti, M.G., Eisenhuth, S., McGrath, B., Walsh, C.A., Kreidberg, J.A., and Anton, E.S. (2000). Reelin binds alpha3beta1 integrin and inhibits neuronal migration. Neuron *27*, 33-44.

Dzhala, V.I., Talos, D.M., Sdrulla, D.A., Brumback, A.C., Mathews, G.C., Benke, T.A., Delpire, E., Jensen, F.E., and Staley, K.J. (2005). NKCC1 transporter facilitates seizures in the developing brain. Nat Med *11*, 1205-1213.

Elias, L.A., Potter, G.B., and Kriegstein, A.R. (2008). A time and a place for nkx2-1 in interneuron specification and migration. Neuron *59*, 679-682.

Faedo, A., Tomassy, G.S., Ruan, Y., Teichmann, H., Krauss, S., Pleasure, S.J., Tsai, S.Y., Tsai, M.J., Studer, M., and Rubenstein, J.L. (2008). COUP-TFI coordinates cortical patterning, neurogenesis, and laminar fate and modulates MAPK/ERK, AKT, and beta-catenin signaling. Cereb Cortex *18*, 2117-2131.

Fairen, A., Cobas, A., and Fonseca, M. (1986). Times of generation of glutamic acid decarboxylase immunoreactive neurons in mouse somatosensory cortex. J Comp Neurol *251*, 67-83.

Flames, N., Long, J.E., Garratt, A.N., Fischer, T.M., Gassmann, M., Birchmeier, C., Lai, C., Rubenstein, J.L., and Marin, O. (2004). Short- and long-range attraction of cortical GABAergic interneurons by neuregulin-1. Neuron *44*, 251-261.

Flames, N., Pla, R., Gelman, D.M., Rubenstein, J.L., Puelles, L., and Marin, O. (2007). Delineation of multiple subpallial progenitor domains by the combinatorial expression of transcriptional codes. J Neurosci *27*, 9682-9695.

Fogarty, M., Grist, M., Gelman, D., Marin, O., Pachnis, V., and Kessaris, N. (2007). Spatial genetic patterning of the embryonic neuroepithelium generates GABAergic interneuron diversity in the adult cortex. J Neurosci *27*, 10935-10946.

Friocourt, G., Liu, J.S., Antypa, M., Rakic, S., Walsh, C.A., and Parnavelas, J.G. (2007). Both doublecortin and doublecortin-like kinase play a role in cortical interneuron migration. J Neurosci *27*, 3875-3883.

Fukumitsu, H., Ohtsuka, M., Murai, R., Nakamura, H., Itoh, K., and Furukawa, S. (2006). Brain-derived neurotrophic factor participates in determination of neuronal laminar fate in the developing mouse cerebral cortex. J Neurosci *26*, 13218-13230.

Gelman, D.M., and Marin, O. (2010). Generation of interneuron diversity in the mouse cerebral cortex. Eur J Neurosci *31*, 2136-2141.

Gelman, D.M., Martini, F.J., Nobrega-Pereira, S., Pierani, A., Kessaris, N., and Marin, O. (2009). The embryonic preoptic area is a novel source of cortical GABAergic interneurons. J Neurosci *29*, 9380-9389.

Giguere, V. (1999). Orphan nuclear receptors: from gene to function. Endocr Rev *20*, 689-725.

Gilmore, E.C., and Herrup, K. (2001). Neocortical cell migration: GABAergic neurons and cells in layers I and VI move in a cyclin-dependent kinase 5-independent manner. J Neurosci *21*, 9690-9700.

Glickstein, S.B., Alexander, S., and Ross, M.E. (2007a). Differences in cyclin D2 and D1 protein expression distinguish forebrain progenitor subsets. Cereb Cortex *17*, 632-642.

Glickstein, S.B., Moore, H., Slowinska, B., Racchumi, J., Suh, M., Chuhma, N., and Ross, M.E. (2007b). Selective cortical interneuron and GABA deficits in cyclin D2-null mice. Development *134*, 4083-4093.

Gonchar, Y., and Burkhalter, A. (1999). Connectivity of GABAergic calretinin-immunoreactive neurons in rat primary visual cortex. Cereb Cortex *9*, 683-696.

Gong, S., Zheng, C., Doughty, M.L., Losos, K., Didkovsky, N., Schambra, U.B., Nowak, N.J., Joyner, A., Leblanc, G., Hatten, M.E*., et al.* (2003). A gene expression atlas of the central nervous system based on bacterial artificial chromosomes. Nature *425*, 917-925.

Gotz, M., and Huttner, W.B. (2005). The cell biology of neurogenesis. Nat Rev Mol Cell Biol *6*, 777-788.

Grigoriou, M., Tucker, A.S., Sharpe, P.T., and Pachnis, V. (1998). Expression and regulation of Lhx6 and Lhx7, a novel subfamily of LIM homeodomain encoding genes, suggests a role in mammalian head development. Development *125*, 2063-2074.

Grinvald, A., and Hildesheim, R. (2004). VSDI: a new era in functional imaging of cortical dynamics. Nat Rev Neurosci *5*, 874-885.

Groticke, I., Hoffmann, K., and Loscher, W. (2007). Behavioral alterations in the pilocarpine model of temporal lobe epilepsy in mice. Exp Neurol *207*, 329-349.

Gupta, A., Wang, Y., and Markram, H. (2000). Organizing principles for a diversity of GABAergic interneurons and synapses in the neocortex. Science *287*, 273-278.

Hammond, V., So, E., Gunnersen, J., Valcanis, H., Kalloniatis, M., and Tan, S.S. (2006). Layer positioning of late-born cortical interneurons is dependent on Reelin but not p35 signaling. J Neurosci *26*, 1646-1655.

Hammond, V., Tsai, L.H., and Tan, S.S. (2004). Control of cortical neuron migration and layering: cell and non cell-autonomous effects of p35. J Neurosci *24*, 576-587.

Hartfuss, E., Galli, R., Heins, N., and Gotz, M. (2001). Characterization of CNS precursor subtypes and radial glia. Dev Biol *229*, 15-30.

Hashimoto, H., Yabe, T., Hirata, T., Shimizu, T., Bae, Y., Yamanaka, Y., Hirano, T., and Hibi, M. (2000). Expression of the zinc finger gene fez-like in zebrafish forebrain. Mech Dev *97*, 191-195.

Haubensak, W., Attardo, A., Denk, W., and Huttner, W.B. (2004). Neurons arise in the basal neuroepithelium of the early mammalian telencephalon: a major site of neurogenesis. Proc Natl Acad Sci U S A *101*, 3196-3201.

Heins, N., Malatesta, P., Cecconi, F., Nakafuku, M., Tucker, K.L., Hack, M.A., Chapouton, P., Barde, Y.A., and Gotz, M. (2002). Glial cells generate neurons: the role of the transcription factor Pax6. Nat Neurosci *5*, 308-315.

Hensch, T.K. (2005). Critical period plasticity in local cortical circuits. Nat Rev Neurosci *6*, 877-888.

Hensch, T.K., and Fagiolini, M. (2005). Excitatory-inhibitory balance and critical period plasticity in developing visual cortex. Prog Brain Res *147*, 115-124.

Hevner, R.F., Daza, R.A., Englund, C., Kohtz, J., and Fink, A. (2004). Postnatal shifts of interneuron position in the neocortex of normal and reeler mice: evidence for inward radial migration. Neuroscience *124*, 605-618.

Hiesberger, T., Trommsdorff, M., Howell, B.W., Goffinet, A., Mumby, M.C., Cooper, J.A., and Herz, J. (1999). Direct binding of Reelin to VLDL receptor and ApoE receptor 2 induces tyrosine phosphorylation of disabled-1 and modulates tau phosphorylation. Neuron *24*, 481-489.

Hirata, T., Suda, Y., Nakao, K., Narimatsu, M., Hirano, T., and Hibi, M. (2004). Zinc finger gene fez-like functions in the formation of subplate neurons and thalamocortical axons. Dev Dyn *230*, 546-556.

Hoshizaki, D.K., Blackburn, T., Price, C., Ghosh, M., Miles, K., Ragucci, M., and Sweis, R. (1994). Embryonic fat-cell lineage in Drosophila melanogaster. Development *120*, 2489-2499.

Howell, B.W., Hawkes, R., Soriano, P., and Cooper, J.A. (1997). Neuronal position in the developing brain is regulated by mouse disabled-1. Nature *389*, 733-737.

Howell, B.W., Herrick, T.M., and Cooper, J.A. (1999). Reelin-induced tyrosine [corrected] phosphorylation of disabled 1 during neuronal positioning. Genes Dev *13*, 643-648.

Inoue, K., Terashima, T., Nishikawa, T., and Takumi, T. (2004). Fez1 is layer-specifically expressed in the adult mouse neocortex. Eur J Neurosci *20*, 2909-2916.

Inta, D., Alfonso, J., von Engelhardt, J., Kreuzberg, M.M., Meyer, A.H., van Hooft, J.A., and Monyer, H. (2008). Neurogenesis and widespread forebrain migration of distinct GABAergic neurons from the postnatal subventricular zone. Proc Natl Acad Sci U S A *105*, 20994-20999.

Jimenez, D., Lopez-Mascaraque, L.M., Valverde, F., and De Carlos, J.A. (2002). Tangential migration in neocortical development. Dev Biol *244*, 155-169.

Jonk, L.J., de Jonge, M.E., Pals, C.E., Wissink, S., Vervaart, J.M., Schoorlemmer, J., and Kruijer, W. (1994). Cloning and expression during development of three murine members of the COUP family of nuclear orphan receptors. Mech Dev *47*, 81-97.

Kanai, M.I., Okabe, M., and Hiromi, Y. (2005). seven-up Controls switching of transcription factors that specify temporal identities of Drosophila neuroblasts. Dev Cell *8*, 203-213.

Kanatani, S., Yozu, M., Tabata, H., and Nakajima, K. (2008). COUP-TFII is preferentially expressed in the caudal ganglionic eminence and is involved in the caudal migratory stream. J Neurosci *28*, 13582-13591.

Kappeler, C., Saillour, Y., Baudoin, J.P., Tuy, F.P., Alvarez, C., Houbron, C., Gaspar, P., Hamard, G., Chelly, J., Metin, C.*, et al.* (2006). Branching and nucleokinesis defects in migrating interneurons derived from doublecortin knockout mice. Hum Mol Genet *15*, 1387-1400.

Karagiannis, A., Gallopin, T., David, C., Battaglia, D., Geoffroy, H., Rossier, J., Hillman, E.M., Staiger, J.F., and Cauli, B. (2009). Classification of NPY-expressing neocortical interneurons. J Neurosci *29*, 3642-3659.

Karlsson, G., Kolb, C., Hausdorf, A., Portet, C., Schmutz, M., and Olpe, H.R. (1992). GABAB receptors in various in vitro and in vivo models of epilepsy: a study with the GABAB receptor blocker CGP 35348. Neuroscience *47*, 63-68.

Kastner, P., Mark, M., and Chambon, P. (1995). Nonsteroid nuclear receptors: what are genetic studies telling us about their role in real life? Cell *83*, 859-869.

Koralek, K.A., and Killackey, H.P. (1990). Callosal projections in rat somatosensory cortex are altered by early removal of afferent input. Proc Natl Acad Sci U S A *87*, 1396-1400.

Kriegstein, A., Noctor, S., and Martinez-Cerdeno, V. (2006). Patterns of neural stem and progenitor cell division may underlie evolutionary cortical expansion. Nat Rev Neurosci *7*, 883-890.

Kriegstein, A.R., and Gotz, M. (2003). Radial glia diversity: a matter of cell fate. Glia *43*, 37-43.

Kriegstein, A.R., and Noctor, S.C. (2004). Patterns of neuronal migration in the embryonic cortex. Trends Neurosci *27*, 392-399.

Ladias, J.A., and Karathanasis, S.K. (1991). Regulation of the apolipoprotein AI gene by ARP-1, a novel member of the steroid receptor superfamily. Science *251*, 561-565.

Lai, T., Jabaudon, D., Molyneaux, B.J., Azim, E., Arlotta, P., Menezes, J.R., and Macklis, J.D. (2008). SOX5 Controls the Sequential Generation of Distinct Corticofugal Neuron Subtypes. Neuron *57*, 232-247.

Laudet, V. (1997). Evolution of the nuclear receptor superfamily: early diversification from an ancestral orphan receptor. J Mol Endocrinol *19*, 207-226.

Lavdas, A.A., Grigoriou, M., Pachnis, V., and Parnavelas, J.G. (1999). The medial ganglionic eminence gives rise to a population of early neurons in the developing cerebral cortex. J Neurosci *19*, 7881-7888.

Lee, S., Hjerling-Leffler, J., Zagha, E., Fishell, G., and Rudy, B. (2010). The largest group of superficial neocortical GABAergic interneurons expresses ionotropic serotonin receptors. J Neurosci *30*, 16796-16808.

Leone, D.P., Srinivasan, K., Chen, B., Alcamo, E., and McConnell, S.K. (2008). The determination of projection neuron identity in the developing cerebral cortex. Curr Opin Neurobiol *18*, 28-35.

Letinic, K., Zoncu, R., and Rakic, P. (2002). Origin of GABAergic neurons in the human neocortex. Nature *417*, 645-649.

Li, G., Adesnik, H., Li, J., Long, J., Nicoll, R.A., Rubenstein, J.L., and Pleasure, S.J. (2008). Regional distribution of cortical interneurons and development of inhibitory tone are regulated by Cxcl12/Cxcr4 signaling. J Neurosci *28*, 1085-1098.

Liang, F.Y., Moret, V., Wiesendanger, M., and Rouiller, E.M. (1991). Corticomotoneuronal connections in the rat: evidence from double-labeling of motoneurons and corticospinal axon arborizations. J Comp Neurol *311*, 356-366.

Lindwall, C., Fothergill, T., and Richards, L.J. (2007). Commissure formation in the mammalian forebrain. Curr Opin Neurobiol *17*, 3-14.

Liodis, P., Denaxa, M., Grigoriou, M., Akufo-Addo, C., Yanagawa, Y., and Pachnis, V. (2007). Lhx6 activity is required for the normal migration and specification of cortical interneuron subtypes. J Neurosci *27*, 3078-3089.

Lopez-Bendito, G., Sanchez-Alcaniz, J.A., Pla, R., Borrell, V., Pico, E., Valdeolmillos, M., and Marin, O. (2008). Chemokine signaling controls intracortical migration and final distribution of GABAergic interneurons. J Neurosci *28*, 1613-1624.

Lopez-Bendito, G., Sturgess, K., Erdelyi, F., Szabo, G., Molnar, Z., and Paulsen, O. (2004). Preferential origin and layer destination of GAD65-GFP cortical interneurons. Cereb Cortex *14*, 1122-1133.

Loscher, W., Honack, D., Fassbender, C.P., and Nolting, B. (1991). The role of technical, biological and pharmacological factors in the laboratory evaluation of anticonvulsant drugs. III. Pentylenetetrazole seizure models. Epilepsy Res *8*, 171-189.

Lutz, B., Kuratani, S., Cooney, A.J., Wawersik, S., Tsai, S.Y., Eichele, G., and Tsai, M.J. (1994). Developmental regulation of the orphan receptor COUP-TF II gene in spinal motor neurons. Development *120*, 25-36.

Magavi, S.S., and Macklis, J.D. (2001). Manipulation of Neural Precursors in situ. Induction of Neurogenesis in the Neocortex of Adult Mice. Neuropsychopharmacology *25*, 816-835.

Malatesta, P., Appolloni, I., and Calzolari, F. (2008). Radial glia and neural stem cells. Cell Tissue Res *331*, 165-178.

Malatesta, P., Hack, M.A., Hartfuss, E., Kettenmann, H., Klinkert, W., Kirchhoff, F., and Gotz, M. (2003). Neuronal or glial progeny: regional differences in radial glia fate. Neuron *37*, 751-764.

Malatesta, P., Hartfuss, E., and Gotz, M. (2000). Isolation of radial glial cells by fluorescent-activated cell sorting reveals a neuronal lineage. Development *127*, 5253-5263.

Mangelsdorf, D.J., and Evans, R.M. (1995). The RXR heterodimers and orphan receptors. Cell *83*, 841-850.

Marin, O., and Rubenstein, J.L. (2001). A long, remarkable journey: tangential migration in the telencephalon. Nat Rev Neurosci *2*, 780-790.

Marin, O., and Rubenstein, J.L. (2003). Cell migration in the forebrain. Annu Rev Neurosci *26*, 441-483.

Markram, H., Toledo-Rodriguez, M., Wang, Y., Gupta, A., Silberberg, G., and Wu, C. (2004). Interneurons of the neocortical inhibitory system. Nat Rev Neurosci *5*, 793-807.

Martini, F.J., Valiente, M., Lopez Bendito, G., Szabo, G., Moya, F., Valdeolmillos, M., and Marin, O. (2009). Biased selection of leading process branches mediates chemotaxis during tangential neuronal migration. Development *136*, 41-50.

Matsuo-Takasaki, M., Lim, J.H., Beanan, M.J., Sato, S.M., and Sargent, T.D. (2000). Cloning and expression of a novel zinc finger gene, Fez, transcribed in the forebrain of Xenopus and mouse embryos. Mech Dev *93*, 201-204.

McConnell, S.K. (1988). Fates of visual cortical neurons in the ferret after isochronic and heterochronic transplantation. J Neurosci *8*, 945-974.

McConnell, S.K., and Kaznowski, C.E. (1991). Cell cycle dependence of laminar determination in developing neocortex. Science *254*, 282-285.

Meyer, G., Perez-Garcia, C.G., Abraham, H., and Caput, D. (2002). Expression of p73 and Reelin in the developing human cortex. J Neurosci *22*, 4973-4986.

Miller, M.W. (1985). Cogeneration of retrogradely labeled corticocortical projection and GABA-immunoreactive local circuit neurons in cerebral cortex. Brain Res *355*, 187-192.
Mitchell, B.D., and Macklis, J.D. (2005). Large-scale maintenance of dual projections by callosal and frontal cortical projection neurons in adult mice. J Comp Neurol *482*, 17-32.

Miyajima, N., Kadowaki, Y., Fukushige, S., Shimizu, S., Semba, K., Yamanashi, Y., Matsubara, K., Toyoshima, K., and Yamamoto, T. (1988). Identification of two novel members of erbA superfamily by molecular cloning: the gene products of the two are highly related to each other. Nucleic Acids Res *16*, 11057-11074.

Miyoshi, G., Butt, S.J., Takebayashi, H., and Fishell, G. (2007). Physiologically distinct temporal cohorts of cortical interneurons arise from telencephalic Olig2-expressing precursors. J Neurosci *27*, 7786-7798.

Miyoshi, G., and Fishell, G. (2010). GABAergic Interneuron Lineages Selectively Sort into Specific Cortical Layers during Early Postnatal Development. Cereb Cortex.

Miyoshi, G., Hjerling-Leffler, J., Karayannis, T., Sousa, V.H., Butt, S.J., Battiste, J., Johnson, J.E., Machold, R.P., and Fishell, G. (2010). Genetic fate mapping reveals that the caudal ganglionic eminence produces a large and diverse population of superficial cortical interneurons. J Neurosci *30*, 1582-1594.

Mizutani, K., and Saito, T. (2005). Progenitors resume generating neurons after temporary inhibition of neurogenesis by Notch activation in the mammalian cerebral cortex. Development *132*, 1295-1304.

Mlodzik, M., Hiromi, Y., Weber, U., Goodman, C.S., and Rubin, G.M. (1990). The Drosophila seven-up gene, a member of the steroid receptor gene superfamily, controls photoreceptor cell fates. Cell *60*, 211-224.

Molnar, Z., Metin, C., Stoykova, A., Tarabykin, V., Price, D.J., Francis, F., Meyer, G., Dehay, C., and Kennedy, H. (2006). Comparative aspects of cerebral cortical development. Eur J Neurosci *23*, 921-934.

Molyneaux, B.J., Arlotta, P., Fame, R.M., MacDonald, J.L., MacQuarrie, K.L., and Macklis, J.D. (2009). Novel subtype-specific genes identify distinct subpopulations of callosal projection neurons. J Neurosci *29*, 12343-12354.

Molyneaux, B.J., Arlotta, P., Hirata, T., Hibi, M., and Macklis, J.D. (2005). Fezl is required for the birth and specification of corticospinal motor neurons. Neuron *47*, 817-831.

Molyneaux, B.J., Arlotta, P., Menezes, J.R., and Macklis, J.D. (2007). Neuronal subtype specification in the cerebral cortex. Nat Rev Neurosci *8*, 427-437.

Naka, H., Nakamura, S., Shimazaki, T., and Okano, H. (2008a). Requirement for COUP-TFI and II in the temporal specification of neural stem cells in CNS development. Nat Neurosci.

Naka, H., Nakamura, S., Shimazaki, T., and Okano, H. (2008b). Requirement for COUP-TFI and II in the temporal specification of neural stem cells in CNS development. Nat Neurosci *11*, 1014-1023.

Nery, S., Fishell, G., and Corbin, J.G. (2002). The caudal ganglionic eminence is a source of distinct cortical and subcortical cell populations. Nat Neurosci *5*, 1279-1287.

Nobrega-Pereira, S., Kessaris, N., Du, T., Kimura, S., Anderson, S.A., and Marin, O. (2008). Postmitotic Nkx2-1 controls the migration of telencephalic interneurons by direct repression of guidance receptors. Neuron *59*, 733-745.

Noctor, S.C., Flint, A.C., Weissman, T.A., Dammerman, R.S., and Kriegstein, A.R. (2001). Neurons derived from radial glial cells establish radial units in neocortex. Nature *409*, 714-720.

Noctor, S.C., Flint, A.C., Weissman, T.A., Wong, W.S., Clinton, B.K., and Kriegstein, A.R. (2002). Dividing precursor cells of the embryonic cortical ventricular zone have morphological and molecular characteristics of radial glia. J Neurosci *22*, 3161-3173.
Noctor, S.C., Martinez-Cerdeno, V., Ivic, L., and Kriegstein, A.R. (2004). Cortical neurons arise in symmetric and asymmetric division zones and migrate through specific phases. Nat Neurosci *7*, 136-144.

Ogawa, M., Miyata, T., Nakajima, K., Yagyu, K., Seike, M., Ikenaka, K., Yamamoto, H., and Mikoshiba, K. (1995). The reeler gene-associated antigen on Cajal-Retzius neurons is a crucial molecule for laminar organization of cortical neurons. Neuron *14*, 899-912.

Ohira, K., Hagihara, H., Toyama, K., Takao, K., Kanai, M., Funakoshi, H., Nakamura, T., and Miyakawa, T. (2010). Expression of tryptophan 2,3-dioxygenase in mature granule cells of the adult mouse dentate gyrus. Mol Brain *3*, 26.

Olsson, M., Campbell, K., and Turnbull, D.H. (1997). Specification of mouse telencephalic and mid-hindbrain progenitors following heterotopic ultrasound-guided embryonic transplantation. Neuron *19*, 761-772.

Pastorcic, M., Wang, H., Elbrecht, A., Tsai, S.Y., Tsai, M.J., and O'Malley, B.W. (1986). Control of transcription initiation in vitro requires binding of a transcription factor to the distal promoter of the ovalbumin gene. Mol Cell Biol *6*, 2784-2791.

Peduzzi, J.D. (1988). Genesis of GABA-immunoreactive neurons in the ferret visual cortex. J Neurosci *8*, 920-931.

Pereira, F.A., Qiu, Y., Tsai, M.J., and Tsai, S.Y. (1995). Chicken ovalbumin upstream promoter transcription factor (COUP-TF): expression during mouse embryogenesis. J Steroid Biochem Mol Biol *53*, 503-508.

Pereira, F.A., Qiu, Y., Zhou, G., Tsai, M.J., and Tsai, S.Y. (1999). The orphan nuclear receptor COUP-TFII is required for angiogenesis and heart development. Genes Dev *13*, 1037-1049.

Petanjek, Z., Berger, B., and Esclapez, M. (2009). Origins of cortical GABAergic neurons in the cynomolgus monkey. Cereb Cortex *19*, 249-262.

Petryniak, M.A., Potter, G.B., Rowitch, D.H., and Rubenstein, J.L. (2007). Dlx1 and Dlx2 control neuronal versus oligodendroglial cell fate acquisition in the developing forebrain. Neuron *55*, 417-433.

Pla, R., Borrell, V., Flames, N., and Marin, O. (2006). Layer acquisition by cortical GABAergic interneurons is independent of Reelin signaling. J Neurosci *26*, 6924-6934.

Pleasure, S.J., Anderson, S., Hevner, R., Bagri, A., Marin, O., Lowenstein, D.H., and Rubenstein, J.L. (2000). Cell migration from the ganglionic eminences is required for the development of hippocampal GABAergic interneurons. Neuron *28*, 727-740.

Polleux, F., Whitford, K.L., Dijkhuizen, P.A., Vitalis, T., and Ghosh, A. (2002). Control of cortical interneuron migration by neurotrophins and PI3-kinase signaling. Development *129*, 3147-3160.

Pontious, A., Kowalczyk, T., Englund, C., and Hevner, R.F. (2008). Role of intermediate progenitor cells in cerebral cortex development. Dev Neurosci *30*, 24-32.

Porteus, M.H., Bulfone, A., Liu, J.K., Puelles, L., Lo, L.C., and Rubenstein, J.L. (1994). DLX-2, MASH-1, and MAP-2 expression and bromodeoxyuridine incorporation define molecularly distinct cell populations in the embryonic mouse forebrain. J Neurosci *14*, 6370-6383.

Powell, E.M., Campbell, D.B., Stanwood, G.D., Davis, C., Noebels, J.L., and Levitt, P. (2003). Genetic disruption of cortical interneuron development causes region- and GABA cell type-specific deficits, epilepsy, and behavioral dysfunction. J Neurosci *23*, 622-631.

Pozas, E., and Ibanez, C.F. (2005). GDNF and GFRalpha1 promote differentiation and tangential migration of cortical GABAergic neurons. Neuron *45*, 701-713.

Qiu, Y., Cooney, A.J., Kuratani, S., DeMayo, F.J., Tsai, S.Y., and Tsai, M.J. (1994a). Spatiotemporal expression patterns of chicken ovalbumin upstream promoter-transcription factors in the developing mouse central nervous system: evidence for a role in segmental patterning of the diencephalon. Proc Natl Acad Sci U S A *91*, 4451-4455.

Qiu, Y., Pereira, F.A., DeMayo, F.J., Lydon, J.P., Tsai, S.Y., and Tsai, M.J. (1997). Null mutation of mCOUP-TFI results in defects in morphogenesis of the glossopharyngeal ganglion, axonal projection, and arborization. Genes Dev *11*, 1925-1937.

Qiu, Y., Tsai, S.Y., and Tsai, M.J. (1994b). COUP-TF an orphan member of the steroid/thyroid hormone receptor superfamily. Trends Endocrinol Metab *5*, 234-239.

Rakic, P. (1972). Mode of cell migration to the superficial layers of fetal monkey neocortex. J Comp Neurol *145*, 61-83.

Rakic, P. (1974). Neurons in rhesus monkey visual cortex: systematic relation between time of origin and eventual disposition. Science *183*, 425-427.

Rakic, P. (2003). Developmental and evolutionary adaptations of cortical radial glia. Cereb Cortex *13*, 541-549.

Rakic, S., Yanagawa, Y., Obata, K., Faux, C., Parnavelas, J.G., and Nikolic, M. (2009). Cortical interneurons require p35/Cdk5 for their migration and laminar organization. Cereb Cortex *19*, 1857-1869.

Rallu, M., Machold, R., Gaiano, N., Corbin, J.G., McMahon, A.P., and Fishell, G. (2002). Dorsoventral patterning is established in the telencephalon of mutants lacking both Gli3 and Hedgehog signaling. Development *129*, 4963-4974.

Reiner, A., Jiao, Y., Del Mar, N., Laverghetta, A.V., and Lei, W.L. (2003). Differential morphology of pyramidal tract-type and intratelencephalically projecting-type corticostriatal neurons and their intrastriatal terminals in rats. J Comp Neurol *457*, 420-440.

Rice, D.S., and Curran, T. (2001). Role of the reelin signaling pathway in central nervous system development. Annu Rev Neurosci *24*, 1005-1039.

Richards, L.J., Plachez, C., and Ren, T. (2004). Mechanisms regulating the development of the corpus callosum and its agenesis in mouse and human. Clin Genet *66*, 276-289.

Rouaux, C., and Arlotta, P. (2010). Fezf2 directs the differentiation of corticofugal neurons from striatal progenitors in vivo. Nat Neurosci *13*, 1345-1347.

Rubin, A.N., Alfonsi, F., Humphreys, M.P., Choi, C.K., Rocha, S.F., and Kessaris, N. (2010). The germinal zones of the basal ganglia but not the septum generate GABAergic interneurons for the cortex. J Neurosci *30*, 12050-12062.

Rymar, V.V., and Sadikot, A.F. (2007). Laminar fate of cortical GABAergic interneurons is dependent on both birthdate and phenotype. J Comp Neurol *501*, 369-380.

Sagami, I., Tsai, S.Y., Wang, H., Tsai, M.J., and O'Malley, B.W. (1986). Identification of two factors required for transcription of the ovalbumin gene. Mol Cell Biol *6*, 4259-4267.

Saito, T., and Nakatsuji, N. (2001). Efficient gene transfer into the embryonic mouse brain using in vivo electroporation. Dev Biol *240*, 237-246.

Sanchez-Alcaniz, J.A., Haege, S., Mueller, W., Pla, R., Mackay, F., Schulz, S., Lopez-Bendito, G., Stumm, R., and Marin, O. (2011). Cxcr7 controls neuronal migration by regulating chemokine responsiveness. Neuron *69*, 77-90.

Seah, C., Levy, M.A., Jiang, Y., Mokhtarzada, S., Higgs, D.R., Gibbons, R.J., and Berube, N.G. (2008). Neuronal death resulting from targeted disruption of the Snf2 protein ATRX is mediated by p53. J Neurosci *28*, 12570-12580.

Senzaki, K., Ogawa, M., and Yagi, T. (1999). Proteins of the CNR family are multiple receptors for Reelin. Cell *99*, 635-647.

Sheldon, M., Rice, D.S., D'Arcangelo, G., Yoneshima, H., Nakajima, K., Mikoshiba, K., Howell, B.W., Cooper, J.A., Goldowitz, D., and Curran, T. (1997). Scrambler and yotari disrupt the disabled gene and produce a reeler-like phenotype in mice. Nature *389*, 730-733.

Smart, I.H. (1976). A pilot study of cell production by the ganglionic eminences of the developing mouse brain. J Anat *121*, 71-84.

Sousa, V.H., Miyoshi, G., Hjerling-Leffler, J., Karayannis, T., and Fishell, G. (2009). Characterization of Nkx6-2-derived neocortical interneuron lineages. Cereb Cortex *19 Suppl 1*, i1-10.

Staiger, J.F., Masanneck, C., Schleicher, A., and Zuschratter, W. (2004). Calbindin-containing interneurons are a target for VIP-immunoreactive synapses in rat primary somatosensory cortex. J Comp Neurol *468*, 179-189.

Stenman, J., Toresson, H., and Campbell, K. (2003). Identification of two distinct progenitor populations in the lateral ganglionic eminence: implications for striatal and olfactory bulb neurogenesis. J Neurosci *23*, 167-174.

Stumm, R.K., Zhou, C., Ara, T., Lazarini, F., Dubois-Dalcq, M., Nagasawa, T., Hollt, V., and Schulz, S. (2003). CXCR4 regulates interneuron migration in the developing neocortex. J Neurosci *23*, 5123-5130.

Sturrock, R.R., and Smart, I.H. (1980). A morphological study of the mouse subependymal layer from embryonic life to old age. J Anat *130*, 391-415.
Sun, H., Ma, C.L., Kelly, J.B., and Wu, S.H. (2006). GABAB receptor-mediated presynaptic inhibition of glutamatergic transmission in the inferior colliculus. Neurosci Lett *399*, 151-156.

Sussel, L., Marin, O., Kimura, S., and Rubenstein, J.L. (1999). Loss of Nkx2.1 homeobox gene function results in a ventral to dorsal molecular respecification within the basal telencephalon: evidence for a transformation of the pallidum into the striatum. Development *126*, 3359-3370.

Taglialatela, P., Soria, J.M., Caironi, V., Moiana, A., and Bertuzzi, S. (2004). Compromised generation of GABAergic interneurons in the brains of Vax1-/- mice. Development *131*, 4239-4249.

Takiguchi-Hayashi, K., Sekiguchi, M., Ashigaki, S., Takamatsu, M., Hasegawa, H., Suzuki-Migishima, R., Yokoyama, M., Nakanishi, S., and Tanabe, Y. (2004). Generation of reelin-positive marginal zone cells from the caudomedial wall of telencephalic vesicles. J Neurosci *24*, 2286-2295.

Tamamaki, N., Fujimori, K.E., and Takauji, R. (1997). Origin and route of tangentially migrating neurons in the developing neocortical intermediate zone. J Neurosci *17*, 8313-8323.

Tamamaki, N., Yanagawa, Y., Tomioka, R., Miyazaki, J., Obata, K., and Kaneko, T. (2003). Green fluorescent protein expression and colocalization with calretinin, parvalbumin, and somatostatin in the GAD67-GFP knock-in mouse. J Comp Neurol *467*, 60-79.

Tamas, G., Lorincz, A., Simon, A., and Szabadics, J. (2003). Identified sources and targets of slow inhibition in the neocortex. Science *299*, 1902-1905.

Tan, S.S., Kalloniatis, M., Sturm, K., Tam, P.P., Reese, B.E., and Faulkner-Jones, B. (1998). Separate progenitors for radial and tangential cell dispersion during development of the cerebral neocortex. Neuron *21*, 295-304.

Tanaka, D., Nakaya, Y., Yanagawa, Y., Obata, K., and Murakami, F. (2003a). Multimodal tangential migration of neocortical GABAergic neurons independent of GPI-anchored proteins. Development *130*, 5803-5813.

Tanaka, J., Fujisawa, S., and Nomura, M. (2003b). GABAergic modulation of the ANG II-induced drinking response in the rat medial preoptic nucleus. Pharmacol Biochem Behav *76*, 43-51.

Thummel, C.S. (1995). From embryogenesis to metamorphosis: the regulation and function of Drosophila nuclear receptor superfamily members. Cell *83*, 871-877.

Tissir, F., and Goffinet, A.M. (2003). Reelin and brain development. Nat Rev Neurosci *4*, 496-505.

Tiveron, M.C., Rossel, M., Moepps, B., Zhang, Y.L., Seidenfaden, R., Favor, J., Konig, N., and Cremer, H. (2006). Molecular interaction between projection neuron precursors and invading interneurons via stromal-derived factor 1 (CXCL12)/CXCR4 signaling in the cortical subventricular zone/intermediate zone. J Neurosci *26*, 13273-13278.

Tomassy, G.S., De Leonibus, E., Jabaudon, D., Lodato, S., Alfano, C., Mele, A., Macklis, J.D., and Studer, M. (2010a). Area-specific temporal control of corticospinal motor neuron differentiation by COUP-TFI. Proc Natl Acad Sci U S A *107*, 3576-3581.

Tomassy, G.S., Lodato, S., Trayes-Gibson, Z., and Arlotta, P. (2010b). Development and regeneration of projection neuron subtypes of the cerebral cortex. Sci Prog *93*, 151-169.

Tricoire, L., Pelkey, K.A., Daw, M.I., Sousa, V.H., Miyoshi, G., Jeffries, B., Cauli, B., Fishell, G., and McBain, C.J. (2010). Common origins of hippocampal Ivy and nitric oxide synthase expressing neurogliaform cells. J Neurosci *30*, 2165-2176.

Trommsdorff, M., Gotthardt, M., Hiesberger, T., Shelton, J., Stockinger, W., Nimpf, J., Hammer, R.E., Richardson, J.A., and Herz, J. (1999). Reeler/Disabled-like disruption of neuronal migration in knockout mice lacking the VLDL receptor and ApoE receptor 2. Cell *97*, 689-701.

Tsai, M.J., and O'Malley, B.W. (1994). Molecular mechanisms of action of steroid/thyroid receptor superfamily members. Annu Rev Biochem *63*, 451-486.

Tsai, S.Y., Sagami, I., Wang, H., Tsai, M.J., and O'Malley, B.W. (1987). Interactions between a DNA-binding transcription factor (COUP) and a non-DNA binding factor (S300-II). Cell *50*, 701-709.

Tsai, S.Y., and Tsai, M.J. (1997). Chick ovalbumin upstream promoter-transcription factors (COUP-TFs): coming of age. Endocr Rev *18*, 229-240.

Valcanis, H., and Tan, S.S. (2003). Layer specification of transplanted interneurons in developing mouse neocortex. J Neurosci *23*, 5113-5122.

Vucurovic, K., Gallopin, T., Ferezou, I., Rancillac, A., Chameau, P., van Hooft, J.A., Geoffroy, H., Monyer, H., Rossier, J., and Vitalis, T. (2010). Serotonin 3A receptor subtype as an early and protracted marker of cortical interneuron subpopulations. Cereb Cortex *20*, 2333-2347.

Wahlsten, D., Metten, P., and Crabbe, J.C. (2003). Survey of 21 inbred mouse strains in two laboratories reveals that BTBR T/+ tf/tf has severely reduced hippocampal commissure and absent corpus callosum. Brain Res *971*, 47-54.

Wang, L.H., Ing, N.H., Tsai, S.Y., O'Malley, B.W., and Tsai, M.J. (1991). The COUP-TFs compose a family of functionally related transcription factors. Gene Expr *1*, 207-216.

Wang, L.H., Tsai, S.Y., Cook, R.G., Beattie, W.G., Tsai, M.J., and O'Malley, B.W. (1989). COUP transcription factor is a member of the steroid receptor superfamily. Nature *340*, 163-166.

Wang, L.H., Tsai, S.Y., Sagami, I., Tsai, M.J., and O'Malley, B.W. (1987). Purification and characterization of chicken ovalbumin upstream promoter transcription factor from HeLa cells. J Biol Chem *262*, 16080-16086.

Wang, Y., Li, G., Stanco, A., Long, J.E., Crawford, D., Potter, G.B., Pleasure, S.J., Behrens, T., and Rubenstein, J.L. (2011). CXCR4 and CXCR7 Have Distinct Functions in Regulating Interneuron Migration. Neuron *69*, 61-76.

Ware, M.L., Tavazoie, S.F., Reid, C.B., and Walsh, C.A. (1999). Coexistence of widespread clones and large radial clones in early embryonic ferret cortex. Cereb Cortex *9*, 636-645.

Wichterle, H., Garcia-Verdugo, J.M., Herrera, D.G., and Alvarez-Buylla, A. (1999). Young neurons from medial ganglionic eminence disperse in adult and embryonic brain. Nat Neurosci *2*, 461-466.

Wichterle, H., Turnbull, D.H., Nery, S., Fishell, G., and Alvarez-Buylla, A. (2001). In utero fate mapping reveals distinct migratory pathways and fates of neurons born in the mammalian basal forebrain. Development *128*, 3759-3771.

Willi-Monnerat, S., Migliavacca, E., Surdez, D., Delorenzi, M., Luthi-Carter, R., and Terskikh, A.V. (2008). Comprehensive spatiotemporal transcriptomic analyses of the ganglionic eminences demonstrate the uniqueness of its caudal subdivision. Mol Cell Neurosci *37*, 845-856.

Williams, B.P., and Price, J. (1995). Evidence for multiple precursor cell types in the embryonic rat cerebral cortex. Neuron *14*, 1181-1188.

Wonders, C.P., and Anderson, S.A. (2006). The origin and specification of cortical interneurons. Nat Rev Neurosci *7*, 687-696.

Wonders, C.P., Taylor, L., Welagen, J., Mbata, I.C., Xiang, J.Z., and Anderson, S.A. (2008). A spatial bias for the origins of interneuron subgroups within the medial ganglionic eminence. Dev Biol *314*, 127-136.

Xu, Q., Cobos, I., De La Cruz, E., Rubenstein, J.L., and Anderson, S.A. (2004). Origins of cortical interneuron subtypes. J Neurosci *24*, 2612-2622.

Xu, Q., Tam, M., and Anderson, S.A. (2008). Fate mapping Nkx2.1-lineage cells in the mouse telencephalon. J Comp Neurol *506*, 16-29.
Xu, X., and Callaway, E.M. (2009). Laminar specificity of functional input to distinct types of inhibitory cortical neurons. J Neurosci *29*, 70-85.

Yabut, O., Renfro, A., Niu, S., Swann, J.W., Marin, O., and D'Arcangelo, G. (2007). Abnormal laminar position and dendrite development of interneurons in the reeler forebrain. Brain Res *1140*, 75-83.

Yamaguchi, H., Zhou, C., Lin, S.C., Durand, B., Tsai, S.Y., and Tsai, M.J. (2004). The nuclear orphan receptor COUP-TFI is important for differentiation of oligodendrocytes. Dev Biol *266*, 238-251.

Yang, Z., Liu, N., and Lin, S. (2001). A zebrafish forebrain-specific zinc finger gene can induce ectopic dlx2 and dlx6 expression. Dev Biol *231*, 138-148.

Young-Pearse, T.L., Bai, J., Chang, R., Zheng, J.B., LoTurco, J.J., and Selkoe, D.J. (2007). A critical function for beta-amyloid precursor protein in neuronal migration revealed by in utero RNA interference. J Neurosci *27*, 14459-14469.

Yozu, M., Tabata, H., and Nakajima, K. (2005). The caudal migratory stream: a novel migratory stream of interneurons derived from the caudal ganglionic eminence in the developing mouse forebrain. J Neurosci *25*, 7268-7277.

Zhadanov, A.B., Provance, D.W., Jr., Speer, C.A., Coffin, J.D., Goss, D., Blixt, J.A., Reichert, C.M., and Mercer, J.A. (1999). Absence of the tight junctional protein AF-6 disrupts epithelial cell-cell junctions and cell polarity during mouse development. Curr Biol *9*, 880-888.

Zhou, C., Qiu, Y., Pereira, F.A., Crair, M.C., Tsai, S.Y., and Tsai, M.J. (1999). The nuclear orphan receptor COUP-TFI is required for differentiation of subplate neurons and guidance of thalamocortical axons. Neuron *24*, 847-859.

Zhou, H.M., and Walthall, W.W. (1998). UNC-55, an orphan nuclear hormone receptor, orchestrates synaptic specificity among two classes of motor neurons in Caenorhabditis elegans. J Neurosci *18*, 10438-10444.